Structural Studies of the Bacterial Histidine Kinases RetS and GacS, Key Components of the Multikinase Network that Controls the Switch Between a Motile Invasive Lifestyle and a Sessile Biofilm Lifestyle in *Pseudomonas aeruginosa*

Kylie Meghan Ryan

Dissertation submitted to the faculty of the Virginia Polytechnic Institute and State University in partial fulfillment of the requirements for the degree of:

Doctor of Philosophy
in
Biological Sciences

Florian D. Schubot, Chair
Clayton C. Caswell
Birgit Scharf
Zhaomin Yang

October 27, 2021
Blacksburg, VA

Keywords: bacterial histidine kinase, two-component systems, crosstalk

Structural Studies of the Bacterial Histidine Kinases RetS and GacS, Key Components of the Multikinase Network that Controls the Switch Between a Motile Invasive Lifestyle and a Sessile Biofilm Lifestyle in *Pseudomonas aeruginosa*

Kylie Meghan Ryan

Abstract

Signal transduction networks enable organisms to respond to environmental stimuli. Bacteria utilize two-component systems (TCSs) and phosphorelays as their primary means of signal transduction. Histidine kinase (HK) and response regulator (RR) proteins comprise these TCSs and phosphorelays. Previously, signal transduction within TCSs and phosphorelays was thought to only occur through a linear series of phosphotransfers between HKs and RRs. Recently multikinase networks have been shown to be involved in TCS and phosphorelay signal transmission. A multikinase network that includes the HKs RetS and GacS controls the switch between the motile invasive lifestyle and the sessile biofilm lifestyle of the opportunistic human pathogen *Pseudomonas aeruginosa*. GacS promotes the sessile biofilm lifestyle, while RetS promotes the motile invasive lifestyle via the inhibition of GacS. This inhibition occurs through three distinct mechanisms. Two of the mechanisms are dephosphorylating mechanisms and the third mechanism is a direct interaction between RetS and GacS which results in the inhibition of GacS autophosphorylation. This study examines the direct binding interaction between RetS and GacS using structural biology. We observed a heterodimeric RetS-GacS complex in which the canonical homodimerization interface was replaced with a heterodimeric interface. Heterodimerization between bacterial HKs is currently a novel observation, but it is likely that other HKs heterodimerize. The RetS-GacS direct interaction can serve as a model for HK-HK binding in multikinase networks.

Structural Studies of the Bacterial Histidine Kinases RetS and GacS, Key Components of the Multikinase Network that Controls the Switch Between a Motile Invasive Lifestyle and a Sessile Biofilm Lifestyle in *Pseudomonas aeruginosa*

Kylie Meghan Ryan

General Audience Abstract

The way in which bacteria assess and respond to their environment is of great interest to microbiologists. Bacteria transmit environmental signals via protein interactions. Some of these interactions involve the transfer of phosphate groups, and some involve a direct binding interaction between proteins. We are investigating a direct binding interaction between two proteins, RetS and GacS. These proteins control whether *Pseudomonas aeruginosa*, an opportunistic pathogen of humans, causes an acute infection, which is characterized by motility and invasiveness, or a chronic infection, which is characterized by a sessile biofilm lifestyle, in a human host. Through the use of structural biology techniques we have visualized the three-dimensional structure of the complex between RetS and GacS. This complex has provided insight into the role of the RetS-GacS interaction in controlling the infection state of *P. aeruginosa*.

Acknowledgments

I would like to thank my advisor, Florian Schubot, for his help and guidance throughout the years as my mentor. I would also like to thank my committee members, Clay Caswell, Birgit Scharf and Zhaomin Yang, for all of their thoughtful suggestions regarding my research and for the support that they provided. Thank you to the numerous graduate students that have aided me and have made this journey enjoyable. Particularly, I thank Dr. Jordan Mancl and Dr. Manisha Shrestha who taught me many laboratory techniques. Finally, I would like to thank my family for supporting me throughout my graduate education.

Chapter 1: Literature Review

Bacterial Signal Transduction

Bacterial Two-Component Systems and Phosphorelays

Signaling pathways such as bacterial two-component systems (TCSs) and phosphorelays allow organisms to adapt to changing environmental conditions (1). Bacterial TCSs and phosphorelays enable an extracellular or intracellular signal to be transmitted and coupled to a response via the transfer of phosphate groups (2, 3). A classical TCS is comprised of two proteins, a sensor histidine kinase (HK) and a response regulator (RR) (Fig. 1.1) (2, 4, 5). HKs are modular proteins that combine diverse N-terminal sensory input domains with more conserved catalytic domains in the HK region (5). The majority of known HKs have an extracytoplasmic sensory domain that interacts with extracellular stimuli, followed by a transmembrane region, but there are HKs that have cytosolic sensory domains that interact with intracellular stimuli (6, 7). The conserved C-terminal HK region is comprised of two domains, the N-terminal dimerization and histidine phosphotransfer (DHp) domain and the C-terminal catalytic and ATP binding (CA) domain. The DHp domain is responsible for homodimerization and contains a highly conserved catalytic histidine residue that undergoes ATP-dependent autophosphorylation (2, 4, 5). The CA domain binds and hyrdrolyzes ATP via a highly conserved ATP binding pocket (2, 5). The RR has an N-terminal conserved receiver domain that contains a highly conserved aspartate residue that undergoes phosphorylation via the catalytic histidine residue of the HK followed by a variable output domain (8). The transfer of the phosphate group causes a conformational change in the output domain of the RR, which results in a regulatory response, often the regulatory response is a form of transcriptional regulation (4).

Phosphorelay systems expand upon the classical TCS and are termed due to their use of a three step phosphotransfer between conserved histidine residues and conserved aspartate residues (1, 8). The greater number of phosphotransfers allows for more adaptability in signaling and a more stringent regulatory control of the phosphorelay itself (5, 9, 10). Unorthodox HKs integrate additional domains into a signal polypeptide. Following the HK region, they possess a receiver domain with a conserved aspartate residue and a histidine phosphotransferase (HPt) domain (Fig. 1.1) (4, 11). Hybrid HKs may contain one or more RR domains but interact with a separate HPt domain (4, 8, 9, 12).

HKs function as dimers (3, 5, 7). The CA domain binds and hydrolyzes ATP to transfer the γ-phosphate to the catalytic histidine residue in the DHp domain (5). The transfer of phosphate from the CA domain to the DHp domain usually occurs in *trans*—the CA domain of one subunit phosphorylates the conserved histidine residue in the DHp domain of the other subunit—but it can also occur in *cis*—the CA domain of one subunit phosphorylates the conserved histidine residue in the DHp domain of the same subunit (5, 7, 13). The phosphorylation of histidine results in a high energy, unstable N-P bond between phosphate and the imidazole ring of histidine which allows for the transfer of the phosphate group to the next conserved aspartate residue in the TCS (5).

Many, but not all HKs are bifunctional in that they possess kinase and phosphatase activity (14, 15). The phosphatase activity of HKs allows for a greater degree of regulation of RR output (14, 16). Research on the EnvZ/OmpR pathway, a TCS in *Escherichia coli*, suggests that the DHp domain of the HK is sufficient for moderate phosphatase activity *in vitro*, while the inclusion of the CA domain with the DHp domain greatly enhances phosphatase activity (14, 17). Interestingly, the conserved histidine residue in the EnvZ DHp domain is not necessary for

phosphatase activity, but does further increases phosphatase activity. On the other hand, substitution at the conserved threonine residue—a residue found in many HKs that is located four residues C-terminal to the conserved histidine—results in a major decrease in phosphatase activity (17). The conserved threonine residue is thought to be the primary residue involved in the transmitter phosphatase activity by which an HK dephosphorylates its cognate RR (17, 18).

Structural examinations of HKs have revealed a potential relationship between the symmetry of the homodimeric HK region and the catalytic state, with symmetric HK regions primed for phosphatase activity, while asymmetric HK regions are primed for the autophosphorylation and phosphotransfer (3, 19). In the asymmetric conformation the α1 helix of the DHp domain is bent while the ATP binding pocket of the CA domain is brought close to the catalytic histidine in preparation for autophosphorylation (13). Consequently, autophosphorylation does not occur for both subunits simultaneously as is suggested by structural studies that have observed asymmetrical hemiphosphorylated homodimeric HKs (13).

Several common topologies exist for HK sensory domains, with the most common being sensory domains that are extracytoplasmic which are sandwiched between two or more transmembrane helices (5, 20, 21). There are also HKs which lack an extracytoplasmic sensory domain and instead rely on their transmembrane regions to interact with membrane associated signals such as cell envelope stress, ionic strength, electrochemical gradients and osmolarity (5, 20). Finally, there are those which utilize cytoplasmic sensory domains to interact with internal signals (5, 20, 21). There are several defined extracytoplasmic sensory domain families. The PDBb (periplasmic solute-binding proteins bacterial) domain binds amino acids and opines (plant derived compounds which are metabolized by bacteria, in particular by the genus *Agrobacterium*) (20, 22, 23). CACHE (calcium channels and chemotaxis receptors) domain

senses small molecules (20, 23). The CHASE (cyclase, histidine kinase associated sensing extracellular) domain senses amino acids, peptides and cytokines (20, 23). The DISM2 (diverse intracellular signaling module 2) domain senses carbohydrates (20). Lastly, the related PAS (Per Arnt Sim)-like fold and the PAS-like PDC (PhoQ, DcuS, CitA) folds are found in extracytoplasmic sensory domains (5, 21, 23). PAS domains have high primary sequence variability with a conserved α/β fold and sense metabolites (in particular dicarboxylic acids), oxygen, redox potential and light (5, 24–27). PAS domains also play a role in signal transmission as the β sheet of the PAS domain undergoes conformational changes upon signal transduction which enabled signal transmission to the C-terminal catalytic domains (13, 24, 28). There are also two common cytoplasmic sensory domains; the PAS domain and the GAF (cGMP phosphodiesterases, adenylyl cyclases and FhlA) domain (5, 13, 29). GAF domains also have high primary sequence variability with a tertiary structure similar to that of PAS domains (20). GAF domains sense redox potential, c-di-GMP and photopigments (13, 20, 23, 29).

Found in most HKs, the signaling helix (S helix), an approximately 40 residue α helical region that connects the helical transmembrane regions with the HK region. Signal transduction through the S helix occurs via helical rotation (which can result in supercoiling of the S helix), helical bending or helical displacements (3, 30–32). These helical movements cause rotation of the helices in the HK region thereby modifying the accessibility of the catalytic histidine and the autophosphorylation state of the HK (3, 30). S helix helical rotation also results in conformational changes to the CA domain that activate the HK (3).

The ubiquitous HAMP domain (termed due to its inclusion in **h**istidine kinases, **a**denylyl cyclases, **m**ethyl-accepting chemotaxis proteins and **p**hosphatases) is frequently found adjacent to the S helix in many histidine kinases, most often N-terminal to the S helix although other

arrangements have been observed (31, 32). It is comprised of approximately 50 residues and consists of a pair of α helices which form a dimeric four helix bundle (32–34). Helical displacement, helical rotations, diagonal scissoring and piston motions have been implicated in signal transmission through HAMP domains, as have the looseness of the four helix bundle (13, 34, 35).

The HK region contains two domains: The α helical DHp domain contains approximately 60 residues and comprises a helix-loop-helix fold that forms a four helix bundle in the HK homodimer (36). The catalytic histidine is located within the H box motif on the α1 helix of the DHp domain (5). The CA domain contains approximately 160 residues and comprises an α/β sandwich fold (36). The ATP binding pocket of the CA domain is defined by the conserved N, G1, F and G2 box motifs, and the ATP lid is the flexible loop between the F and G2 box motifs that covers the ATP binding pocket upon nucleotide binding (5).

Crosstalk in Bacterial TCSs and Phosphorelays

The ability of two-component systems and phosphorelays to maintain specificity and avoid crosstalk is of great interest due to the paralogous and modular nature of the HK and RR proteins, which results in a high degree of amino acid sequence similarity and tertiary structural relatedness among the component proteins (14, 37). Many HKs maintain specificity for their cognate RRs through molecular recognition via specificity residues (3, 14, 19, 37–40). Specificity residues are covarying residues found within the base of the α1 and α2 helices that make up the four helix bundle in the DHp domains of a homodimeric HK and within the loop that connects the β4 strand and the α4 helix of the receiver domains of RRs (3, 19, 40). Hybrid HKs that have tethered receiver domains are not under the same selective pressure to maintain

specificity residues for their tethered domains as some specificity is provided by spatial localization (1, 41). HK transmitter phosphatase activity has been implicated in buffering the effects of crosstalk via the removal of phosphoryl groups that are attached to RRs through cross-phosphorylation (14, 42–44). HKs also have three homodimerization specificity residues that maintain the formation of homodimeric HKs and prevent the formation of HK heterodimers (45). These three key residues are located within the DHp domain at the base of the four helix bundle formed by the α1 and α2 helices (38, 45).

Examples of crosstalk are becoming more commonplace, although many examples found in the literature only demonstrate crosstalk when components of the original signal transduction pathway are removed, or when the HK is overexpressed resulting in a non-native signal transduction pathway (14). There are instances of interactions between HKs and RRs in which multiple HKs phosphorylate one RR (termed a many-to-one relationship) and in which one HK phosphorylates multiple RRs (termed a one-to-many relationship) (14). Recently multikinase networks (MKNs) have been discovered in which multiple HKs interact with each other resulting in a more complex signal transduction pathway (46, 47). Phosphotransfer between HKs results in a MKN, such as in the case of the early sporulation pathway in *Myxococcus xanthus* in which the hybrid HK EspA phosphorylates the receiver domain of the hybrid HK EspC resulting in the proteolysis of the developmental regulatory protein MrpC through an unknown factor, which overall disrupts sporulation (47). There are several examples of direct interactions between HKs which result in a MKN (36, 46–51). In *Pseudomonas aeruginosa* the MKN controlling the switch between a motile invasive lifestyle and a sessile biofilm lifestyle, is facilitated by several such interactions (36, 46, 48–51). The hybrid HK RetS binds and inhibits the unorthodox HK GacS but is in turn blocked through binding of the hybrid HK PA1611, whereas GacS also

interacts with the hybrid HK LadS, which funnels additional phosphates into the GacS/GacA system to counteract RetS.

Two-Component System and Phosphorelay Protein Evolution

Proteins evolve through point mutations (substitutions, insertions, and deletions) and rearrangements or recombinations (gene fusion, gene fission, gene duplication, and retrotransposition) of the DNA that encodes them (52–54). The fate of the mutation depends on whether the mutation is deleterious, neutral, or advantageous. Deleterious mutations are removed from the population via purifying selection (53). Neutral mutations may be maintained within the population providing time for further mutation and are subject to genetic drift (53). Advantageous mutations tend to become stabilized within a population via positive selection, although genetic drift can result in the removal of advantageous mutations from a small population (53).

Gene duplication followed by divergence, or lineage-specific expansion, is the predominant mechanism by which new genes emerge and it is one of the primary mechanisms by which bacterial signal transduction proteins have evolved, in particular it has resulted in the paralogous families of histidine kinases and response regulators (38, 53, 55, 56). Protein redundancy immediately after duplication allows for mutations to arise in one or both of the duplicated genes that result in the divergence of the proteins (38, 55, 57). For example, the Pho2 and Pho3 TCSs in *M. xanthus* have arisen via gene duplication and divergence (1). Pho2 and Pho3 appear to have redundant roles in *M. xanthus*, as both respond to phosphate limitation via the regulation of phosphatase expression and secretion, and both regulate multicellular development (58, 59). The HKs PhoR2 and PhoR3 also maintain the ability to cross

phosphorylate each other's RR *in vitro*, demonstrating that they have not diverged to the point where they are no longer able to communicate (1). The Nar system in *Escherichia coli* is also thought to have evolved via gene duplication and divergence (1). *In vitro* phosphorylation assays have demonstrated the cross phosphorylation by the HK NarX for its non-cognate RR NarP and the cross phosphorylation by the HK NarQ for its non-cognate RR NarL (1).

Horizontal gene transfer (HGT) is another mechanism by which bacterial signal transduction proteins have evolved (38, 56). Genes acquired by HGT tend to maintain the same functionality as their orthologous counterparts due to the lack of shared sequence space within an individual organism (56). Many horizontally transferred genes tend to be transferred with other genes in their operon, or those that are neighbors. Horizontally transferred genes may be incompatible with the new host due to differences in codon usage or the host may not contain all genes necessary for a functional unit (53). The VanR/VanS TCS in the genus *Enterococcus* which responds to vancomycin is encoded on a plasmid and is thought to have been acquired through HGT (38). The SsrA/SsrB TCS in *Salmonella* which promotes the lifestyle switch from that of an extracellular to an intracellular human pathogen is encoded by a chromosomal pathogenicity island and is believed to have been acquired through HGT (38, 60).

The CA domain has a common tertiary structure that is similar to the ATP binding domains of the GHKL (gyrase, heat shock protein 90, histidine kinase, MutL DNA mismatch repair protein) superfamily ATPases, suggesting that catalytic region of bacterial HKs has evolved from this family of enzymes (38, 61, 62). The ATP binding pocket is still conserved between both families and allows for ATP to bind within the pocket while the γ phosphate of ATP is sticking out of the pocket poised for the hydrolysis reactions (61). There are no known evolutionary homologs of RR proteins (38).

Hybrid and unorthodox HKs are believed to result from the fusion of genes encoding an HK and an RR (1, 63, 64). This could occur through the fusion of operonic HK and RR genes or via HK and RR genes that are located in different positions on the chromosome (1, 64). The kinase region and receiver domains of many hybrid HKs have phylogenetically distinct origins lending support to the belief that hybrid HKs evolve via gene fusion (64). Hybrid HKs have also been acquired through duplication and divergence of genes encoding pre-existing hybrid HKs (1, 64). Similarly, sensory domains are predicted to be acquired via gene fusion events (1, 64).

Pseudomonas aeruginosa

Pseudomonas aeruginosa is a ubiquitous Gram-negative bacterium, found in terrestrial, aquatic, plant and animal environments and like many Pseudomonads, *P. aeruginosa* is highly adaptable to changing environmental conditions (4, 12, 65, 66). 9.3% of the open reading frames of *P. aeruginosa* encode regulatory proteins (48, 65, 67). *P. aeruginosa* is an opportunistic pathogen of plants and animals, including humans (65, 68). The ability of *P. aeruginosa* to cause both acute and chronic infections in immunocompromised individuals is of great medical concern (68–70). *P. aeruginosa* has two distinct lifestyles that result in two distinct infection states within a human host. The acute infection state is characterized by a motile invasive lifestyle in which *P. aeruginosa* promotes host cell cytotoxicity, evades host defenses and spreads rapidly (68, 70–72). Bacteremia caused by *P. aeruginosa* infection of severe burn wounds, commonly leads to sepsis and death (68). Ventilator-associated pneumonia, a nosocomial *P. aeruginosa* infection, often results in a systemic infection followed by death (70, 73). These acute infections are mediated by virulence factors including the type three secretion system (T3SS), the type two secretion system (T2SS), flagella, and type four pili (T4P) (66, 74,

75). The T3SS necessary for acute infection is a multi-protein complex that delivers effector proteins into a host cell (71, 72, 76). Once inside the host cell, effector proteins interact with and alter the function of host proteins, resulting in modifications to the host cell that are cytotoxic and that enable *P. aeruginosa* to evade phagocytosis (71, 76, 77). Similarly, the previously mentioned T2SS used in acute infections is a multiprotein complex that delivers effectors, typically toxins, from the bacterial cytoplasm to the extracellular environment where they promote host cell cytotoxicity (66, 78). The above mentioned bacterial flagellum is a multiprotein assembly that spans the cell envelope and enables swimming and swarming motility via rotational propulsion (79, 80). The T4P machinery is a multiprotein complex that spans the cell envelope and enables the extension and retraction of the pilus filament which is the hallmark of twitching motility via the polymerization and depolymerization of pilin subunits (81).

Conversely, the chronic infection state is characterized by a sedentary lifestyle in which *P. aeruginosa* exists in a biofilm (82). Biofilms are composed of an assemblage of microorganisms surrounded by an extracellular matrix (83). The matrix of *P. aeruginosa* biofilms is primarily composed of exopolysaccharides and, to a lesser extent, proteins, lipids and nucleic acids (82, 84, 85). The exopolysaccharides that comprise the *P. aeruginosa* biofilm are Psl, Pel and alginate, although alginate plays a significant role in biofilm formation in clinical mucoid strains but not in wildtype laboratory or environmental strains (82, 83, 85, 86). The extracellular matrix affords protection to the microorganisms within the biofilm, in particular it provides protection against the host immune response and antimicrobials (87). The majority of individuals with cystic fibrosis, an autosomal recessive disorder in which mutations in the cystic fibrosis transmembrane conductance regulator (*CFTR*) gene result in a nonfunctional chloride ion channel protein, eventually die due to chronic *P. aeruginosa* lung infections (68, 69).

P. aeruginosa has intrinsic resistance to many antibiotics. The low permeability of the outer membrane which is comprised of an inner leaflet of phospholipids and an outer layer of lipopolysaccharide (LPS) helps *P. aeruginosa* evade many antimicrobial agents, and ABC-multidrug transporters and multidrug efflux pumps remove antibiotics from the cell (85, 88, 89). *P. aeruginosa* also possesses periplasmic β-lactamases which cleave and inactivate β-lactam antibiotics (penicillins, carbapenems, cephalosporins, monobactams) (88–90). Biofilm matrix materials restrict the ability of antimicrobials to reach the cells, and those cells within the interior of the biofilm have a reduced metabolic rate which reduces the effectiveness of those antimicrobials that do reach them (85, 90).

Biofilm Formation in *Pseudomonas aeruginosa*

Biofilms are assemblages of microbial cells associated via cell-to-cell attachments and via matrix components such as exopolysaccharides, extracellular DNA (eDNA), lipids and proteins (85). The biofilm lifestyle offers numerous benefits to the cells living within them (i.e. nutrient proximity, proximity for the exchange of genetic material, protection from environmental stresses, protection from protozoa and host immune system, protection from antibiotics) (91–94). *P. aeruginosa* forms a complex biofilm via the progression from motile-planktonic cells through a series of biofilm stages to the final complex macrocolony biofilm (95). Chemotaxis and flagellar motility direct planktonic *P. aeruginosa* to a surface (94). Initial reversible attachment occurs via the polar flagellum which acts as a tether to the surface (92, 96, 97). This is followed by surface-associated motility (swarming and twitching motility) that enables the bacteria to locate a suitable niche for biofilm formation (94, 97, 98). A defect in either flagellar based motility or T4P based motility at this stage inhibits biofilm formation (94).

Two flagellar stators, MotAB and MotCD are necessary during the initial reversible attachment of static biofilm formation (96). During this stage a subpopulation of cells produces exopolysaccharides needed for surface attachment and a subpopulation of cells utilizes surface exploration behaviors (91).

During the next stage of biofilm development, *P. aeruginosa* attaches to the surface irreversibly through the formation of a monolayer of cells that attachvia their horizontal axes (99). T4P are responsible for cell-to-cell attachment and cell-to-surface attachment (97). The production of the exopolysaccharides Psl and Pel, and eDNA are upregulated, as the matrix begins to form (92). Psl and Pel are uncharged and cationic polysaccharides respectively, that are responsible for cell-to-surface and cell-to-cell attachment providing structural support for the biofilm matrix (82, 87, 100, 101). Pel also binds and crosslinks eDNA produced by *P. aeruginosa* and host produced eDNA that is located in sputum within the lungs (75, 100). The crosslinking of Pel with eDNA results in aggregates that are less susceptible to two common treatments for cystic fibrosis lung infections; the antibiotic tobramycin and the treatment of the host with DNAse (100). During the next stage of biofilm development, *P. aeruginosa* forms a microcolony, which is a multilayer biofilm in which cell-to-cell attachments predominate. Matrix elaboration occurs, in which Psl, Pel, eDNA and proteins are secreted to form the extracellular matrix. CdrA, a 150 kDa protein, adheres to Psl in the extracellular matrix, with ensuing cell aggregation and structural support as the microcolony forms (92, 101). The lectin, LecB also binds to Psl providing structural support for the forming microcolony (102). As the biofilm increases in complexity, fluid filled channels linking the interior of the biofilm to the exterior provide a mechanism to introduce nutrients and oxygen into the interior of the biofilm, as well act as a means of waste removal (75, 103, 104). eDNA provides a grid-like structure and

rhamnolipids provide surfactant which allow T4P-mediated motility to move cells vertically and expand the biofilm into the final stage, the mature biofilm, the macrocolony stalk-like structure (95, 105).

Cells can dissociate from the biofilm and enter the planktonic state as a continual process throughout biofilm development, both due to cellular dissociation and due to the passive process of sloughing (106). Eventually, most biofilms undergo dissolution, the process whereby the majority of cells within the biofilm dissociate. During dissolution, induction of flagellar mediated motility gene expression is increased as is gene expression of hydrolases needed to degrade the biofilm matrix (107). While there is an increase in flagella-related gene expression during biofilm dissolution, flagella do appear to be produced throughout all of the stages of biofilm development (106). The production of flagella is energetically costly and may provoke an immune response, so Ozer et al. speculated that flagella may provide a role in the structural support of the growing biofilm (106). There are several dissolution signals; lysis of an interior population of cells, excess rhamnolipid production, oxygen depletion and byproducts of anaerobic respiration (107).

Virulence Regulation in *Pseudomonas aeruginosa*

Quorum Sensing Regulates the Motile to Sessile Switch

Quorum sensing is a form of bacterial cell-to-cell communication that allows bacteria to regulate gene expression based on their surrounding population density (108). Quorum sensing occurs via the production and sensing of small molecules termed autoinducers (108). In Gram negative bacteria autoinducers are synthesized via autoinducer synthases; the prototypical autoinducer synthase is LuxI (108). In Gram negative bacteria, once synthesized, autoinducers

freely diffuse out of the cell and from the environment into neighboring cells. As the concentration of autoinducers increases due to heightened cell density there is a concomitant increase in binding between autoinducers and the cytoplasmic autoinducer receivers, which activates the autoinducer receivers as transcriptional regulators; the prototypical autoinducer receiver is LuxR (108).

P. aeruginosa uses four quorum sensing systems to regulate gene expression, in particular to regulate gene expression related to virulence and biofilm formation. LasI is a LuxI type autoinducer synthase that produces the autoinducer, *N*-3-oxo-dodecanoyl homoserine lactone, which activates the LuxR type receiver, LasR (109–111). Activated LasR transcriptionally upregulates expression of genes associated with eDNA vesicular release and T4P-mediated motility, the exopolysaccharides Pel and Psl and virulence factors not associated with the T3SS (elastases, proteases, pyocyanin, exotoxin A, hydrogen cyanide), all necessary for biofilm formation and maturation (108, 110). LasR also upregulates expression of the genes necessary in the secondary quorum sensing system, the RhlI/RhlR system (109, 111). RhlI is a LuxI type autoinducer synthase that synthesizes the autoinducer butyryl homoserine lactone which activates RhlR, a LuxR type receiver (109–111). RhlR activates transcription of genes associated with rhamnolipid production and T4P-mediated motility, both necessary for biofilm maturation, as well as upregulates pyocyanin and hydrogen cyanide synthesis (85, 108, 110). LasR upregulates transcription of the genes necessary for production of the autoinducer for the third quorum sensing system, the PQS system (111). PqsABCDE and PqsH synthesize the autoinducers, 2-heptyl-3-hydroxy-4-quinolone also termed *Pseudomonas* quinolone signal (PQS) and 2-heptyl-4-hydroxyquinolone also termed HHQ which in turn activate the receiver PqsR (109, 110, 112). PqsR upregulates expression of genes associated with eDNA vesicular release,

cellular autolysis, and hydrolases (proteases, lipases, glycoside hydrolases, elastases), rhamnolipids and pyocyanin all needed during the maturation and dissolution of the *P. aeruginosa* biofilm (85, 113). PQS appears to play a role in *P. aeruginosa* virulence outside of its quorum sensing capabilities. PQS acts as an iron chelator, possesses antimicrobial activity, produces reactive oxygen species that result in oxidative stress to host immune cells and epithelial cells, and produces immunomodulatory effects in host cells (113). *P. aeruginosa* has a fourth, newly discovered quorum sensing system termed the IQS quorum sensing system (112, 113). The autoinducer for the IQS system is 2-(2-hydroxyphenyl)-thiazole-4-carbaldehyde which the synthesis of is a contentious issue as some research suggests that it is synthesized via the gene products of *ambBCDE* and other research suggests that it is synthesized as a byproduct of the siderophore pyochelin synthesis (112, 114–117). Current research suggests that the IQS system is activated by LasR as well as phosphate limitation (112, 115). Similar to PQS, IQS plays a role in *P. aeruginosa* virulence outside of its quorum sensing capabilities, as IQS induces host cell apoptosis (114).

c-di-GMP Regulates the Motile to Sessile Switch

Cyclic diguanylate monophosphate (c-di-GMP) is a bacterial intracellular signaling molecule implicated in the motile-to-sessile switch in *P. aeruginosa*, with low c-di-GMP levels associated with the motile lifestyle and high c-di-GMP levels associated with the sessile, biofilm lifestyle (92, 93, 98, 118). A c-di-GMP control module comprises a diguanylate cyclase that catalyzes the cyclization of two guanylate monophosphate (GMP) molecules into c-di-GMP, one or more phosphodiesterases, which catalyze the hydrolysis of c-di-GMP into the linear molecule 5’-phosphoguanylyl-(3’5’)-guanosine (pGpG) or into two GMP molecules, and the effector

protein which is activated or deactivated by c-di-GMP binding (93, 118). *P. aeruginosa* has up to 41 diguanylate cyclases and phosphodiesterases depending on the strain (92, 93). How can a global signaling molecule like c-di-GMP act at a local level and avoid crosstalk? Avoidance of crosstalk is achieved through three mechanisms, temporal regulation, effector binding affinity, and spatial localization. In temporal regulation, differential gene expression, translation, and/or activation of diguanylate cyclases and phosphodiesterases can alter which cyclic-di-GMP control modules are active at one time (118). C-di-GMP effector binding affinity varies as does affinity among diguanylate cyclases for c-di-GMP inhibition via the diguanylate cyclase inhibitory site (I-site) (118). In *Salmonella enterica*, YcgR (flagellar clutch protein with the homologue FlgZ in *P. aeruginosa*) has a 43-fold higher affinity for c-di-GMP than BscA (a protein in part responsible for production of exopolysaccharides needed for progression into a biofilm) (119). This disparity in c-di-GMP binding affinity allows YcgR to be activated at lower concentrations of c-di-GMP during the early stages of transitioning to a sessile lifestyle, whereas BscA is activated at higher concentrations of c-di-GMP during later stages of biofilm formation. Spatial localization of diguanylate cyclases and phosphodiesterases with their cognate c-di-GMP effector proteins can result in avoidance of crosstalk (16). In *P. aeruginosa* the diguanylate cyclase and response regulator WspR forms clusters when phosphorylated allowing for the localized production of c-di-GMP (67).

During the initial stage of biofilm development, *P. aeruginosa* reversibly attaches to a surface via its polar flagellum. Surface interaction results in activation of the Wsp system (through an unknown mechanism) (75, 120). The diguanylate cyclase WspR increases the level of c-di-GMP which increases expression of the *psl* and *pel* operons, thus beginning the processes of cell-to-surface attachment and cell-to-cell attachment (92, 93, 118, 121). C-di-GMP binding

inhibits the ability of FleQ to activate expression of flagellar motility genes and inhibits the ability of FleQ to repress expression of the *pel* operon (83, 92, 93, 122, 123). SadB, a c-di-GMP binding protein has a higher affinity for c-di-GMP than does FleQ and upon activation via c-di-GMP SadB negatively regulates flagellar mediated motility (99). FlgZ (YcgR in *E. coli* and *S. enterica*) acts as a flagellar clutch interacting with FliG, the flagellar motor protein, and MotA, the flagellar stator protein, to inhibit flagellar rotation under high c-di-GMP conditions (92). T4P production is promoted upon surface contact which correlates with an increase in c-di-GMP (124).

During the irreversible attachment stage of biofilm development inhibition of the post-transcriptional regulator RsmA via the GacS/GacA phosphorelay promotes translation of the diguanylate cyclases, SiaD, GcbA and SadC as well as synthesis of the exopolysaccharides Psl and Pel (67, 93). SiaD promotes production of biofilm matrix components (93). GcbA promotes cell-to-cell and cell-to-surface attachment (93). The diguanylate cyclase, SadC is activated by the exopolysaccharides Psl and Pel, and downregulates swarming motility (16, 93). The diguanylate cyclase RoeA enhances the production of Pel through a unknown mechanism (16, 92, 93). PelD, an inner membrane protein necessary for the transport of Pel to the extracellular environment is activated via c-di-GMP (125, 126).

The diguanylate cyclase WspR is also implicated in biofilm maturation via increased expression of the *psl* and *pel* operons (92, 93, 118). SiaD and SadC are responsible for increased expression of the c-di-GMP binding protein CdrA (92). CdrA adheres to Psl in the extracellular matrix, resulting in aggregation of cells and biofilm microcolony and macrocolony formation (92, 101). Dispersal of the biofilm community is triggered by low levels of c-di-GMP, which is precipitated by the activation of phosphodiesterases. The phosphodiesterase DipA is predicted to

respond to nutrient limitation via the promotion of flagella-mediated motility and the phosphodiesterase RbdA is predicted to respond to anoxic conditions within the biofilm (92, 93).

A Role for cAMP in Biofilm Formation

The second messenger cyclic adenosine monophosphate (cAMP) is known to regulate carbon catabolism repression in bacteria (127). cAMP has also been implicated in biofilm formation and virulence in many bacteria, although the effect varies depending on the bacterial species (127–129). In *P. aeruginosa* cAMP promotes acute virulence via binding to the CRP family protein transcription factor Vfr (virulence factor regulator) (128–130). cAMP-Vfr regulates expression of genes necessary for acute virulence factors such as exotoxin A, the type three secretion system and its effectors, the type two secretion system, type four pili and proteases (66, 76, 130). While overall, in *P. aeruginosa* an increase in cAMP results in disruption to later stage biofilms and enhancement of acute virulence factors, cAMP does appear to enhance biofilm production at the initial stage of biofilm development (127). At the initial stage of biofilm development when the bacterial cell attaches to the surface via its polar flagellum, the adenylate cyclases CyaA and CyaB are activated to produce cAMP (127). cAMP bound to Vfr inhibits expression of *fleQ*, which encodes the regulator for flagellar biosynthesis thus resulting in downregulation of flagellar biosynthesis (127). cAMP-Vfr activates expression of genes necessary for type four pili, which act in cell-to-cell and cell-to-surface adhesion in the initial stages of biofilm development (127). cAMP production is inhibited by heightened levels of c-di-GMP which increase as the biofilm progresses, resulting in the decrease of cAMP levels as the biofilm matures (129).

The Gac/Rsm Pathway Regulates the Motile to Sessile Switch

The Gac/Rsm (BarA/UvrY in *E. coli*) pathway is a TCS signal transduction pathway conserved in γ-proteobacteria (131). In γ-proteobacteria, the Gac/Rsm pathway controls expression of 1-5 genes that encode sRNAs that are characterized by repeated GGA motifs (132). The GGA motifs are essential for binding and sequestering small, dimeric RNA binding proteins of the RsmA (CsrA) family (132, 133). The RsmA family of proteins are translational repressors of certain mRNAs that contain an RsmA/CsrA binding site at or near the Shine Dalgarno sequence. The output of the Gac/Rsm pathway varies among the γ-proteobacteria, with the management of carbon storage and expression of virulence factors being the most prominent outputs (131).

The Gac/Rsm pathway allows *P. aeruginosa* to switch between the acute infection state characterized by a motile invasive lifestyle and the chronic infection state characterized by a sessile biofilm lifestyle (66, 93, 134). At the head of the pathway sits the GacS/GacA phosphorelay. Phosphorylated GacS activates GacA via phosphorylation (48). The phosphorylation of GacA results in conformational changes that enable it to act as a transcriptional activator of two genes encoding the sRNAs, RsmY and RsmZ (Fig. 1.2) (131). RsmY and RsmZ bind and inhibit the posttranscriptional regulator RsmA (Fig. 1.2) (135). The RsmA regulon comprises over 500 genes, many of which encode virulence factors (136). When RsmA is sequestered the T3SS and T2SS are downregulated and the production of the exopolysaccharides Psl and Pel is upregulated, as are the Rhl and Las quorum sensing systems and the diguanylate cyclases SiaD, GcbA and SadC resulting in a chronic infection state (66, 137). Conversely, active RsmA results in an acute infection state (66, 137).

HKs GacS, LadS and RetS Interact to Tune Virulence Gene Expression

The unorthodox HK GacS (global activator for antibiotics and cyanide synthesis) has a periplasmic sensory PDC/PAS domain, followed by the HK region comprising the DHp and CA domains, a receiver domain and an Hpt domain (Fig. 1.3) (26, 65, 134, 138, 139). While the PDC/PAS domain suggests that GacS may sense metabolites (in particular carboxylic acids, such as in the case of the citrate sensing PDC/PAS domain of CitA in *Klebsiella pneumoniae* and the C_4 dicarboxylate sensing domain of DcuS in *E. coli*), oxygen, redox potential or light, the ligand for GacS remains elusive (5, 24–27, 139, 140).

GacS is reciprocally regulated by two hybrid sensor kinases, LadS and RetS. Through a unique signal transduction pathway, LadS enhances the phosphotransfer activity of GacS via the phosphorylation of the Hpt domain of GacS (141, 142). LadS contains a periplasmic sensory 7-transmembrane receptor with DISM2 (7 TMR-DISM2) domain, followed by a 7-transmembrane receptor with DISM 7-transmembrane region (7 TMR-DISM-7TM), a histidine kinase region comprising the DHp and CA domains and a receiver domain (Fig. 1.3) (142). While the 7 TMR-DISM2 domain suggests that LadS may sense a carbohydrate, LadS is activated by calcium binding to the 7 TMR-DISM2 domain (21, 142, 143). It is predicted that an elevated concentration of calcium signals a transition from an acute infection state to a chronic infection state in a human host, as heightened levels of calcium are observed in the chronic infection state and reduced calcium levels are observed in an acute infection state (143).

In counteraction to LadS, RetS (regulator of exopolysaccharide and type three secretion) has been shown to inhibit GacS via three distinct mechanisms (46, 48, 70, 135, 144). RetS possesses a periplasmic sensory 7 TMR-DISM2 domain, followed by a 7 TMR-DISM-7TM, a histidine kinase region comprising the DHp and CA domains, and a tandem of receiver domains,

each with a conserved aspartate residue (Fig. 1.3) (49, 142). In the first mechanism of GacS inhibition, RetS dephosphorylates the DHp domain of GacS via its C-terminal receiver domain, resulting in RetS outcompeting GacS's own receiver domain in the phosphotransfer reaction (46). In the second inhibitory mechanism, the HK region of RetS dephosphorylates the receiver domain of GacS via transmitter phosphatase activity in which a conserved threonine residue four residues C-terminal to the conserved catalytic histidine residue is required (46). RetS also inhibits GacS autophosphorylation via a direct interaction between the DHp domains of RetS and GacS at the canonical homodimerization interface (36, 46, 48, 145).

RetS is a unique hybrid histidine kinase in that it does not possess the canonical kinase activity of bacterial HKs (48). Conserved residues involved in ATP binding and hydrolysis located in the N, G1, F and G2 box motifs were found to lack conservation in RetS (36, 46). The canonical ATP binding pocket has collapsed in RetS, resulting in a lack of ATP binding and thus a lack of autophosphorylation (36). RetS does maintain conserved residues that are critical to transmitter phosphatase activity (46).

The 7 TMR-DISM2 domain of RetS possesses a β-sandwich fold that is distinctive of the ligand binding domains of carbohydrate binding proteins, suggesting that RetS may interact with a polysaccharide such as Psl or Pel (142, 144). A component of kin cell lysate (cell lysate from neighboring *P. aeruginosa*) binds to the periplasmic domain of RetS resulting in the relief of GacS inhibition (146). Host cell mucins also bind to the sensory domain of RetS resulting in inhibition to GacS (147). This suggests that RetS may possess the ability to respond to multiple signals that present information regarding the virulence state of *P. aeruginosa*.

The current model for the interaction between RetS and GacS involves RetS binding GacS during the motile-invasive lifestyle inhibiting GacS autophosphorylation and enabling the

two dephosphorylating mechanisms of RetS to further inhibit GacS (46). The formation of the heteromeric HK region likely provides the spatial arrangement and specificity needed for the two dephosphorylating mechanisms. The reasons for the existence of three distinct mechanisms are not fully clear. However, the initial inhibition of autophosphorylation may not be sufficient because either some *trans* autophosphorylation occurs even in the presence of RetS or GacS may be capable of both *cis* and *trans* autophosphorylation. Moreover, the second mechanism may be required to counteract the phosphorylation of GacS by LadS, which circumvents the other two mechanisms.

GacS, LadS and RetS are Part of a Multikinase Network Mediating the Motile to Sessile Switch

RetS, GacS and LadS are part of a much larger multikinase network (MKN) (46, 47). RetS itself is inhibited via the direct binding of the hybrid HK PA1611 at an interface that is distinct from the canonical homodimerization DHp-DHp interface, between the DHp domain of PA1611 and the CA domain of RetS (Fig. 1.2) (50, 51, 67). RetS interacts with the histidine phosphotransferase protein HptB (Fig. 1.2) (67, 135, 148). The hybrid HKs PA1611, ErcS and SagS also interact with HptB via phosphotransfer (Fig. 1.2) (149, 150). Phosphorylated HptB in turn transphosphorylates its cognate RR HsbR. Phosphorylated HsbR acts as a phosphatase toward the anti-anti-sigma factor HsbA (Fig. 1.2) (150, 151). When HsbA is dephosphorylated it sequesters the anti-sigma factor FlgM and this sequestration of FlgM indirectly upregulates flagellar-related gene expression via the release of the sigma factor FliA resulting in the promotion of the motile invasive lifestyle (150, 151). Conversely, when HsbA is phosphorylated it activates expression of the diguanylate cyclase HsbD which produces c-di-GMP that results in

the upregulation of expression of the sRNA RsmY ultimately resulting in promotion of the sessile biofilm lifestyle and inhibition of the motile invasive lifestyle (Fig. 1.2) (150). SagS also inhibits the hybrid HK BfiS under planktonic conditions and activates BfiS under biofilm conditions (152, 153). Uninhibited BfiS transphosphorylates its cognate RR BfiR which in turn downregulates expression of the sRNA RsmZ. Remarkably, the BfiS/R phosphorelay is responsible for promotion of the transition to the irreversible biofilm stage (152–154). While the majority of evidence suggests that a downregulation of the sRNAs RsmY and RsmZ result in an inhibition to biofilm formation, Petrova and Sauer (2010) demonstrated that reduced levels of RsmZ are essential for biofilm development post irreversible attachment (152, 153). This suggests that the regulation of the sessile biofilm lifestyle is much more complex than an on/off switch but entails the integration of multiple signals that result in variable outputs. This signal transduction pathway, which controls the switch between the motile invasive lifestyle and the sessile biofilm lifestyle, is one of the most complex examples of a multikinase network to date (Fig. 1.2) (47).

Research Goals

The mechanism by which RetS inhibits GacS autophosphorylation was previously unknown. Inhibition of GacS autophosphorylation was initially proposed to occur via the formation of a RetS-GacS heterodimer (48). Prior work in our lab demonstrated that RetS-GacS binding occurs between the DHp domains of RetS and GacS (36). Mancl et al. also determined that binding between the cytoplasmic region of RetS and the cytoplasmic region of GacS did not disrupt the GacS homodimer (36). This led Mancl et al. to propose a model in which RetS and GacS DHp domains bind at an interface that is distinct from the homodimeric DHp interface, and

that the binding between RetS and GacS results in a dimer of dimers or a higher order oligomer (36). The aim of this research was to determine the mechanism by which RetS inhibits GacS autophosphorylation through the identification of the RetS DHp-GacS DHp interface using a structural examination of a RetS-GacS co-complex. Identification of the RetS DHp-GacS DHp interface provides insight into the role of RetS-GacS binding in controlling output through the Gac/Rsm pathway. The Gac/Rsm pathway is the pathway through which *Pseudomonas aeruginosa*, an opportunistic human pathogen, switches between an acute infection state characterized by a motile invasive lifestyle and chronic infection state characterized by a sessile biofilm-associated lifestyle. The interaction between RetS and GacS is key to understanding how *P. aeruginosa* mediates its lifestyle and infection state.

Figures

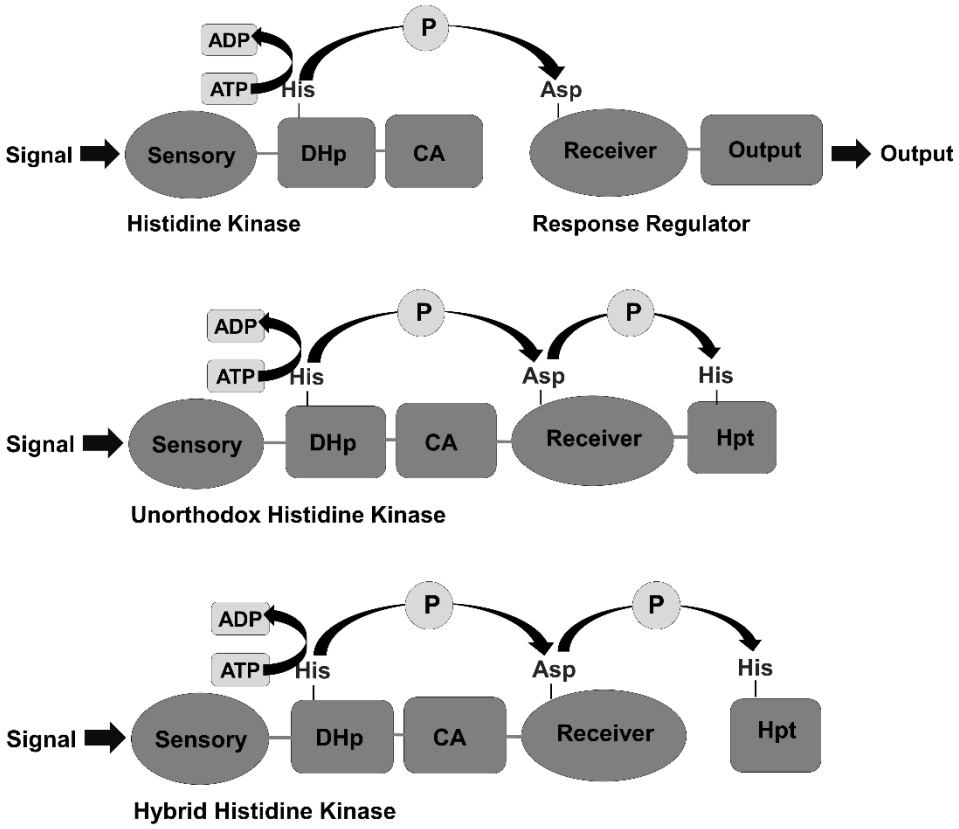

Figure 1.1. Two component system (TCS), unorthodox histidine kinase andhybrid histidine kinase. Phosphate signal transmission via a TCS from the histidine kinase (HK) to the response regulator (RR). Sensory domain stimulation results in ATP dependent autophosphorylation of the conserved catalytic histidine residue. The phosphate group is then transferred to the conserved aspartate residue on the receiver domain of the RR resulting in a conformational change to the output domain that alters the functionality of the RR (top). Phosphate signal transmission within an unorthodox HK and a hybrid HK. Sensory domain stimulation results in ATP dependent autophosphorylation of the conserved catalytic histidine residue. The phosphate group is then transferred to the conserved aspartate residue of the HK's receiver domain and from there it is transferred to the conserved histidine of the Hpt domain or protein prior to phosphotransfer to the RR (bottom).

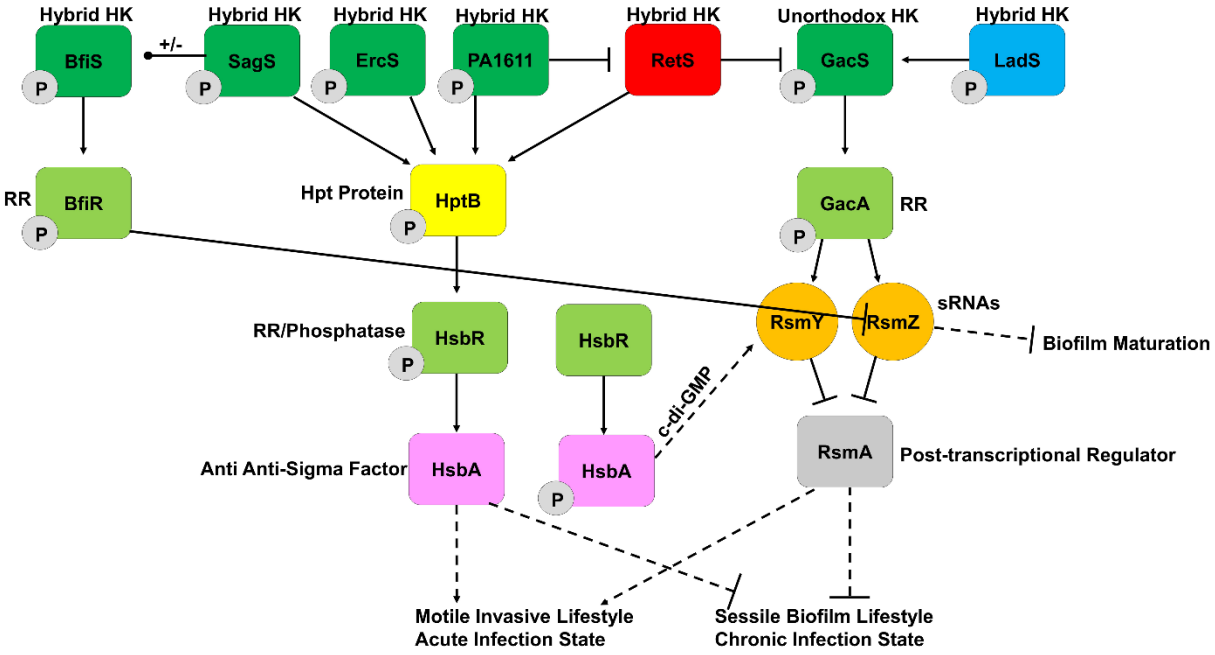

Figure 1.2. Multikinase network controls switch between motile invasive lifestyle and sessile biofilm lifestyle. GacS undergoes autophosphorylation and in turn activates its cognate RR GacA via phosphotransfer (48). GacA acts as a transcriptional activator of two sRNAs, RsmY and RsmZ (131). RsmY and RsmZ bind to and sequester the posttranscriptional regulator RsmA (135). Sequestration of RsmA results in upregulation of the sessile biofilm lifestyle and the downregulation of the motile virulent lifestyle. RetS inhibits GacS through three distinct mechanisms, two dephosphorylating mechanisms and via a direct interaction that inhibits GacS autophosphorylation (46, 48, 135). LadS further activates GacS via the direct transfer of phophates to the Hpt domain of GacS (141, 142). PA1611 inhibits RetS through a direct interaction. PA1611, ErcS and SagS transphosphorylate HptB (150). HptB in turn transphosphorylates the RR HsbR activating it as a phosphatase for the anti anti-sigma factor HsbA (150). When HsbA is not phosphorylated it promotes the motile invasive lifestyle (150). When HsbA is phosphorylated it in turn activates a diguanylate cyclase, HsbD, which produces c-di-GMP that activates expression of the sRNA RsmY, thus promoting the sessile biofilm lifestyle (150). SagS also inhibits the HK BfiS during the planktonic lifestyle and activates BfiS during the biofilm lifestyle (152). While the majority of evidence suggests that a downregulation of the sRNAs RsmY and RsmZ result in an inhibition to biofilm formation, Petrova and Sauer

(2010) have demonstrated that reduced levels of the sRNA RsmZ are essential for biofilm maturation post irreversible attachment (152, 153).

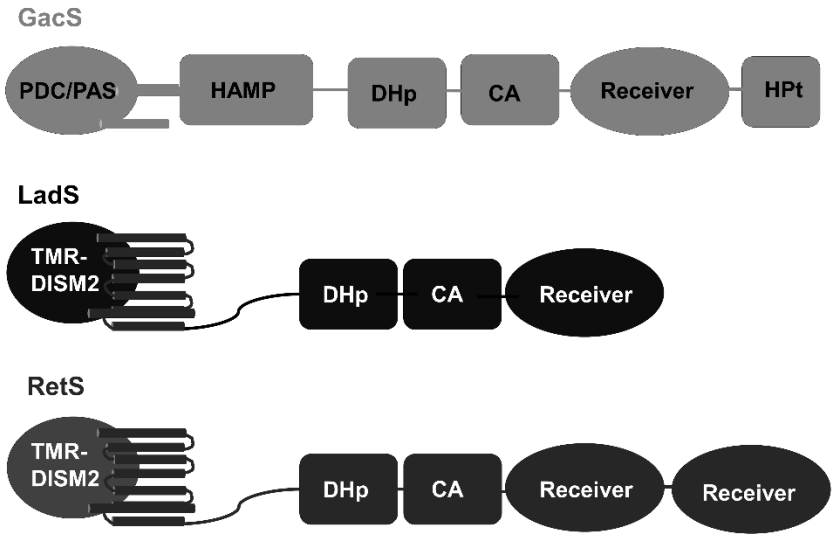

Figure 1.3. Domain organization of GacS, LadS and RetS. GacS comprises a periplasmic PDC/PAS sensory domain (26). Following the PDC/PAS sensory domain is the single transmembrane region followed by a HAMP domain, the HK region containing the DHp domain and the CA domain, a receiver domain and an Hpt domain (48). LadS contains a periplasmic 7 TMR-DISM2 domain, followed by a 7 TMR-DISM-7TM region, a histidine kinase region comprised of a DHp domain and a CA domain, and a receiver domain (142). RetS possesses a periplasmic sensory 7 TMR-DISM2, followed by a 7 TMR-DISM-7TM region, a histidine kinase region comprised of a DHp domain and a CA domain, and two tandem receiver domains (49, 142).

Chapter 2

RetS inhibits *Pseudomonas aeruginosa* Biofilm Formation by Disrupting the Canonical Histidine Kinase Dimerization Interface of GacS

Kylie M. Ryan Kaler[1], Jay C. Nix[2], Florian D. Schubot[1]

[1]Department of Biological Sciences, Virginia Polytechnic Institute and State University, Blacksburg, VA, USA; [2]Advanced Light Source, Lawrence Berkeley National Laboratory, Berkeley, CA, USA

This work has been published on September 13, 2021 in *The Journal of Biological Chemistry*:

> Ryan Kaler, K. M., Nix, J. C., and Schubot, F. D. (2021) RetS inhibits *Pseudomonas aeruginosa* biofilm formation by disrupting the canonical histidine kinase dimerization interface of GacS. *J. Biol. Chem.* **297**, 101193

Abstract

Bacterial signaling histidine kinases (HKs) have long been postulated to function exclusively through linear signal transduction chains. However, several HKs have recently been shown to form complex multikinase networks (MKNs). The most prominent MKN, involving the enzymes RetS and GacS, controls the switch between the motile and biofilm lifestyles in the pathogenic bacterium *Pseudomonas aeruginosa*. While GacS promotes biofilm formation, RetS counteracts GacS using three distinct mechanisms. Two are dephosphorylating mechanisms. The third, a direct binding between the RetS and GacS HK regions, blocks GacS autophosphorylation. Focusing on the third mechanism, we determined the crystal structure of a co-complex between the HK region of RetS and the dimerization and histidine phosphotransfer (DHp) domain of GacS. This is the first reported structure of a complex between two distinct bacterial signaling HKs. In the complex the canonical HK homodimerization interface is replaced by a strikingly similar heterodimeric interface between RetS and GacS. We further demonstrate that GacS autophosphorylates in *trans*, thus explaining why the formation of a RetS-GacS complex inhibits GacS autophosphorylation. Using mutational analysis in conjunction with bacterial two-hybrid and biofilm assays we not only corroborate the biological role of the observed RetS-GacS interactions, but also identify a residue critical for the equilibrium between the RetS-GacS complex and the respective RetS and GacS homodimers. Collectively, our findings suggest that RetS and GacS form a domain-swapped hetero-oligomer during the planktonic growth phase of *P. aeruginosa* before unknown signals cause its dissociation and a relief of GacS inhibition to promote biofilm formation.

Introduction

Sensor histidine kinase-linked signal transduction systems are the primary means whereby bacteria sense extracellular signals to shape an adaptive response (2, 5, 155). The classic two-component signaling system consists of autophosphorylation of the histidine kinase (HK) followed by phosphate transfer to a cognate response regulator (RR). In the closely related phosphorelay systems there are two additional transfer steps. Here, the phosphate moves from the HK region to a receiver domain with no coupled output domain, then to a histidine phosphotransfer (HPt) protein, and from there finally to a RR (3, 12). The additional phosphotransfers allow for finer-tuned output regulation (5, 10). Hybrid signaling HKs contain a sensory domain, HK region and a receiver domain within a single polypeptide chain, while unorthodox HKs contain a sensory domain, HK region, a receiver domain and an HPt domain (3). Because the tethering of the HK region to the receiver domain confers specificity to the associated phospho-transfer step, the otherwise stringent evolutionary requirement for HK-RR complementarity are more relaxed in hybrid and unorthodox HKs (41). Crosstalk between distinct phosphorelay chains was long thought to be undesirable and therefore forbidden (14, 37, 156). However, mounting evidence suggests the presence of intricately webbed multikinase networks (MKNs) (46). At this point, we have gained a reasonably clear understanding of how the linear phosphotransfer events are facilitated within a single relay, we have only a cursory understanding of how such crosstalk occurs and is regulated. To date the best studied example of interactions within a MKN is perhaps the multilayered interplay between the HK family enzymes RetS and GacS in the opportunistic pathogen *Pseudomonas aeruginosa.* The unorthodox HK GacS and its cognate RR GacA sit at the heart of the Gac/Rsm signal transduction pathway (48). This pathway allows *P. aeruginosa* to switch between a motile, invasive lifestyle—which causes

an acute infection in a human host—and a sessile, biofilm-associated lifestyle—which often results in a chronic infection in a human host (66, 134). Once phosphorylated, GacA acts as a transcriptional activator, indirectly upregulating genes associated with the sessile biofilm lifestyle (75, 131, 135). Conversely, GacA indirectly downregulates genes associated with a motile, invasive lifestyle, such as the expression of flagella-mediated motility-related genes and Type Three Secretion System-related genes necessary for producing the observed cytotoxic effects in an acute infection (131, 135).

GacS is reciprocally regulated by two HK family proteins, LadS and RetS (46). LadS enhances the phosphotransfer activity of GacS via phosphorylation of the HPt domain of GacS (141, 142). RetS, on the other hand, inhibits GacS via three distinct mechanisms (summarized in Fig. 2.S1) (46, 48, 49). RetS has an unusual architecture consisting of a periplasmic sensor domain, an HK region and two receiver domains. RetS uses its HK region and C-terminal receiver domain to siphon phosphate groups from the receiver and DHp domains of GacS, respectively (46, 49). Mediated by direct interactions between the HK regions of the two enzymes, RetS also interferes with the initial autophosphorylation of GacS (36, 46, 48). This mode of inhibition is not well understood and is the focus of the present study. Initial models suggested that RetS might form a heterodimeric complex with GacS (48). However, our recent work demonstrated that the GacS dimer remains intact upon RetS binding (36), suggesting the formation of a larger heteromeric assembly, perhaps a tetramer (36). In the same study we also demonstrated that a structurally dynamic region of the RetS DHp domain is important for GacS binding and might be involved in regulating the interaction.

In the present study, we report the crystal structure of a complex between the RetS HK region and the GacS DHp domain. The RetS-GacS interface closely resembles the canonical

interface in homodimeric enzymes. Consistent with the proposed role of helix cracking in the regulation of the interaction, the structurally dynamic helix of RetS DHp is fully formed and involved in GacS binding. We experimentally determined that GacS autophosphorylates *in trans*. Thus, the $RetS_{HK}$-$GacS_{DHp}$ structure also answers the question how RetS prevents GacS autophosphorylation, because RetS binding disrupts the spatial arrangements needed for *trans*-autophosphorylation.

Results

RetS and GacS Form a DHp-DHp Interface that Closely Resembles the Dimerization Interface in Canonical Signaling Histidine Kinases

Co-crystallization of the HK region of RetS ($RetS_{HK}$, amino acid residues 413-649) and the DHp domain of GacS ($GacS_{DHp}$, amino acid residues 270-349) yielded crystals that gave X-ray diffraction data up to 2.3 Å resolution using a $CC_{1/2}$ threshold of 0.3 as cut-off (data collection and structure refinement statistics are provided in Table 2.1) (157). The structure was solved via molecular replacement using a single molecule of the previously solved $RetS_{HK}$ dimer as search model (36). The complex consists of a 1:1 heterodimer wherein the DHp domain of RetS and GacS form an extensive interface (Fig. 2.1). The final model contains residues 414 – 573, 604 – 639 of RetS and GacS residues 285 – 344. RetS residues 413, 574 – 603, and 640-649 appear to be structurally dynamic in the complex because no electron density was observed for these sections of the molecule. Similarly, there was no interpretable electron density for GacS residues 270-284 and 345-349. $RetS_{HK}$ consists of a CA and a DHp domain. The overall folds of the individual domains mirror those observed in the crystal structure of the $RetS_{HK}$ homodimer (36). The RetS-DHp domain assumes the canonical helix-loop-helix fold wherein the conserved

histidine residue H424 is located on the α1 helix and solvent exposed. The RetS-CA domain assumes the expected α/β sandwich fold comprising the α3 – α4 helices, the α7 helix, and strands β1 to β7. The residues that formed helices α5 and α6 helices in the $RetS_{HK}$ homodimer show no electron density in the RetS-GacS complex (residues 574 – 603) (Fig. 2.S2). The DHp domain of GacS forms the anticipated helix-loop-helix structure. The conserved catalytic histidine residue H293 is also solvent exposed.

The DHp domains of RetS and GacS form a four-helix bundle, closely resembling the canonical interface observed in homodimeric bacterial histidine kinases (2, 5, 158) (Fig. 2.2*A*). The same section of $RetS_{HK}$ also partakes in RetS homodimerization or, in the case of GacS, would also be predicted to form the binding surface in a GacS homodimer. Altogether 25 GacS residues corresponding to a surface area of 1351 $Å^2$ and 23 RetS residues that cover 1348 $Å^2$ of surface area form the extensive interface. The 89 non-bonded contacts are largely hydrophobic, containing only four hydrogen bonds (Fig. 2.2*B*).

In HKs the α1 helix is kinked N-terminal at highly conserved threonine and proline residues. The kinking provides the plasticity needed for autophosphorylation, phosphotransfer, and phosphatase activity (29). This kink is also observable N-terminal to Thr428 and Pro429 of RetS, and N-terminal to Thr297 and Pro298 in GacS (Fig. 2.3*A*). The kink angle for GacS is 28.7° and the angle for RetS is 22.8° (Fig. 2.3*A*). In the $RetS_{HK}$ homodimer the corresponding section is unfolded in one molecule and displays a kink angle of 33.3° in the other molecule (Fig. 2.3). While RetS is not a functional kinase the kink does play a role in regulating the equilibrium between a domain-swapped RetS-GacS oligomer and the individual homodimers (36). We previously demonstrated that this section is critical for GacS binding but not RetS homodimerization and predicted that it would be helical in the heteromeric complex (36).

Consistent with these predictions the dynamic N-terminal section of RetS α1 helix is now helical and forms part of the interface in the complex with GacS (Fig. 2.3*B*).

GacS Binding Forces Conformational Changes in RetS$_{HK}$

In the RetS-GacS complex RetS$_{HK}$ assumes a distinct conformation compared to those observed in the RetS$_{HK}$ homodimer. Overall, it closely resembles Chain A (PDB code 6dk7) with an RMSD of 0.359 Å between the DHp domains. Here, the positions of the CA domains are very similar as demonstrated by the 5.3° angle of rotation between the two CA domains (Fig. 2.4). A larger angle of rotation between the two CA domains of 35.4° accounts for the larger overall RMSD of 1.53Å between the RetS$_{HK}$ molecule in the RetS-GacS complex and Chain B of the RetS$_{HK}$ homodimer (Fig. 2.4).

Beyond the relative movements of the CA and DHp domains GacS binding significantly impacts regions that were previously implicated in the regulation of the RetS-GacS interaction. In the RetS$_{HK}$-GacS$_{DHp}$ complex residues 574 to 603 encompassing a section of the molecule containing the so-called ATP lid loop is not structured. In the asymmetric RetS$_{HK}$ homodimer the ATP lid loop regions assume two distinct but well-defined conformations consisting of a short N-terminal helix and the lid loop (36) (Fig. 2.S2). The ATP lid loop of other histidine kinases also displays conformational plasticity, such as in the histidine kinase from *Bacillus subtilis* DesK (159). However, RetS has lost the ability to bind ATP (36). Instead, the lid region from one RetS$_{HK}$ molecule forms a short helix that displaces an unfolded section of α1 helix from the other molecule at the DHp-DHp interface (36). The biological significance of these interactions was corroborated *in vitro* and *in vivo* (36). In the RetS-GacS complex the α1 helix of

GacS DHp is fully folded, while the lid region is now dislodged from the interface and apparently unstructured.

GacS Autophosphorylates in *Trans*

Because RetS binding disrupts the DHp-DHp interface of the GacS dimer, we reasoned, this interaction should interfere with GacS autophosphorylation if GacS actually autophosphorylates in *trans*. Many HKs are predicted to autophosphorylate in *trans*, although some HKs have been demonstrated to autophosphorylate in *cis* (19, 160). BarA, the GacS homolog in *E. coli* has been demonstrated to autophosphorylate in *trans* (161). The handedness of the loop between the α1 and α2 helices of the DHp domain predict whether a HK will autophosphorylate in *trans* or in *cis* (160). A right-handed loop predicts that the HK will autophosphorylate in *trans* due to the position of the conserved histidine as being more proximal to the CA domain in the other subunit as compared to the CA domain of its own subunit. Given that the GacS homolog autophosphorylates in *trans* and in the structure, GacS has a right-handed loop between the α1 and α2 helices of the DHp domain, GacS is predicted to autophosphorylate in *trans*. An autophosphorylation assay followed by Zn^{2+}-Phos-tag SDS-PAGE was used to assess if GacS autophosphorylates in *trans* (Fig. 2.5). $GacS_{cyt}$ (GacS 219-925) and the $GacS_{cyt}$ variants H293A and G472A G474A were examined in the autophosphorylation assay. Variation of the conserved HK region histidine residue (H293) to an alanine inhibits GacS autophosphorylation (161). The variation of conserved G2 box residues G472 and G474 to alanines inhibit the ability of $GacS_{cyt}$ to bind ATP. The G2 box is a conserved region in histidine kinases located within the CA domain which binds ATP (161). Individual variant constructs ($GacS_{cyt}$ H293A and $GacS_{cyt}$ G472A G474A) are unable to autophosphorylate in *cis*, but when

both variant constructs are introduced into the autophosphorylation assay they can autophosphorylate in *trans*. The observed mobility shift when both $GacS_{cyt}$ H293A and $GacS_{cyt}$ G272A G474A were present in the autophosphorylation assay demonstrated that GacS autophosphorylates in *trans*, thus providing evidence for the mechanism by which RetS inhibits GacS autophosphorylation (Fig. 2.5).

GacS L309 and I302 are Critical for Promoting Complex Formation with RetS

In order to experimentally corroborate the RetS-GacS interface found in the crystal structure a number of interface residues were mutated and the variants examined via the bacterial adenylate cyclase two-hybrid (BACTH) assay. The DHp domains of RetS and GacS share a 56.9% amino acid sequence identity (Fig. 2.1), whereas the entire HK regions of RetS and GacS share 40.4% sequence identity. The high degree of conservation in the DHp domain might explain the overall complementarity of their molecular surfaces. Yet, we also sought to identify distinctive residues that promote the formation of a RetS-GacS complex at the DHp-DHp interface over the formation of the typical homodimers. The interactions of the cytoplasmic region of GacS ($GacS_{cyt}$) with itself and with the cytoplasmic region of RetS ($RetS_{cyt}$) were used as positive controls and reference points (Fig. 2.6). The GacS homodimer is expected to contain multiple dimerization interfaces including HAMP-HAMP and DHp-DHp domains (162). Therefore, the RetS-GacS interactions are expected to be more sensitive to mutations disrupting the interactions between the DHp domains than the more extensively paired GacS homodimer. A complicating factor in this analysis was the observation we made in prior experiments that monomeric RetS and GacS are not stable proteins. A variant that has completely lost the ability to dimerize could either be misfolded or simply be unstable because it can no longer dimerize.

Therefore, we were particularly interested in identifying GacS residues that are critical for RetS binding but not for GacS dimerization. A number of residues were probed. The GacS L309R mutation attenuated homodimerization but completely disrupted the $RetS_{cyt}$-$GacS_{cyt}$ interaction (Figs. 2.6 and 2.S3) confirming that L309 is important in the RetS-GacS complex. The $GacS_{cyt}$ I325R mutation abrogated both $GacS_{cyt}$ homodimerization and the $RetS_{cyt}$-$GacS_{cyt}$ interaction (Figs. 2.6 and 2.S3). $GacS_{cyt}$ I302V formed a stable homodimer, while binding to $RetS_{cyt}$ was partially disrupted (Figs. 2.6 and 2.S3). This suggests that the $GacS_{cyt}$I302V construct is stable and, as predicted by the crystal structure, that I302 is involved in RetS binding. Two $RetS_{cyt}$ variant constructs were also examined in the BACTH assay. $RetS_{cyt}$ L463R could no longer form homodimers or bind to GacS (Fig. 2.S4). The $RetS_{cyt}$ V433I mutation was too subtle as the substitution had no significant impact on $RetS_{cyt}$ homodimerization or the $RetS_{cyt}$-$GacS_{cyt}$ interface (Fig. 2.S4).

Because the GacS L309R and GacS I302V mutations showed differential binding profiles in the BACTH assays we decided to examine their impact on *P. aeruginosa* biofilm formation. Both substitutions were introduced into the full length *gacS* gene and the resulting proteins were expressed *in trans* in a PAKΔ*gacS* strain. A crystal violet assay was used to monitor production of biofilm formation associated carbohydrates. At the early growth stage biofilm formation is closely held in check by RetS and the *gacS* deletion strain is essentially indistinguishable from the wild-type or a complemented strain (Fig. 2.7). However, we predicted that GacS mutations that selectively prevent RetS binding but not GacS dimerization should cause a hyper-biofilm phenotype akin to what is observed in a *ΔretS* strain because here RetS would no longer be able to block GacS autophosphorylation. Indeed, the I302V mutation, which had resulted in a moderate disruption to the heterodimeric interface in the BACTH assay produced a gain-of-

function phenotype comparable to the hyperbiofilm phenotype of the *retS* mutant (Fig. 2.7) (66). The L309R variant on the other hand, produced no phenotypic change, suggesting that the local impact of this substitution on the DHp-DHp interface not only interferes with RetS binding but also prevents GacS autophosphorylation (Fig. 2.7).

Discussion

Initially, the Gac/Rsm pathway was discovered as a central signal transduction pathway in Pseudomonads that regulates the production of secondary metabolites (e.g. antimicrobials, hydrogen cyanide, siderophores) and also the switch between a motile, invasive lifestyle and a sessile biofilm-associated lifestyle (131, 139, 163–165). However, beyond the biological significance of this particular signaling pathway, the GacS-GacA system has become the model for studying crosswise interactions between multiple signaling kinases. HKs have been demonstrated to maintain a high degree of fidelity for their cognate RRs and vice versa, but we are beginning to recognize that multikinase networks (MKNs) are often necessary to control complex outputs (14, 47). Such MKNs were once postulated to be prohibited but it now appears many bacterial species use them to integrate diverse extracellular signals to regulate adaptive responses (47). MKNs control transitions associated with virulence, response to switching from aerobic to anaerobic conditions, the integration of diverse quorum sensing signals, as well as sporulation and fruiting body formation (47). However, none is more complex than the MKN associated with the regulation of the GacS-GacA system. At least seven HKs coordinate their signaling to fine-tune *P. aeruginosa* gene expression. LadS and RetS do so through direct interactions with GacS (46, 48, 49, 141), while PA1611 appears to sequester RetS to promote GacS signaling (50, 51). However, RetS, PA1611, ErcS, and SagS all appear to also interact with

HptB to modulate RsmY levels (148–150, 152). SagS interacts with BfiS to integrate the BfiS/BfiR system which promotes biofilm formation into the MKN (152). The mechanism whereby these signaling pathways integrate are varied and, in some cases, multifaceted as the interactions can be both activating and suppressing. Often, the molecular mechanisms underlying the MKNs can be readily understood as they involve well-characterized protein-protein interactions mirroring canonical signaling pathways. The basis for the direct pairwise interactions of the HK regions observed for RetS-GacS but also RetS-PA1611, and SagS-BfiS in *P. aeruginosa*, as well as the DivL-CckA interactions in *Caulobacter crescentus* are less well understood (166). The present evidence of domain-swapping between DHp domains in the RetS-GacS complex suggests that once again MKN signaling evolved from known contact interfaces of regular linear HK systems. Although, earlier work suggests that the interface formed between PA1611 and RetS involves the DHp domain of PA1611 and the beta-sheet of the CA domain of RetS, suggesting an interface that does not have an equivalent in known HK contacts (51). The present structure may broadly represent the basis for how heteromeric HK-HK interactions inhibit autophosphorylation in MKNs.

The $RetS_{HK}$-$GacS_{DHp}$ complex structure answers the question of how binding between the RetS and GacS DHp domains prevents GacS autophosphorylation because the formation of a heterodimeric DHp-DHp interface should inhibit GacS *trans*-autophosphorylation (46, 48). However, perhaps this inhibition is not complete, thus explaining why RetS uses not one but three distinct mechanisms to inhibit GacS signaling (Fig. 2.S1). Potential *trans*-autophosphorylation of GacS in a heteromeric RetS-GacS complex is at this point only speculative, however, the siphoning of phosphates from the catalytic histidine in GacS-HK by the second receiver domain of RetS would otherwise appear to be redundant. Yet, Francis et al.

demonstrated that this phosphatase activity is critical for inhibiting GacS signling *in vivo* (46). The RetS HK region also dephosphorylates the receiver domain of GacS in a manner similar to transmitter phosphatase activity (5, 44, 46). It is not known if RetS-GacS binding through the DHp-DHp increases the efficiency or is in fact a prerequisite for the efficient working of the two other inhibitory mechanisms. In recent years, some progress has been made toward elucidating the roles of periplasmic sensory domains of RetS and GacS in regulating their interplay. Remarkably, the sensory domain of RetS appears to promote the inhibition of GacS when exposed to host cell derived mucins, while *P. aeruginosa* lysis releases a molecular signal, also recognized by the RetS sensory domain, that causes GacS activation (146, 147). The sensory domain of GacS, on the other hand is required for GacS activation, but the longstanding hunt for the elusive ligand is ongoing (139).

Overall, the present study has uncovered the novel heteromeric DHp-DHp of a RetS-GacS complex, which readily explains, how direct binding of RetS-HK to GacS-HK interferes with GacS *trans*-autophosphorylation. The observed $RetS_{HK}$-$GacS_{DHp}$ structure is also consistent with the proposed model for regulation of RetS-GacS binding via RetS helix-cracking, which predicted that a structurally dynamic section of RetS would form the N-terminal end of the DHp α1 helix and interact with GacS (36). Another structurally dynamic feature of the RetS-HK dimer, the so-called ATP lid loop was shown to play an important role in stabilizing the RetS homodimer but not the RetS-GacS complex (36). Consistent with this prediction the ATP lid loop region and a short α helix N-terminal to the ATP lid loop region of the RetS CA domain are unstructured in the $RetS_{HK}$-$GacS_{DHp}$ complex. The mutational analysis of the DHp-DHp interface offered additional insight into which residues might be critical in providing specificity for the unusual heteromeric RetS-GacS interactions in favor of the RetS-RetS and GacS-GacS

interfaces. We demonstrated upon variation of select residues (GacS I302, GacS L309) an inhibition to binding in the heterodimeric interface of the cytoplasmic regions, but not an equivalent inhibition to binding in the homodimeric interface of the cytoplasmic regions. We also demonstrated a phenotype comparable to the hyperbiofilm *retS* mutant for the GacS I302V strain in an *in vivo* assay, demonstrating the importance of I302 in RetS binding (66).

There is a disparity between the observation that RetS disrupts the GacS DHp-DHp dimerization interface and our previous finding that RetS overall does not disrupt the GacS homodimer (20). This apparent contradiction may be explained by the fact that the GacS protein construct used in the original FRET measurements included not only the histidine kinase region but also the HAMP domain of GacS (36). HAMP domains are ubiquitous signaling domains of signaling histidine kinases and methyl accepting chemotaxis proteins; and facilitate homodimerization and signal transduction by forming structurally dynamic intermolecular four-helix bundles (34). The GacS HAMP domain appears to maintain GacS-GacS association even in the presence of RetS (Fig. 2.8). This observation is also consistent with the finding that the HAMP domain is required for GacS homodimerization in *Pseudomonas fluorescens* (162). Similarly, the periplasmic domain of RetS has also been demonstrated to dimerize *in vitro* (144, 167). If and how this interaction is affected by GacS binding is unknown.

Collectively, the present work and previous results support a model in which RetS and GacS form a domain-swapped complex (Fig. 2.8). The exact stoichiometry and size of this complex remains to be determined. While the presence of additional GacS-GacS and RetS-RetS interfaces might make it tempting to propose the formation of a symmetric hetero-tetramer (Fig. 2.8, Model 2), steric factors may create an asymmetric complex, cause dissociation of the RetS

dimer, or may even facilitate the formation of a larger polymeric structure consisting of alternating RetS and GacS dimers.

Experimental Procedures

Cloning and Site-directed Mutagenesis

The plasmid construct for the expression of $RetS_{HK}$ (residues 413-649) from the pDEST-HisMBP plasmid was created previously (36). For the expression of the $GacS_{DHp}$ protein the section of the *gacS* gene that encodes residues 270-349 was amplified via PCR from pDEST-HisMBP-$GacS_{HK}$ using GacS_350_stop_F and GacS_350_stop_R primers. The PCR product was cloned into pDONR221 and from there into pDEST-HisMBP using Gateway recombinational cloning (Thermo Fisher) to create pDEST-HisMBP-$GacS_{DHp}$.

Constructs for the BACTH assay were generated using standard cloning protocols. pKT25-$RetS_{cyt}$-GFP, encoding RetS residues 387-942 in frame with the *gfp* gene, was generated previously (36). pKT25-$RetS_{cyt}$-GFP L463R and V433I variants were created using Agilent QuickChange XL site-directed mutagenesis kit (Agilent) following the manufacturer's protocol. A pUT18c-$GacS_{HK}$ plasmid was created by introducing a stop codon after *gacS* codon 509 into the previously generated pUT18c-$GacS_{cyt}$ ($GacS_{cyt}$ includes residues 219-925) plasmid using the Agilent QuickChange XL site-directed mutagenesis kit (Agilent) and GacS509STPx2_F and GacS509STPx2_R primers following the manufacturer's protocol (36). Agilent QuickChange XL site-directed mutagenesis kit (Agilent) was also used to create the pUT18c-$GacS_{HK}$ constructs expressing variants L309R, I325R, and I302V following the manufacturer's protocol. Ultimately, the pUT18c-$GacS_{HK}$ constructs expressing the original *gacS* sequence and the three mutated genes were only used in this study as templates to cut-and-paste the L309R, I325R, and

I302V associated mutations into the pUT18c-$GacS_{cyt}$ vector via internal restriction sites (XbaI and StuI) using standard restriction cloning protocols.

$GacS_{cyt}$ variants $GacS_{cyt}$ H293A and $GacS_{cyt}$ G472A G474A used for the *in vitro* autophosphorylation assays were also generated with the Agilent QuickChange XL site-directed mutagenesis kit (Agilent) using the pQE60-$GacS_{cyt}$vector as template, which was previously generated and generously shared with us by Dr. Steven Porter's group (University of Exeter) (46).

The Agilent QuickChange XL site-directed mutagenesis kit (Agilent) was also used to create pHERD20T-*gacS* L309R and pHERD20T-*gacS* I302V variants using the previously generated pHERD20T-*gacS* vector as a template following the manufacturer's protocol (168, 169). Cloning and site-directed mutagenesis primers are listed in Table 2.S1. Recombinant DNA used in this study is listed in Table 2.S2.

Recombinant Protein Expression and Purification

BL-21(DE3)(RIL) pDEST-HisMBP-$RetS_{HK}$ was grown in 6 L Lysogeny broth (LB) with 100 μg/mL ampicillin, 30 μg/mL chloramphenicol and 10 g glucose/L at 37℃, shaking at 250 rpm. The cultures were induced with 1 mM isopropyl β-D-1-thiogalactopyranoside (IPTG) after the OD_{600} reached 0.6, and incubated at 18 ℃ for 18 hours, again shaking at 250 rpm. A 35.5 g cell pellet was resuspended in 200 mL NiNTA A buffer (buffer compositions are listed in Table 2.S3) and 0.3 mM phenylmethanesulfonyl fluoride (PMSF) and lysed via sonication (36). The soluble fraction was collected via centrifugation for 1 hour at 100,000 x g, 4 ℃. HisMBP-$RetS_{HK}$ was purified via Ni-NTA affinity chromatography using a 30 mL Ni-NTA Superflow column (Qiagen) and a 150 mL linear gradient elution with Ni-NTA B buffer. SDS-PAGE was used to

assess purification of HisMBP-RetS$_{HK}$. To remove the HisMBP-tag, the collected protein was incubated with 1 mg His$_6$TEV protease per 50 mg protein, as estimated by the UV$_{280}$ absorption and extinction coefficient of the fusion protein, and dialyzed into Ni-NTA A buffer. A second 30 mL Ni-NTA Superflow column (Qiagen) was used to separate RetS$_{HK}$ from the HisMBP tag and the His$_6$TEV protease. SDS-PAGE was used to assess purification of RetS$_{HK}$. RetS$_{HK}$ was further purified using a HiTrap Q HP column (GE Life Sciences) with a 150 mL linear gradient of anion exchange buffer A and anion exchange buffer B. SDS-PAGE was used to assess purification of RetS$_{HK}$. The eluted sample was polished on a 26/60 Superdex 200 column (GE Life Sciences) pre-equilibrated in RetS$_{HK}$ gel filtration buffer (36). SDS-PAGE was used to assess purification of RetS$_{HK}$. Expression and purification protocols for GacS$_{DHp}$ from the pDEST-HisMBP-GacS$_{DHp}$ plasmid followed the same protocol as that for RetS$_{HK}$ (36).

Selenomethionine-substituted RetS$_{HK}$ was produced by altering the growth conditions prior to protein purification. BL-21(DE3)(RIL) pDEST-HisMBP-RetS$_{HK}$ was grown in 1 L Lysogeny broth (LB) with 100 μg/mL ampicillin, 30 μg/mL chloramphenicol and 10 g glucose/L at 37°C, shaking at 250 rpm until the OD$_{600}$ was 0.5. The culture was incubated on ice for 30 minutes, after which the cells were pelleted via centrifugation at 4000 x g, 4 °C for 15 minutes. The cell pellet was resuspended in 100 mL of M9 salts plus Medicilon non-inhibitory amino acid cocktail (NIAAC), pelleted a second time at 4000 x g, 4 °C for 15 minutes and then resuspended in 100 mL of M9 salts plus Medicilon NIAAC (Medicilon). Medicilon selenomethionine M9 medium (Medicilon) with 100 μg/mL ampicillin and 30 μg/mL chloramphenicol was inoculated with the resuspended pellet. The cultures were incubated at 37 °C for 30 minutes, after which time protein expression was induced with 1 mM IPTG and the cultures were incubated at 18 °C

for 18 hours. Protein purification of selenomethionine-substituted $RetS_{HK}$ followed the same protocol as that for $RetS_{HK}$ (36).

To produce $GacS_{cyt}$ the pQE60-$GacS_{cyt}$ plasmid was transformed into the *E. coli* JM109 cell line. Cells were grown in LB medium with 100 μg/mL ampicillin at 37 °C for approximately 3 hours until the OD_{600} was 0.6. The temperature was reduced to 18 °C and expression was induced with the addition of 1 mM IPTG. Induction continued for 18 hours, after which cell pellets were harvested. Cell pellets were resuspended in 10 mL $GacS_{cyt}$ NiNTA A buffer per gram cell pellet with 0.3 mM PMSF, and then lysed via sonication. After centrifugation at 100,000 x g, 4 °C for 1 hour, the supernatant was applied to a Ni-NTA Superflow column (Qiagen) for FPLC and eluted using a 150 mL linear gradient of $GacS_{cyt}$ Ni-NTA A buffer and $GacS_{cyt}$ Ni-NTA B buffer. SDS-PAGE was used to assess the purification of $GacS_{cyt}$. The sample was then applied to a 26/60 Superdex 200 gel filtration column (GE Life Sciences) for the final purification step using $GacS_{cyt}$ gel filtration buffer. SDS-PAGE was used to assess $GacS_{cyt}$ purification. (Buffer compositions are listed in Table 2.S3.)

$GacS_{cyt}$ pQE60 variants $GacS_{cyt}$ H293A and $GacS_{cyt}$ G472A G474A were expressed in *E. coli* JM109 cell line following the same protocol as for $GacS_{cyt}$. The purification followed the same protocol as for $GacS_{cyt}$.

$RetS_{HK}$-$GacS_{DHp}$ Crystallization and Structure Determination

Crystals containing the complex of seleno-methionine-substituted $RetS_{HK}$ with $GacS_{DHp}$ were grown by vapor diffusion in a 6 μL hanging drop containing a 5:1 volume ratio of protein:mother liquor, with 440 μM of each $RetS_{HK}$ and $GacS_{DHp}$ in gel filtration buffer. The mother liquor was composed of 30% PEG3350, 0.2 M Li_2SO_4, 0.1 M Tris-HCl, pH 8.5. The

reservoir contained 0.4 mL of mother liquor. Crystals grew over a two-week period at room temperature. The crystals were loop-mounted and flash frozen in liquid nitrogen. X-ray diffraction data were collected at Advanced Light Source Beamline 4.2.2 at Lawrence Berkeley National Laboratory. The diffraction images were processed and integrated with XDS and intensities converted to amplitudes using Aimless (170–172). The resolution was cut off at 2.3 Å using a $CC_{1/2}$ threshold of 0.3 (157). The anomalous signal of the selenium atoms was not strong enough to facilitate structure solution. Therefore, the structure was solved with the PHASER molecular replacement tool within the Phenix suite using the structure of $RetS_{HK}$ (PDB 6DK8) as the search model (36, 173, 174). Iterative cycles of model building in Coot and automated refinements in Phenix and RefMac were used to build the $RetS_{HK}$-$GacS_{DHp}$ structure (173, 175–177). The degree of rotation between the CA domain of RetS and the CA domains of the RetS homodimer (PDB 6dk7) were estimated via PyMOL(178). PyMOL was used to determine the kink angle in the α1 helix of GacS, RetS, and the RetS homodimer (PDB 6dk7) (178). PyMOL was also used to generate Figures 2.1-2.4 and 2.S2 (178).

Bacterial Adenylate Cyclase Two-Hybrid (BACTH) Assay

Interface variants were examined in the BACTH MacConkey agar assay and the BACTH β-galactosidase assay (179, 180). For the BACTH MacConkey agar assay, LB cultures containing 100 μg/mL ampicillin and 50 μg/mL kanamycin were incubated for 18 hours at 37 ℃. The OD_{600} was adjusted to 1.0. 2 μL of culture was dispensed onto MacConkey agar containing 0.5 mM IPTG, 1 (w/v) % maltose, 100 μg/mL ampicillin, and 50 μg/mL kanamycin. The MacConkey agar plates were incubated at 32 ℃ for 24 hours. The BACTH MacConkey agar assay was performed in triplicate. For the BACTH β-galactosidase assay, LB cultures with 100

μg/mL ampicillin, 50 μg/mL kanamycin, and 0.5 mM IPTG were incubated for 24 hours at 30 °C. OD_{600} was measured for each culture. 20 μL of culture was added to 80 μL permeabilization solution (100 mM Na_2HPO_4, 20 mM KCl, 2 mM $MgSO_4$, 0.8 mg/mL cetrimonium bromide, 0.4 mg/mL sodium deoxycholate, 5.4 μL β-mercaptoethanol) (180). Samples were incubated for 30 minutes at 30 °C, after which, 0.6 mL of substrate solution (60 mM Na_2PO_4, 40 mM NaH_2PO_4, 1 mg/mL o-nitrophenyl β-D-galactoside, 2.7 μL β-mercaptoethanol) was added to the samples with the time noted (180). The reaction was stopped via the addition of 1 M Na_2CO_3 and the time was recorded (180). The samples were centrifuged at 16,000 x g for 10 minutes and absorbance at 420 nm was recorded (180). Miller Units were calculated using the following formula: 1000 x (Abs_{420} / (OD_{600} * volume of sample in mL * reaction time in minutes) (180). The BACTH β-galactosidase assay was performed in triplicate.

Autophosphorylation Assay and Zn^{2+} Phos-tag SDS-PAGE

The Zn^{2+}-Phos-tag assay closely followed the steps provided in the manufacturer's protocol and all solutions were prepared according to the manufacturer's protocol (FUJIFILM Wako Chemicals). Autophosphorylation was performed via the incubation of 5μM $GacS_{cyt}$ or $GacS_{cyt}$ variant proteins $GacS_{cyt}$ H293A and $GacS_{cyt}$ G472A G474A with 2 mM ATP for 30 minutes at 21 °C (46). The reaction was stopped via the addition of 3x loading buffer to a final concentration of 1x following manufacturer's protocol (FUJIFILM Wako Chemicals). The samples were analyzed via Zn^{2+}-Phos-tag SDS-PAGE following manufacturer's protocol using 100 μM Phos-tag in a 10% acrylamide Zn^{2+}-Phos-tag SDS-PAGE gel (FUJIFILM Wako Chemicals) (161). The autophosphorylation assay and Zn^{2+}-Phos-tag SDS-PAGE were performed in triplicate.

Crystal Violet Biofilm Assay

P. aeruginosa PAK strains were examined in the crystal violet biofilm assay. The strains were plated to LB agar containing 300 μg/mL carbenicillin. Individual colonies were used to inoculate LB containing 300 μg/mL carbenicillin which was then incubated at 37 °C overnight while shaking at 250 rpm. The strains were sub-cultured into modified M63 media containing 0.5% arabinose and 300 μg/mL carbenicillin which were incubated at 37 °C overnight while shaking at 250 rpm (181). The OD_{600} of the cultures was adjusted to 0.05 using modified M63 media containing 0.5% arabinose and 300 μg/mL carbenicillin. 100 μL of each culture was dispensed into 96-well plates (Corning # 2797) (181). Plates were covered with aluminum foil and incubated at 37 °C for 6 hours. Following incubation, the media were removed via pipette and the wells were washed with water via pipette. The wells were stained with 0.1% crystal violet for 10 minutes, and then washed with water via pipette (181). The remaining crystal violet-stained cells were solubilized in 125 μL of 30% acetic acid for 15 minutes (181). 100 μL of the solution was transferred to a 96-well plate (Corning # 3370) and absorbance at 600 nm was measured using a Tecan M200 plate reader.

Figures

Table 2.1. X-ray diffraction data collection and refinement statistics

X-ray Diffraction Data	
Space Group	P 3(1) 2 1
Unit Cell: a, b, c (Å)	103.4, 103.4, 62.0
Unit Cell: α, β, γ (º)	90, 90, 120
Resolution range (Å)	44.76 – 2.29 (2.37 – 2.29)
Total reflections	369,869 (36,066)
Unique reflections	17,507 (1,708)
Multiplicity	21.1 (21.1)
Completeness (%)	100 (100)
I/σ(I)	16.9 (0.4)
R_{merge}	0.147 (13.7)
$CC_{1/2}$ threshold	0.3
Refinement Statistics	
Resolution (Å)	44.76 – 2.30
R_{work}/R_{free}	0.2475/0.2662
Root mean square bonds (Å)	0.004
Root mean square angles (º)	0.815
Average B factor ($Å^2$)	89.6

Outer shell statistics are provided in parentheses.

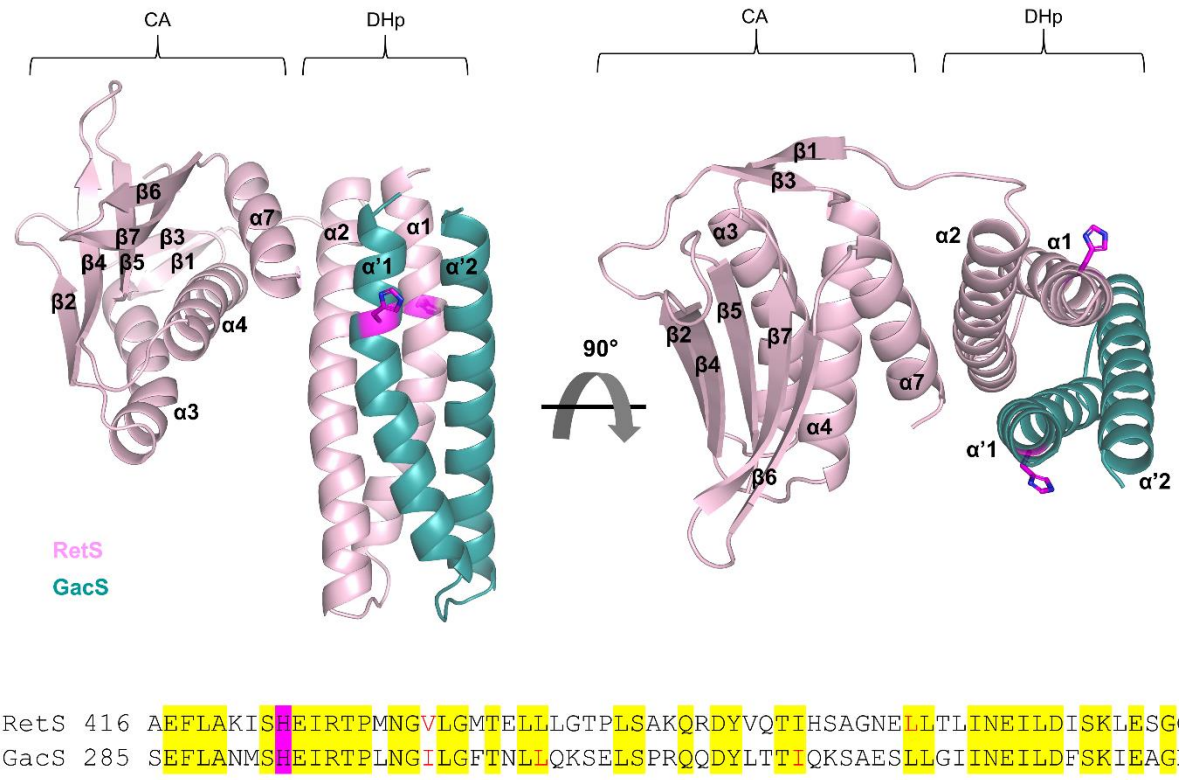


```
RetS 416 AEFLAKISHEIRTPMNGVLGMTELLLGTPLSAKQRDYVQTIHSAGNELLTLINEILDISKLESGQ
GacS 285 SEFLANMSHEIRTPLNGILGFTNLLQKSELSPRQQDYLTTIQKSAESLLGIINEILDFSKIEAGK
```

Figure 2.1. Crystal structure of the 1:1 RetS$_{HK}$-GacS$_{DHp}$ complex. The binding interface replaces the RetS and GacS homodimeric interfaces. RetS is shown in light pink. GacS is shown in turquoise. Catalytic histidine residues are shown in magenta. Shown underneath the structure is a sequence alignment of the DHp domains of RetS and GacS. The conserved catalytic histidine residues are highlighted in magenta. Residues conserved between RetS and GacS are highlighted in yellow. Residues selected for mutagenesis are colored red.

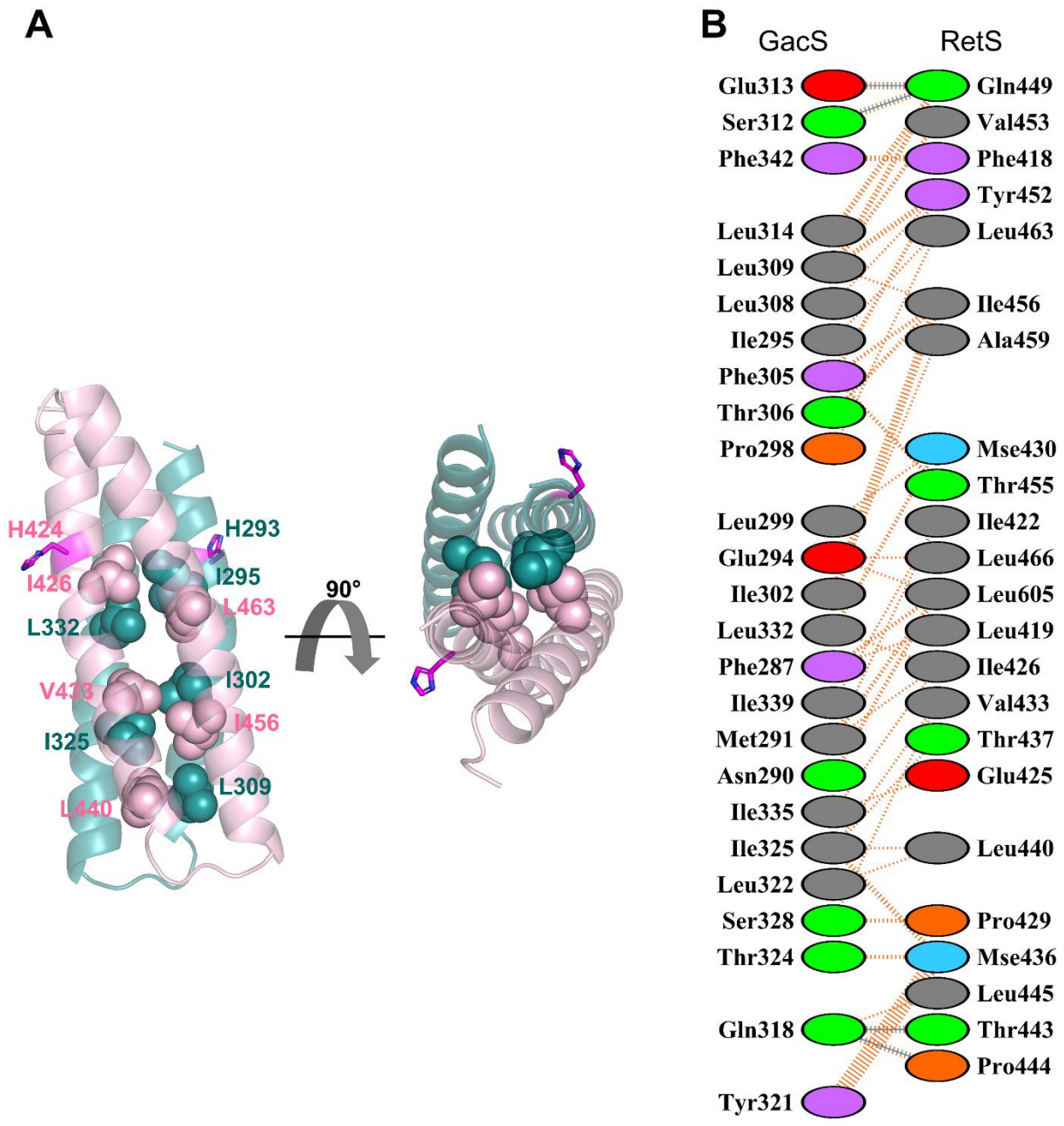

Figure 2.2. The RetS-GacS DHp-DHp interface. *A*, hydrophobic residues form the core of the RetS-GacS heterodimeric four helix bundle. RetS is shown in light pink. GacS is shown in turquoise. Catalytic histidine residues are shown in magenta. Hydrophobic interface residues shown as spheres. *B*, interacting interface residues. PDBsum was used to generate a schematic cataloguing interactions between RetS and GacS. Dashed orange lines represent non-bonded contacts. Blue lines represent hydrogen bonds (182).

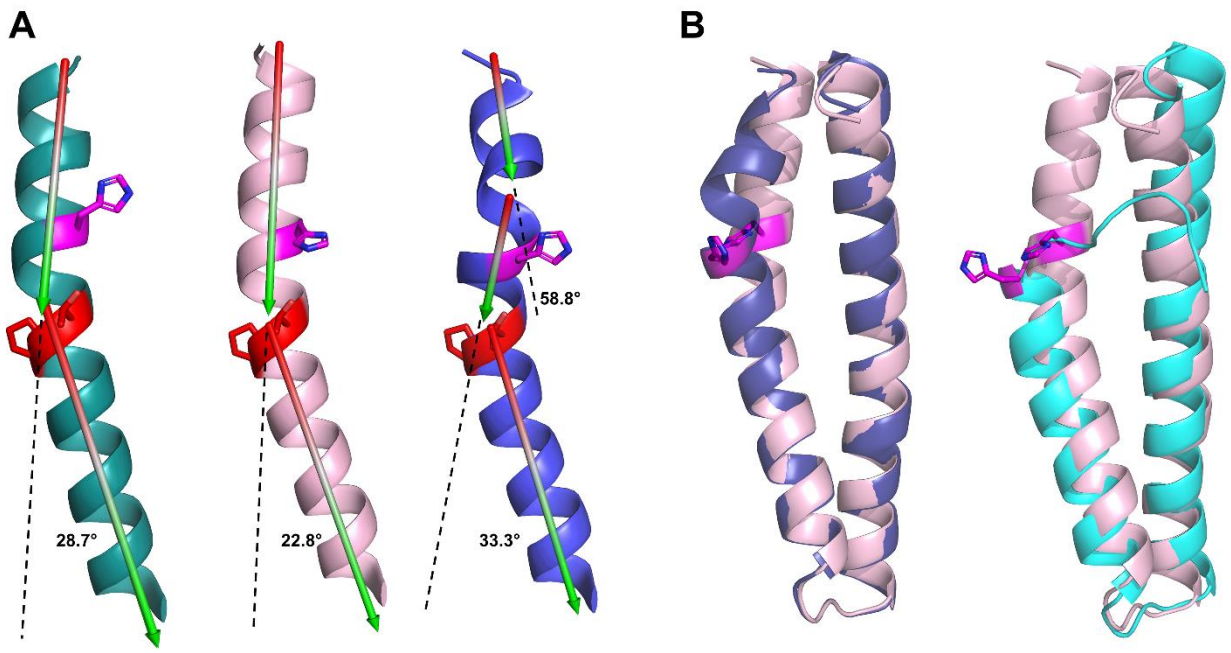

Figure 2.3. Conserved DHp kink in RetS and GacS, and fully folded RetS DHp. *A*, conserved kink in the N-terminal sections of the DHp domain α1 helix. Angles of conserved α1 helix kinks N-terminal to conserved threonine and proline residues (GacS Thr297 and Pro298, and RetS Thr428 and Pro429). GacS is shown in turquoise. RetS is shown in light pink. Shown in blue is the dually-kinked structure of the corresponding section in molecule A of the homodimeric $RetS_{HK}$ structure (PDB 6dk7). The catalytic histidine residues are shown in magenta. The conserved threonine and proline residues are shown in red. *B*, RetS DHp is fully folded in the heterodimeric complex. Alignment of the DHp domain of RetS with the DHp domain of the RetS homodimer Chain A (PDB 6dk7) (RMSD = 0.539) visualizes the fully folded α1 helix of the DHp domain of RetS in the heterodimeric complex (left image). Alignment of the DHp domain of RetS with the DHp domain of the RetS homodimer Chain B (PDB 6dk7) (RMSD = 1.864) visualizes the fully folded α1 helix of the DHp domain of RetS in the heterodimeric complex (right image). RetS is shown in light pink. RetS homodimer Chain A is shown in blue. RetS homodimer Chain B is shown in cyan. The catalytic histidine residues are shown in magenta.

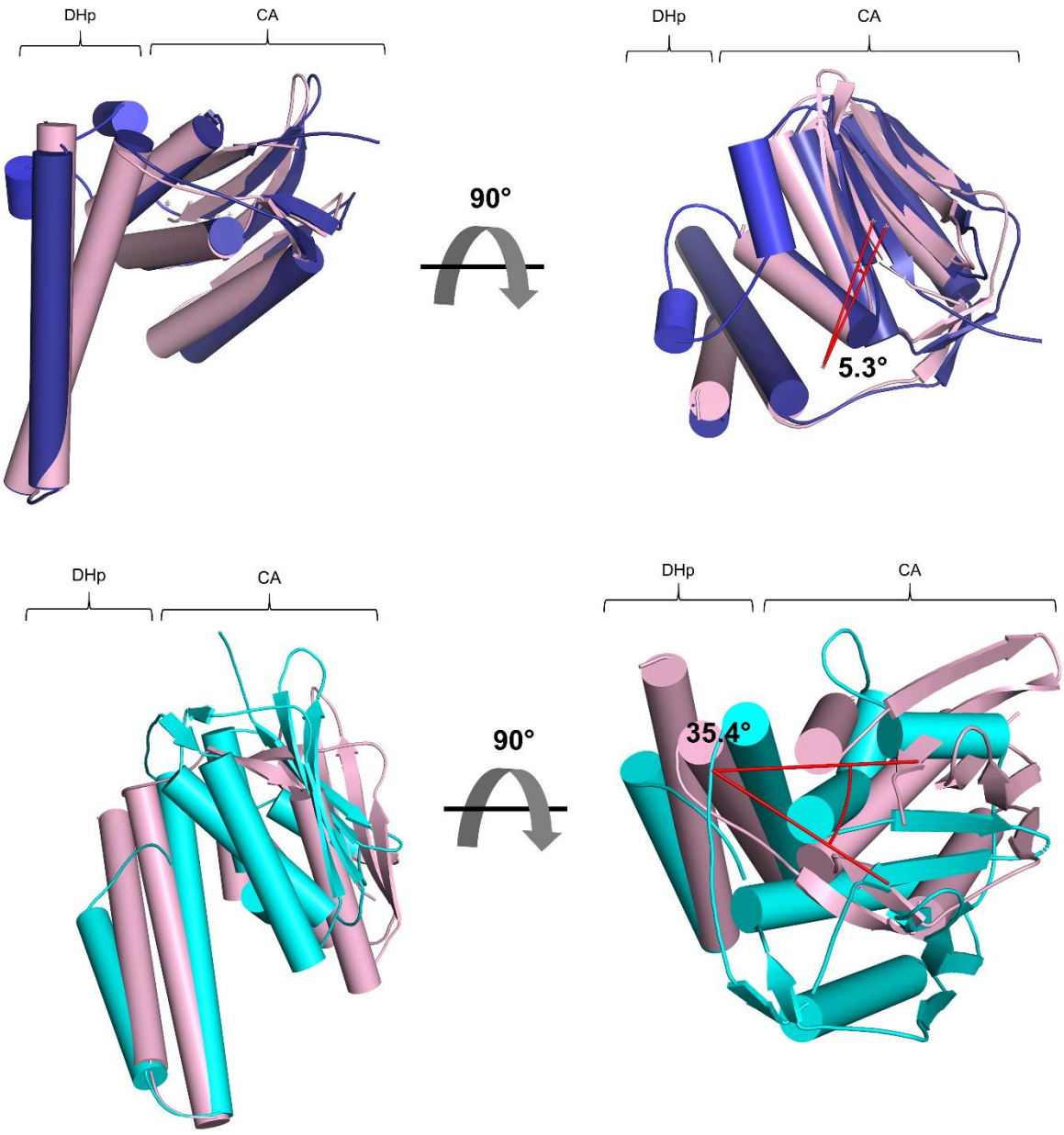

Figure 2.4. RetS CA domain movement. Alignment of the DHp domain of RetS with the DHp domain of the RetS homodimer Chain A (PDB 6dk7) (RMSD = 0.359) visualizes slight movement of the CA domain as demonstrated by the angle of rotation between the CA domains of 5.31° (top image). Alignment of the DHp domain of RetS with the DHp domain of the RetS homodimer Chain B (PDB 6dk7) (RMSD = 1.533) visualizes the greater movement of the CA domain as demonstrated by the angle of rotation between the CA domains of 35.41° (bottom image). RetS is shown in light pink. RetS homodimer Chain A is shown in blue. RetS homodimer Chain B is shown in cyan.

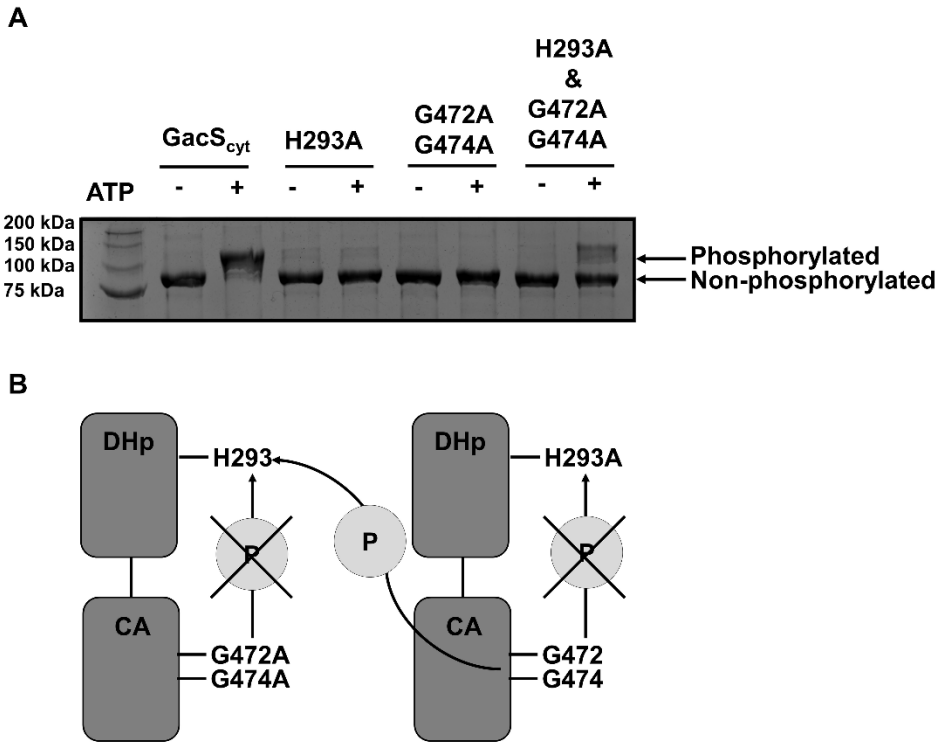

Figure 2.5. GacS autophosphorylates in *trans*. *A*, an autophosphorylation assay followed by Zn^{2+}-Phos-tag SDS-PAGE was used to examine the autophosphorylation of GacS$_{cyt}$ and GacS$_{cyt}$ variants in the absence and presence of ATP. GacS$_{cyt}$ wildtype, GacS$_{cyt}$ H293A (a variant that cannot undergo autophosphorylation), GacS$_{cyt}$ G472A G747A (a variant that cannot bind ATP), and an equimolar ratio of GacS$_{cyt}$ H293A and GacS$_{cyt}$ G472A G474A were used to assess the ability of GacS to autophosphorylate in *trans* or in *cis*. GacS$_{cyt}$ and the GacS$_{cyt}$ variants are 77 kDa. Each lane contains 7.74 μg protein. GacS$_{cyt}$ has three potential phosphorylation sites (the catalytic histidine in the DHp domain, the conserved aspartate in the receiver domain, and the conserved histidine in the Hpt domain). *B*, autophosphorylation assay. Individual variant constructs (GacS$_{cyt}$ H293A and GacS$_{cyt}$ G472A G474A) are unable to undergo *cis* autophosphorylation, but when both variant constructs are introduced into the autophosphorylation assay they can autophosphorylate in *trans*. The histidine kinase region is shown for clarity even though the assay was performed with the cytosolic region of GacS.

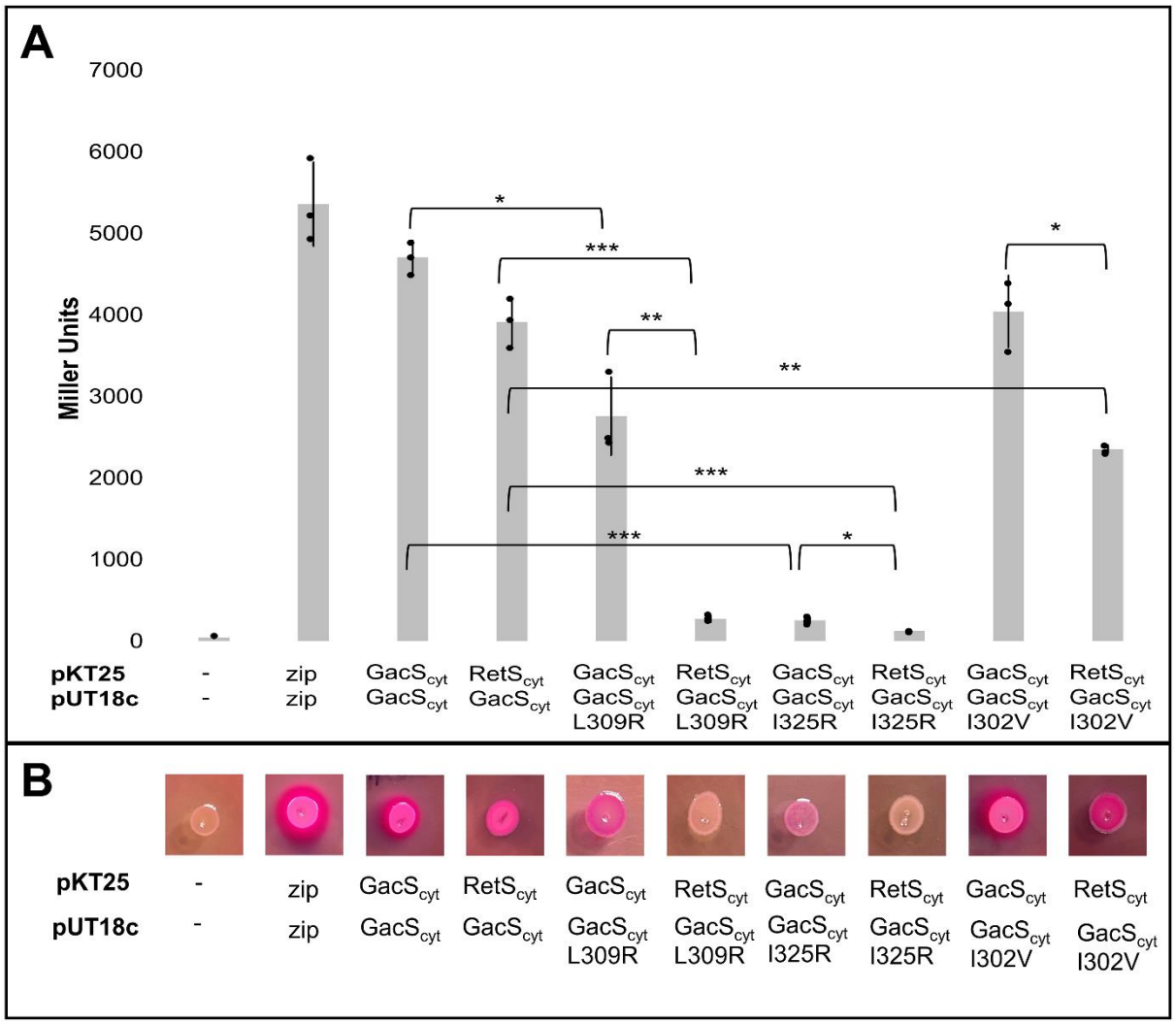

Figure 2.6. Interface variants in the BACTH assay. *A*, examination of interface variants in the BACTH β-galactosidase assay. Interface variants were examined in the BACTH β-galactosidase assay after 24 hours incubation at 30℃. Assay was performed in triplicate. Statistical significance was determined by a two-tailed, non-paired Student's t-test. *$p < 0.01$, **$p < 0.001$, ***$p < 0.0001$. *B*, examination of interface variants in the BACTH MacConkey agar assay. Interface variants were examined in the BACTH MacConkey agar assay after 24 hours incubation at 32℃. Assay was performed in triplicate.

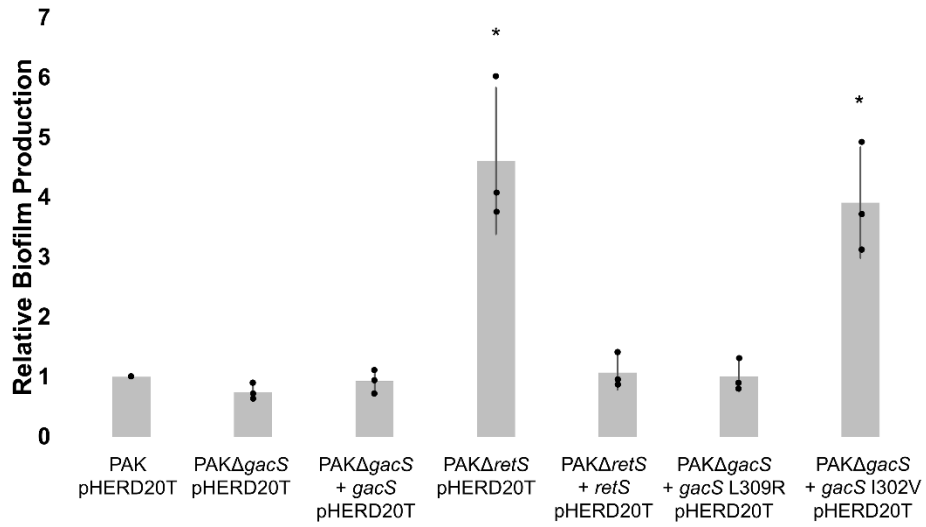

Figure 2.7. *In vivo* biofilm assay assessing GacS variants. Relative biofilm production assessed by the crystal violet biofilm assay. PAKΔ*gacS* + pHERD20T-*gacS* I302V was demonstrated to have a phenotype comparable to that of PAKΔ*retS* pHERD20T in the crystal violet biofilm assay after incubation at 37 °C for 6 hours. The complemented strains and PAKΔ*gacS* + pHERD20T-*gacS* L309R were demonstrated not to be significantly different from PAK pHERD20T. Assay was performed in triplicate. * indicates that the strain demonstrated significantly more biofilm production than PAK pHERD20T. Statistical significance was determined by a two-tailed, non-paired Student's t-test. *$p < 0.01$.

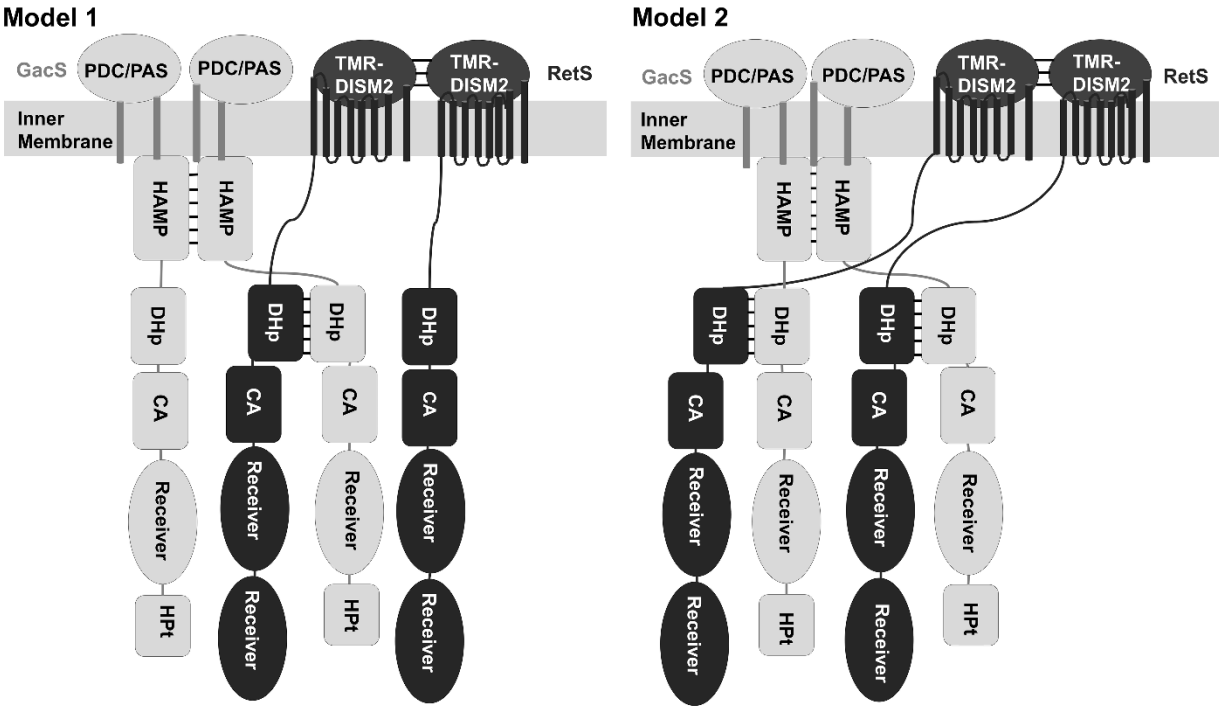

Figure 2.8. Models for RetS-GacS tetramers. Binding between the two proteins could be asymmetric (Model 1), where only one DHp-DHp interface forms. This model allows for the possible formation of a polymer consisting of repeat units of asymmetric tetramers linked through DHp-DHp interactions. Alternatively, RetS and GacS could form a symmetric tetramer with two DHp-DHp interfaces (Model 2).

Supplementary Figures

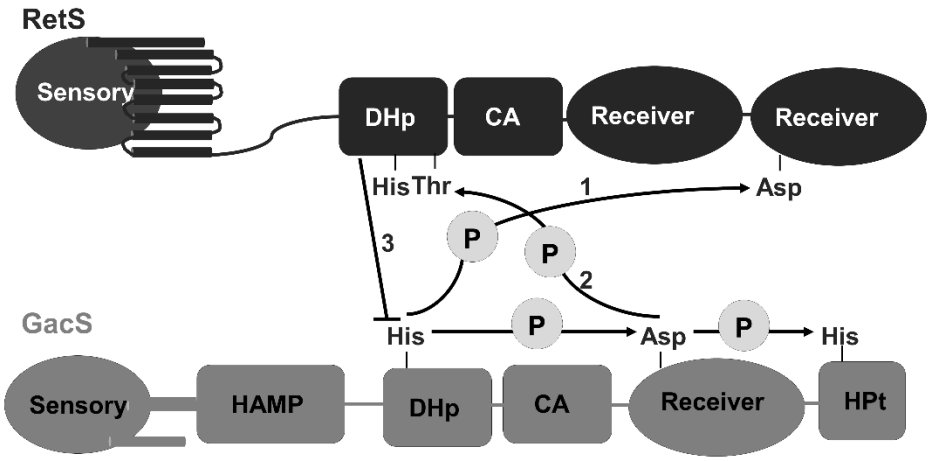

Figure 2.S1. RetS inhibition of GacS. RetS inhibits GacS via three mechanisms as shown by Francis et al., 2018 (46, 49). Mechanism 1 involves the siphoning of phosphates from the catalytic histidine on GacS DHp via the second receiver domain of RetS (46, 49). Mechanism 2 is comparable to transmitter phosphatase activity in which a conserved threonine residue four residues C-terminal to the catalytic histidine on the DHp domain of RetS dephosphorylates the receiver domain of GacS (46). Mechanism 3 is mediated by direct interaction between the DHp domains of RetS and GacS which inhibits GacS autophosphorylation (46, 48).

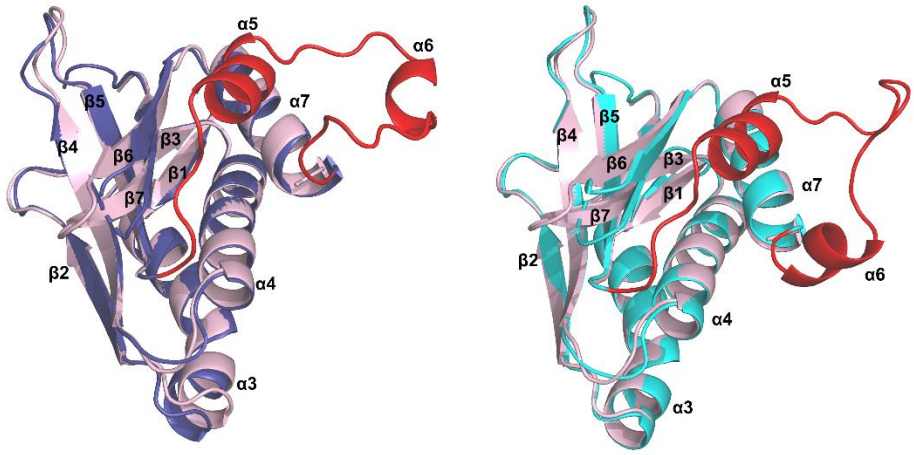

Figure 2.S2. The ATP lid loop region and a short α helix N-terminal to the ATP lid loop region of the RetS CA domain is unstructured (residues 574 – 603) in the RetSHK-GacSDHp structure. In the previous structure of the RetS homodimer (PDB 6dk7), the ATP lid loop region is in two distinct conformations in each of the subunits of the homodimer as observed in the alignments of the CA domain of RetS with the CA domain of the RetS homodimer Chain A (RMSD = 0.289) and with the CA domain of the RetS homodimer Chain B (RMSD = 0.363). RetS is shown in light pink. RetS homodimer Chain A is shown in blue. RetS homodimer Chain B is shown in cyan. The ATP lid loop region is shown in red.

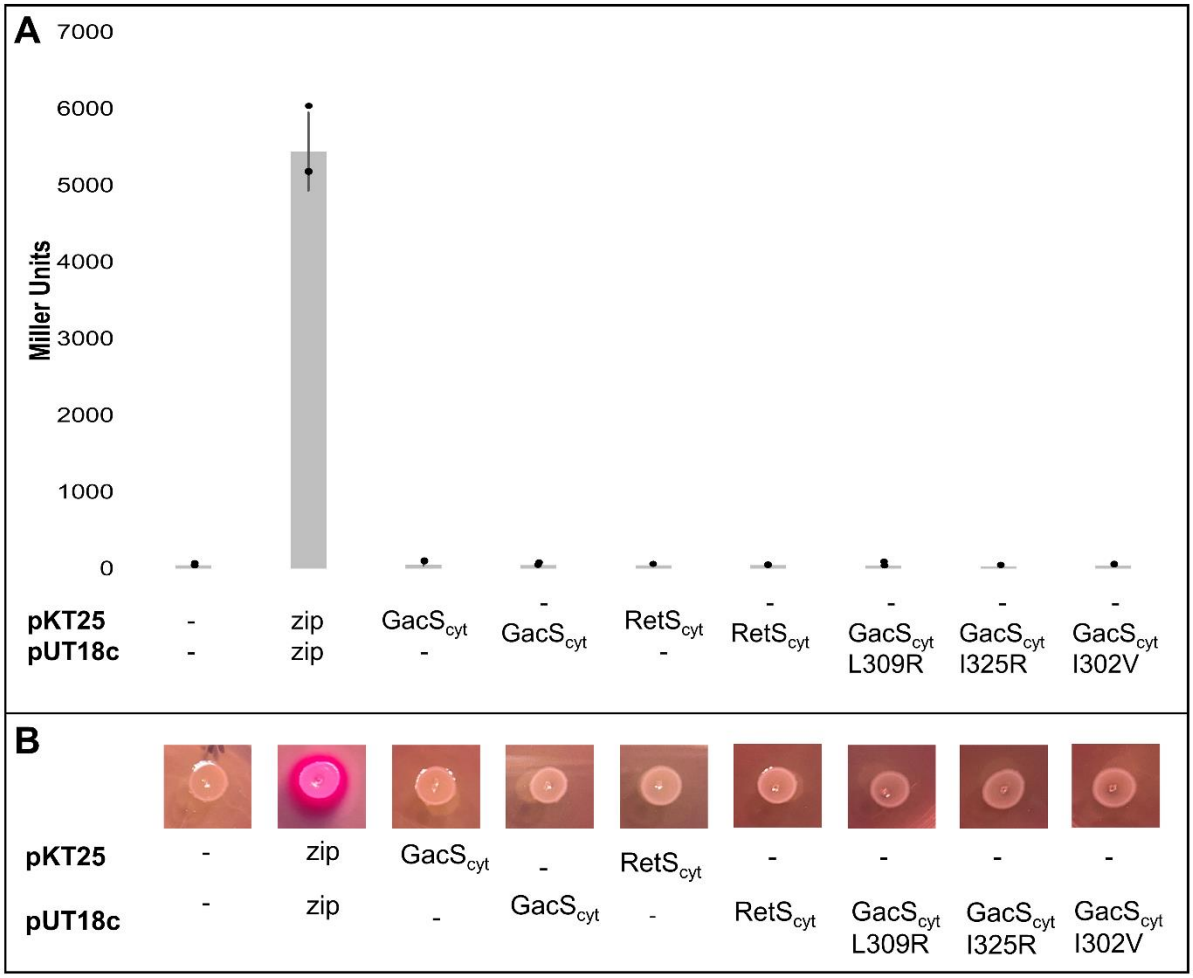

Figure 2.S3. Additional BACTH assay controls. *A*, examination of interface variants in the BACTH β-galactosidase assay. Interface variants were examined in the BACTH β-galactosidase assay after 24 hours incubation at 30℃. Assay was performed in triplicate. *B*, examination of interface variants in the BACTH MacConkey agar assay. Interface variants were examined in the BACTH MacConkey agar assay after 24 hours incubation at 32℃. Assay was performed in triplicate.

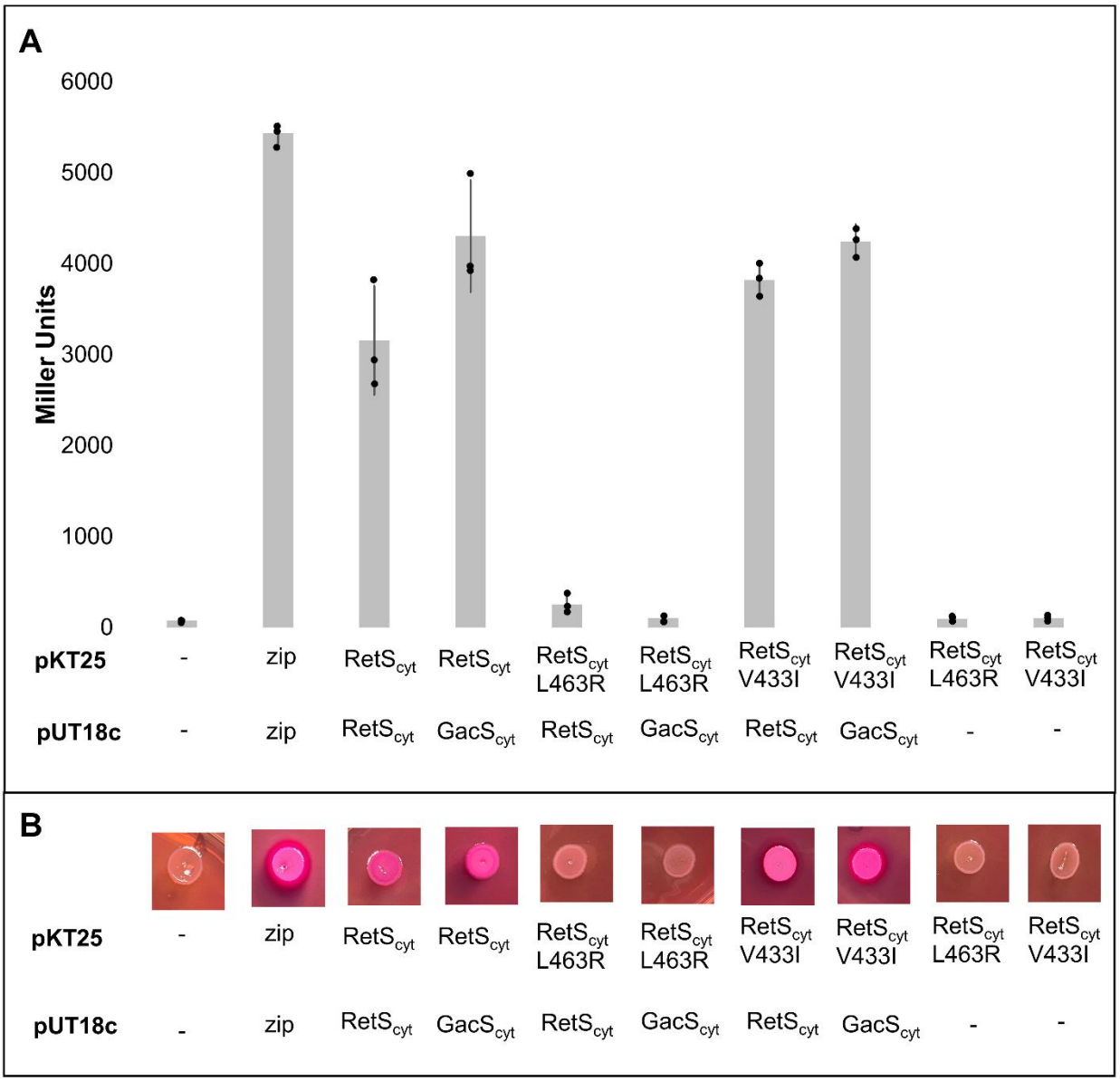

Figure 2.S4. $RetS_{cyt}$ variants in the BACTH assay. *A*, examination of interface variants in the BACTH β-galactosidase assay. Interface variants were examined in the BACTH β-galactosidase assay after 24 hours incubation at 30°C. Assay was performed in triplicate. Statistical significance was determined by a two-tailed, non-paired Student's t-test. *$p < 0.01$, **$p < 0.001$. *B*, examination of interface variants in the BACTH MacConkey agar assay. Interface variants were examined in the BACTH MacConkey agar assay after 24 hours incubation at 32°C. Assay was performed in triplicate.

Table 2.S1. Cloning Primers

GacS_350_stop_F	5’ – gaggttttccagaacctacttgccggcctcgatc – 3’
GacS_350_stop_R	5’ – gatcgaggccggcaagtaggttctggaaaacctc – 3’
attb1.1newTEV_F	5’ – ggggacaagtttgtacaaaaaagcaggctctgagaacctgtacttccag – 3’
GacS509STPx2_F	5’ – tggatcagcctgagtctgtagtaaagtcgcgacgacaacg – 3’
GacS509STPx2_R	5’ – cgttgtcgtcgcgactttactacagactcaggctgatcca – 3’
RetSL463R_F	5’ – gatcagcgtgagccgctcgttgccggc – 3’
RetSL463R_R	5’ – gccggcaacgagcggctcacgctgatc – 3’
RetSV433I_F	5’ – cgcccatgaacggcatactgggcatgaccga – 3’
RetSV433I_R	5’ – tcggtcatgcccagtatgccgttcatgggcg – 3’
GacSL309R_F	5’ – agctcgctcttctgccgcaggttggtgaaac – 3’
GacSL309R_R	5’ – gtttcaccaacctgcggcagaagagcgagct – 3’
GacSI325R_F	5’ – ctttccgccgatttctgcctggtcgtgaggtagtcc – 3’
GacSI325R_R	5’ – ggactacctcacgaccaggcagaaatcggcggaaag – 3’
GacSI302V_F	5’ – cccgctcaacggcgtcctcggtttcac – 3’
GacSI302V_R	5’ – gtgaaaccgaggacgccgttgagcggg – 3’
GacSH293A_F	5’ – tcgccaacatgagcgccgagatccgcaccc – 3’
GacSH293A_R	5’ – gggtgcggatctcggcgctcatgttggcga – 3’
GacSG472A_G474A_F	5’ – caagccggtgccaccgccctgggcctg – 3’
GacSG472A_G474A_R	5’ – caggcccagggcggtggcaccggcttg – 3’

Table 2.S2. Recombinant DNA

Recombinant DNA	Source
pDEST-HisMBP-RetS$_{HK}$	Mancl et al., 2019
pDEST-HisMBP	Invitrogen
pDONR221	Invitrogen
pDEST-HisMBP-GacS$_{HK}$	This study
pDEST-HisMBP-GacS$_{DHp}$	This study
pKT25	Euromedex
pUT18c	Euromedex
pKT25zip	Euromedex
pUT18czip	Euromedex
pKT25-RetS$_{HK}$-GFP	Mancl et al., 2019
pUT18c-GacS$_{HK}$	This study
pUT18c-GacS$_{HK}$ L309R	This study
pUT18c-GacS$_{HK}$ I325R	This study
pUT18c-GacS$_{HK}$ I302V	This study
pKT25-RetS$_{cyt}$-GFP	Mancl et al., 2019
pUT18c-GacS$_{cyt}$	Mancl et al., 2019
pKT25-RetS$_{cyt}$-GFP V433I	This study
pKT25-RetS$_{cyt}$-GFP L463R	This study
pUT18c-GacS$_{cyt}$ L309R	This study
pUT18c-GacS$_{cyt}$ I325R	This study
pUT18c-GacS$_{cyt}$ I302V	This study

pQE60-GacS$_{cyt}$	Francis et al., 2018
pQE60-GacS$_{cyt}$ H293A	This study
pQE60-GacS$_{cyt}$ G472A G474A	This study
pHERD20T	Qiu et al., 2018
pHERD20T-*retS*	Mancl et al., 2019
pHERD20T-*gacS*	Mancl, 2018
pHERD20T-*gacS* L309R	This study
pHERD20T-*gacS* I302V	This study

Table 2.S3. Buffers Used

Buffer	Composition	Purpose
NiNTA A Buffer	50 mM tris pH 7.4, 500 mM NaCl, 5 % glycerol, 25 mM imidazole pH 7.4, 1 mM DTT	Cell resuspension, binding to NiNTA column
NiNTA B Buffer	50 mM tris pH 7.4, 500 mM NaCl, 5 % glycerol, 250 mM imidazole pH 7.4, 1 mM DTT	Elution from NiNTA column
Anion Exchange Buffer A	50 mM tris pH 7.4, 50 mM NaCl, 10 % glycerol, 1 mM DTT	Binding to anion exchange column
Anion Exchange Buffer B	50 mM tris pH 7.4, 500 mM NaCl, 10 % glycerol, 1 mM DTT	Elution from anion exchange column
$RetS_{HK}$ Gel Filtration Buffer	25 mM tris pH 7.4, 125 mM NaCl, 2.5 % glycerol, 2 mM TCEP pH 8.0	Size exclusion gel filtration column elution, crystallization buffer
$GacS_{cyt}$ NiNTA A Buffer	50 mM HEPES pH 7.4, 500 mM NaCl, 5 % glycerol, 25 mM imidazole pH 7.4, 1 mM DTT	Cell resuspension, binding to NiNTA column
$GacS_{cyt}$ NiNTA B Buffer	50 mM HEPES pH 7.4, 500 mM NaCl, 5 % glycerol, 250 mM imidazole pH 7.4, 1 mM DTT	Elution from NiNTA column
$GacS_{cyt}$ Gel Filtration Buffer	50 mM tris pH 7.4, 150 mM NaCl, 10% (v/v) glycerol, 1 mM TCEP pH 8, 5 mM $MgCl_2$, 50 mM KCl, pH adjusted to 8	Size exclusion gel filtration column elution

Author Contributions

K.R.K. designed the research, conducted the research, analyzed results, and wrote the manuscript. J.C.N. performed X-ray diffraction data collection, data processing, and data scaling. F.D.S. designed the research, supervised the research, analyzed results, and wrote the manuscript.

Acknowledgments

We would like to thank Dr. Stephen Porter (University of Exeter) for his gift of pQE60-GacS$_{cyt}$. We would also like to thank Dr. Alain Filloux (Imperial College London) for his gift of *P. aeruginosa* PAK strains.

Chapter 3: Final Discussion

Canonically, two-component systems and phosphorelays are considered to be isolated linear signal transduction pathways (183). Crosswise interactions between proteins involved in these signal transduction pathways, defined as crosstalk by Laub and Goulian, were previously thought to be unfavorable and therefore selected against by evolution (14, 183). However, evidence of crosstalk in two-component systems and phosphorelays has been mounting (14, 42, 156, 184). More recently, the role of multikinase networks (MKNs) linking multiple two-component and phosphorelay signal transduction systems via crosswise HK interactions has become noteworthy (47). The MKN that controls the switch between the motile invasive lifestyle and the sessile biofilm-associated lifestyle in *Pseudomonas aeruginosa* is the most complex MKN studied to date with interactions occurring among seven HKs (GacS, RetS, LadS, PA1611, ErcS, SagS, and BfiS) (47, 50, 51, 67, 135, 148–150, 152, 153). The aforementioned GacS/GacA phosphorelay has a prominent position within this MKN. The HK GacS is reciprocally regulated by two HKs, LadS and RetS, with LadS enhancing the activity of GacS via a phosphotransfer and RetS inhibiting the activity of GacS via three distinct mechanisms (46, 48, 70, 135, 141, 142, 144). Two of the inhibitory mechanisms are dephosphorylating mechanisms and the third mechanism is the inhibition of GacS autophosphorylation via a direct interaction between RetS and GacS (36, 46, 48). It is the direct interaction between RetS and GacS that this work has examined.

In 2009 Goodman et al. discovered the direct interaction between the HKs RetS and GacS and the resulting inhibition of GacS autophosphorylation (48). Goodman et al. proposed the initial model for GacS inhibition by RetS, in which the formation of a heterodimeric RetS-

GacS complex inhibits GacS *trans* autophosphorylation (48). In 2018 Francis et al. furthered our understanding of the interactions between RetS and GacS by demonstrating that RetS not only inhibits GacS autophosphorylation through the already proven direct interaction, but also inhibits GacS via two distinct dephosphorylating mechanisms (46). Both dephosphorylating mechanisms used by RetS appear to have evolved from canonical HK phosphotransfer mechanisms or phosphatase activity (46). In the case of the dephosphorylation of the conserved histidine residue of GacS by the second receiver domain of RetS, the dephosphorylating mechanism is a redirection of the GacS phosphotransfer reaction (46). In the case of the dephosphorylation of the receiver domain of GacS via a conserved threonine residue of RetS, the phosphatase activity mimics the transmitter phosphatase activity that many HKs have for their cognate RRs (46). In 2019 Mancl et al. disproved the initial model for RetS inhibition of GacS via heterodimeric complex formation and instead demonstrated that the GacS homodimer is not disrupted upon RetS binding (36). This finding brought forth a new model in which RetS and GacS bind through their dimerization and histidine phosphotransfer (DHp) domains at an interface that is distinct from the canonical homodimerization DHp-DHp interface (36). In Chapter 2, we demonstrated that, contrary to the model proposed by Mancl et al., the canonical homodimerization interface of GacS is disrupted upon RetS binding due to the formation of a localized heterodimeric HK region between RetS and GacS (36, 145). In other words, similar to the other two mechanisms used by RetS to inhibit GacS, the direct interaction between RetS and GacS HK regions also mimics a canonical HK interface (145). It is likely that the heterodimeric RetS-GacS interface evolved from the canonical homodimerization interfaces. While most often specificity residues provide a means of molecular recognition between an HK and its cognate RR or between the two subunits of HKs in a homodimer, we have identified a residue (GacS I302) that provides

specificity to the RetS-GacS heterodimeric interface, demonstrating that at least one heterodimeric specificity residue has evolved to maintain this interaction (3, 14, 19, 37–40, 145). The apparent contradiction between the findings of Mancl et al. and our recent findings was integrated through an examination of the domains that were used in each experiment. In the binding studies performed by Mancl et al. the RetS and GacS constructs comprised the cytoplasmic portions of the proteins, which includes the HAMP domain in GacS (36). HAMP domains are known to dimerize, and in *Pseudomonas fluorescens* the HAMP domain is necessary for GacS homodimerization (162). Thus, GacS maintained its overall homodimeric form through contacts in the HAMP domain, while RetS and GacS formed a localized heterodimeric HK region at the canonical DHp-DHp dimerization interface (36, 145). The finding that Rets and GacS form a domain swapped heterodimeric HK region explains how RetS binding inhibits GacS autophosphorylation, which was demonstrated to occur in *trans* (46, 48, 150). In Chapter 2, we also discussed dynamic structural features of RetS that were found to play distinct roles in the RetS homodimer and in the RetS-GacS heterodimer (36, 145). These features, the N-terminal region of the RetS DHp domain and the RetS ATP lid loop region, likely play roles in regulating RetS-GacS interactions (36, 145). In particular, the N-terminal region of DHp domains in canonical HKs is highly plastic, and it is this plasticity that is in part responsible for mediating the accessibility of the catalytic histidine and the dynamic changes needed for autophosphorylation, phosphotransfer and phosphatase activity (29, 36, 145). This N-terminal region of the DHp domain of RetS is necessary for the formation of the RetS-GacS complex (36). Therefore, the N-terminal region of the DHp domain of RetS may not only be critical for RetS-GacS binding, but also for stimulating the phosphatase activity of RetS.

While MKNs are known, direct HK-HK interactions are few, with the direct interaction between RetS and GacS being the best characterized. RetS also has a direct interaction with another HK, PA1611 (50, 51). While the heterodimeric DHp-DHp interface between RetS and GacS replaces the canonical homodimeric DHp-DHp interface, RetS appears to use its CA domain to interact with the DHp domain of PA1611 (51, 145). The lack of overlap between the RetS-GacS interface and the RetS-PA1611 interface suggests that interactions between PA1611 and RetS allosterically regulate RetS-GacS binding.

We can speculate about the size of the RetS-GacS complex based upon studies with truncated proteins, but we likely need to examine the interaction between the full-length proteins to understand the extent of the complex. Domains other than the DHp have roles to play in the formation of the heterocomplex. While the inclusion of the GacS HAMP domain in the FRET studies performed by Mancl et al. enabled GacS to maintain its homodimeric form upon RetS binding, the lack of inclusion of the GacS HAMP domain in the structural examination of the RetS-GacS complex resulted in a smaller complex than would be expected for the full-length proteins (36, 145). The periplasmic sensory domain of RetS is known to homodimerize (144). This suggests that RetS may also maintain homodimeric contacts while forming a heterodimeric DHp-DHp interface. While the heterocomplex revealed the RetS-GacS interface, it only established a section of the complex. Future, in *vivo* and in *vitro* experiments with the full-length proteins could focus on the determination of the size of the RetS-GacS assembly and dynamic changes that occur at the onset of biofilm formation or through the binding of other extracellular stimulants such as a component of the *P. aeruginosa* lysate (146).

The ligands of many HKs remain unknown. The GacS PDC/PAS sensory domain is necessary for regulating output through the Gac/Rsm pathway (26). While the PDC/PAS domain

suggests that GacS senses metabolites (specifically carboxylic acids), oxygen, redox potential or light, the actual ligand remains elusive (5, 24–27, 139, 140). We know that sensory domain stimulation through GacS results in promotion of the sessile biofilm lifestyle, which could occur due to the disruption of RetS-GacS binding, the stimulation of GacS autophosphorylation or both (26). Two signals have been identified that interact with the sensory domain of RetS resulting in output through the Gac/Rsm pathway. While a constituent of kin cell lysis interacts with the periplasmic sensory domain of RetS resulting in the reversal of GacS inhibition, the exact component of kin cell lysis is unknown (146). The relief of GacS inhibition upon RetS binding to a component of kin cell lysis suggests that kin cell lysis may act as a danger signal that enables *P. aeruginosa* to react by promoting the sessile biofilm lifestyle, which would enable it to evade antimicrobials and the host immune response (146). Lysis of a subpopulation of cells within the mature biofilm has also been demonstrated to precede biofilm dissolution in *P. aeruginosa* (107). Altogether this suggests that cell lysis may have multiple roles to play in the regulation of biofilm formation. The sensory domain of RetS also binds to host cell mucin glycans which result in GacS inhibition, demonstrating that mucin glycans are a host signal that promotes the motile invasive lifestyle (147). The 7 TMR-DISM2 sensory domain of RetS possesses a carbohydrate binding motif which may mediate mucin glycan binding or mediate binding to a carbohydrate component of kin cell lysis (142, 144). While input signals for RetS have been discovered, it is unknown whether those signals regulate the RetS-GacS complex and/or RetS phosphatase activity. The ability of RetS to sense multiple signals enhances the complexity of the signal transduction pathway. It will be interesting to discover the role of GacS signal sensing in the interaction between RetS and GacS. In the future, the structures of full-length RetS and GacS individually and in complex will be examined in the presence and absence of ligand. This

will allow us to compare ligand bound proteins to apo proteins to assess the impact of ligand binding on the activity of RetS and GacS, such as how ligand binding controls the RetS-GacS complex and the activity state (autophosphorylation, phosphotransfer and phosphatase activity) of the proteins. Combined with the structural studies, we will use molecular techniques to examine the regulation of complex formation and the activity state of the proteins. Autophosphorylation and binding assays post sensory domain stimulation of RetS and GacS may enable the assessment of the impact of sensory domain stimulation on the RetS-GacS complex or the kinase and phosphatase activity of GacS and RetS, respectively. Prior to the above-mentioned studies, the exact ligands need to be identified for RetS and GacS.

The interactions between RetS and GacS exemplify the importance of nonlinear signal transmission in two-component systems and phosphorelays. Heterodimeric bacterial HKs currently appear to be novel, but there are other HKs that also form heteromeric complexes, and the RetS-GacS co-complex can serve as a model (47).

The present work is also of significant biomedical interest. Bacterial HKs are promising targets for antimicrobials in part because they lack homologs in humans and because they are ubiquitous and have tertiary structural conservation among bacteria (185). Antimicrobials capable of disrupting RetS-GacS interactions would alter the infection state of *P. aeruginosa* within a human host. An alteration to the finely regulated Gac/Rsm pathway is likely to impact the fitness of *P.aeruginosa*, possibly resulting in an advantage to the host immune system over that of *P. aeruginosa*. In particular, an antimicrobial that results in the inhibition of GacS during biofilm development may force *P. aeruginosa* into an invasive infection state that is more immunogenic and susceptible to antimicrobial treatment enabling the host immune response in conjunction with antimicrobials to eradicate the *P. aeruginosa* infection. Since the interactions

between RetS and GacS control the outcome of a *P. aeruginosa* infection, a clear understanding of these interactions is necessary to combat *P. aeruginosa* infections.

Bibliography

1. Whitworth, D. E., and Cock, P. J. A. (2009) Evolution of prokaryotic two-component systems: Insights from comparative genomics. *Amino Acids*. **37**, 459–466
2. Stock, A. M., Robinson, V. L., and Goudreau, P. N. (2000) Two-component signal transduction. *Annu. Rev. Biochem.* **69**, 183–215
3. Buschiazzo, A., and Trajtenberg, F. (2019) Two-component sensing and regulation: How do histidine kinases talk with response regulators at the molecular level? *Annu. Rev. Microbiol.* 10.1146/annurev-micro-091018-054627
4. Sevilla, E., Silva-Jiménez, H., Duque, E., Krell, T., and Rojo, F. (2013) The *Pseudomonas putida* HskA hybrid sensor kinase controls the composition of the electron transport chain. *Environ. Microbiol. Rep.* **5**, 291–300
5. Gao, R., and Stock, A. M. (2009) Biological insights from structures of two-component proteins. *Annu. Rev. Microbiol.* **63**, 133–154
6. Wuichet, K., Cantwell, B. J., and Zhulin, I. B. (2010) Evolution and phyletic distribution of two-component signal transduction systems. *Curr. Opin. Microbiol.* **13**, 219–225
7. Krell, T., Lacal, J., Busch, A., Silva-Jiménez, H., Guazzaroni, M. E., and Ramos, J. L. (2010) Bacterial sensor kinases: Diversity in the recognition of environmental signals. *Annu. Rev. Microbiol.* **64**, 539–559
8. Rojo, F. (2010) Carbon catabolite repression in *Pseudomonas*: Optimizing metabolic versatility and interactions with the environment. *FEMS Microbiol. Rev.* **34**, 658–684
9. Dinamarca, M. A., Aranda-Olmedo, I., Puyet, A., and Rojo, F. (2003) Expression of the *Pseudomonas putida* OCT plasmid alkane degradation pathway is modulated by two different global control signals: Evidence from continuous cultures. *J. Bacteriol.* **185**,

4772–4778

10. West, A. H., and Stock, A. M. (2001) Histidine kinases and response regulator proteins in two-component signaling systems. *Trends Biochem. Sci.* **26**, 369–376

11. Wolanin, P. M., Thomason, P. A., and Stock, J. B. (2002) Histidine protein kinases: Key signal transducers outside the animal kingdom. *Genome Biol.* 10.1186/gb-2002-3-10-reviews3013

12. Rodrigue, A., Quentin, Y., Lazdunski, A., Méjean, V., and Foglino, M. (2000) Two-component systems in *Pseudomonas aeruginosa*: Why so many? *Trends Microbiol.* **8**, 498–504

13. Jacob-Dubuisson, F., Mechaly, A., Betton, J. M., and Antoine, R. (2018) Structural insights into the signalling mechanisms of two-component systems. *Nat. Rev. Microbiol.* 10.1038/s41579-018-0055-7

14. Laub, M. T., and Goulian, M. (2007) Specificity in two-component signal transduction pathways. *Annu. Rev. Genet.* **41**, 121–145

15. Casino, P., Rubio, V., and Marina, A. (2010) The mechanism of signal transduction by two-component systems. *Curr. Opin. Struct. Biol.* **20**, 763–771

16. Merritt, J. H., Ha, D. G., Cowles, K. N., Lu, W., Morales, D. K., Rabinowitz, J., Gitai, Z., and O'Toole, G. A. (2010) Specific control of *Pseudomonas aeruginosa* surface-associated behaviors by two c-di-GMP diguanylate cyclases. *MBio*. 10.1128/mBio.00183-10

17. Kenney, L. J. (2010) How important is the phosphatase activity of sensor kinases? *Curr. Opin. Microbiol.* **13**, 168–176

18. Huynh, T. A. N., Noriega, C. E., and Stewart, V. (2010) Conserved mechanism for sensor

phosphatase control of two-component signaling revealed in the nitrate sensor NarX. *Proc. Natl. Acad. Sci. U. S. A.* 10.1073/pnas.1013081107

19. Casino, P., Miguel-Romero, L., and Marina, A. (2014) Visualizing autophosphorylation in histidine kinases. *Nat. Commun.* 10.1038/ncomms4258

20. Cheung, J., and Hendrickson, W. A. (2010) Sensor domains of two-component regulatory systems. *Curr. Opin. Microbiol.* 10.1016/j.mib.2010.01.016

21. Mascher, T., Helmann, J. D., and Unden, G. (2006) Stimulus Perception in Bacterial Signal-Transducing Histidine Kinases. *Microbiol. Mol. Biol. Rev.* 10.1128/mmbr.00020-06

22. Vladimirov, I. A., Matveeva, T. V., and Lutova, L. A. (2015) Opine biosynthesis and catabolism genes of *Agrobacterium tumefaciens* and *Agrobacterium rhizogenes*. *Russ. J. Genet.* 10.1134/S1022795415020167

23. Galperin, M. Y., Nikolskaya, A. N., and Koonin, E. V. (2001) Novel domains of the prokaryotic two-component signal transduction systems. *FEMS Microbiol. Lett.* 10.1016/S0378-1097(01)00326-3

24. Vreede, J., Van der Horst, M. A., Hellingwerf, K. J., Crielaard, W., and Van Aalten, D. M. F. (2003) PAS domains. Common structure and common flexibility. *J. Biol. Chem.* 10.1074/jbc.M301701200

25. Taylor, B. L., and Zhulin, I. B. (1999) PAS Domains: Internal Sensors of Oxygen, Redox Potential, and Light. *Microbiol. Mol. Biol. Rev.* 10.1128/mmbr.63.2.479-506.1999

26. Ali-Ahmad, A., Fadel, F., Sebban-Kreuzer, C., Ba, M., Pélissier, G. D., Bornet, O., Guerlesquin, F., Bourne, Y., Bordi, C., and Vincent, F. (2017) Structural and functional insights into the periplasmic detector domain of the GacS histidine kinase controlling

biofilm formation in *Pseudomonas aeruginosa*. *Sci. Rep.* 10.1038/s41598-017-11361-3

27. Shah, N., Gaupp, R., Moriyama, H., Eskridge, K. M., Moriyama, E. N., and Somerville, G. A. (2013) Reductive evolution and the loss of PDC/PAS domains from the genus *Staphylococcus*. *BMC Genomics*. 10.1186/1471-2164-14-524

28. DuprÃ, E., Clantin, B., Yuan, Y., Lecher, S., Lesne, E., Antoine, R., Villeret, V., and Jacob-Dubuisson, F. (2021) Structural Insight into the Role of the PAS Domain for Signal Transduction in Sensor Kinase BvgS. *J. Bacteriol.* 10.1128/JB.00614-20

29. Bhate, M. A. P., Molnar, K. A. S., Goulian, M., and Degrado, W. F. (2015) Signal Transduction in Histidine Kinases: Insights from New Structures. *Structure*. **23**, 981–994

30. Berntsson, O., Diensthuber, R. P., Panman, M. R., Björling, A., Gustavsson, E., Hoernke, M., Hughes, A. J., Henry, L., Niebling, S., Takala, H., Ihalainen, J. A., Newby, G., Kerruth, S., Heberle, J., Liebi, M., Menzel, A., Henning, R., Kosheleva, I., Möglich, A., and Westenhoff, S. (2017) Sequential conformational transitions and α-helical supercoiling regulate a sensor histidine kinase. *Nat. Commun.* 10.1038/s41467-017-00300-5

31. Möglich, A. (2019) Signal transduction in photoreceptor histidine kinases. *Protein Sci.* 10.1002/pro.3705

32. Stewart, V., and Chen, L. L. (2010) The S helix mediates signal transmission as a HAMP domain coiled-coil extension in the NarX nitrate sensor from *Escherichia coli* K-12. *J. Bacteriol.* 10.1128/JB.00172-09

33. Gushchin, I., Melnikov, I., Polovinkin, V., Ishchenko, A., Yuzhakova, A., Buslaev, P., Bourenkov, G., Grudinin, S., Round, E., Balandin, T., Borshchevskiy, V., Willbold, D., Leonard, G., Büldt, G., Popov, A., and Gordeliy, V. (2017) Mechanism of transmembrane

signaling by sensor histidine kinases. *Science (80-.).* 10.1126/science.aah6345

34. Parkinson, J. S. (2010) Signaling Mechanisms of HAMP domains in chemoreceptors and sensor kinases. *Annu. Rev. Microbiol.* **64**, 101–122

35. Matamouros, S., Hager, K. R., and Miller, S. I. (2015) HAMP domain rotation and tilting movements associated with signal transduction in the PhoQ sensor kinase. *MBio*. 10.1128/mBio.00616-15

36. Mancl, J. M., Ray, W. K., Helm, R. F., and Schubot, F. D. (2019) Helix Cracking Regulates the Critical Interaction between RetS and GacS in *Pseudomonas aeruginosa*. *Structure*. **27**, 785-793.e5

37. Capra, E. J., Perchuk, B. S., Skerker, J. M., and Laub, M. T. (2012) Adaptive mutations that prevent crosstalk enable the expansion of paralogous signaling protein families. *Cell*. **150**, 222–232

38. Capra, E. J., and Laub, M. T. (2012) Evolution of two-component signal transduction systems. *Annu. Rev. Microbiol.* **66**, 325–347

39. Willett, J. W., Tiwari, N., Müller, S., Hummels, K. R., Houtman, J. C. D., Fuentes, E. J., and Kirby, J. R. (2013) Specificity residues determine binding affinity for two-component signal transduction systems. *MBio*. 10.1128/mBio.00420-13

40. Skerker, J. M., Perchuk, B. S., Siryaporn, A., Lubin, E. A., Ashenberg, O., Goulian, M., and Laub, M. T. (2008) Rewiring the Specificity of Two-Component Signal Transduction Systems. *Cell*. **133**, 1043–1054

41. Capra, E. J., Perchuk, B. S., Ashenberg, O., Seid, C. A., Snow, H. R., Skerker, J. M., and Laub, M. T. (2012) Spatial tethering of kinases to their substrates relaxes evolutionary constraints on specificity. *Mol. Microbiol.* **86**, 1393–1403

42. Siryaporn, A., Perchuk, B. S., Laub, M. T., and Goulian, M. (2010) Evolving a robust signal transduction pathway from weak cross-talk. *Mol. Syst. Biol.* 10.1038/msb.2010.105

43. Siryaporn, A., and Goulian, M. (2008) Cross-talk suppression between the CpxA-CpxR and EnvZ-OmpR two-component systems in E. coli. *Mol. Microbiol.* **70**, 494–506

44. Huynh, T. A. N., and Stewart, V. (2011) Negative control in two-component signal transduction by transmitter phosphatase activity. *Mol. Microbiol.* **82**, 275–286

45. Ashenberg, O., Rozen-Gagnon, K., Laub, M. T., and Keating, A. E. (2011) Determinants of homodimerization specificity in histidine kinases. *J. Mol. Biol.* **413**, 222–235

46. Francis, V. I., Waters, E. M., Finton-James, S. E., Gori, A., Kadioglu, A., Brown, A. R., and Porter, S. L. (2018) Multiple communication mechanisms between sensor kinases are crucial for virulence in *Pseudomonas aeruginosa*. *Nat. Commun.* 10.1038/s41467-018-04640-8

47. Francis, V. I., and Porter, S. L. (2019) Multikinase networks: Two-component signaling networks integrating multiple stimuli. *Annu. Rev. Microbiol.* **73**, 199–223

48. Goodman, A. L., Merighi, M., Hyodo, M., Ventre, I., Filloux, A., and Lory, S. (2009) Direct interaction between sensor kinase proteins mediates acute and chronic disease phenotypes in a bacterial pathogen. *Genes Dev.* **23**, 249–259

49. Laskowski, M. A., and Kazmierczak, B. I. (2006) Mutational analysis of RetS, an unusual sensor kinase-response regulator hybrid required for *Pseudomonas aeruginosa* virulence. *Infect. Immun.* **74**, 4462–4473

50. Kong, W., Chen, L., Zhao, J., Shen, T., Surette, M. G., Shen, L., and Duan, K. (2013) Hybrid sensor kinase PA1611 in *Pseudomonas aeruginosa* regulates transitions between acute and chronic infection through direct interaction with RetS. *Mol. Microbiol.* **88**, 784–

797

51. Bhagirath, A. Y., Pydi, S. P., Li, Y., Lin, C., Kong, W., Chelikani, P., and Duan, K. (2017) Characterization of the Direct Interaction between Hybrid Sensor Kinases PA1611 and RetS That Controls Biofilm Formation and the Type III Secretion System in *Pseudomonas aeruginosa*. *ACS Infect. Dis.* **3**, 162–175
52. Weiner, J., Beaussart, F., and Bornberg-Bauer, E. (2006) Domain deletions and substitutions in the modular protein evolution. *FEBS J.* 10.1111/j.1742-4658.2006.05220.x
53. Patthy, L. (2008) *Protein Evolution*, 2nd Ed., Blackwell Publishing Ltd.
54. Björklund, Å. K., Ekman, D., Light, S., Frey-Skött, J., and Elofsson, A. (2005) Domain rearrangements in protein evolution. *J. Mol. Biol.* 10.1016/j.jmb.2005.08.067
55. Ponting, C. P., and Russell, R. R. (2002) The natural history of protein domains. *Annu. Rev. Biophys. Biomol. Struct.* 10.1146/annurev.biophys.31.082901.134314
56. Alm, E., Huang, K., and Arkin, A. (2006) The evolution of two-component systems in bacteria reveals different strategies for niche adaptation. *PLoS Comput. Biol.* 10.1371/journal.pcbi.0020143
57. Bordin, N., Sillitoe, I., Lees, J. G., and Orengo, C. (2021) Tracing Evolution Through Protein Structures: Nature Captured in a Few Thousand Folds. *Front. Mol. Biosci.* 10.3389/fmolb.2021.668184
58. Whitworth, D. E., Holmes, A. B., Irvine, A. G., Hodgson, D. A., and Scanlan, D. J. (2008) Phosphate acquisition components of the *Myxococcus xanthus* pho regulon are regulated by both phosphate availability and development. *J. Bacteriol.* 10.1128/JB.01781-07
59. Moraleda-Muñoz, A., Carrero-Lérida, J., Pérez, J., and Muñoz-Dorado, J. (2003) Role of

two novel two-component regulatory systems in development and phosphatase expression in *Myxococcus xanthus*. *J. Bacteriol.* 10.1128/JB.185.4.1376-1383.2003

60. Pérez-Morales, D., Banda, M. M., Chau, N. Y. E., Salgado, H., Martínez-Flores, I., Ibarra, J. A., Ilyas, B., Coombes, B. K., and Bustamante, V. H. (2017) The transcriptional regulator SsrB is involved in a molecular switch controlling virulence lifestyles of *Salmonella*. *PLoS Pathog.* 10.1371/journal.ppat.1006497

61. Dutta, R., Qin, L., and Inouye, M. (1999) Histidine kinases: Diversity of domain organization. *Mol. Microbiol.* 10.1046/j.1365-2958.1999.01646.x

62. Dutta, R., and Inouye, M. (2000) GHKL, an emergent ATPase/kinase superfamily. *Trends Biochem. Sci.* 10.1016/S0968-0004(99)01503-0

63. Qian, W., Han, Z. J., and He, C. (2008) Two-component signal transduction systems of *Xanthomonas* spp.: A lesson from genomics. *Mol. Plant-Microbe Interact.* 10.1094/MPMI-21-2-0151

64. Zhang, W., and Shi, L. (2005) Distribution and evolution of multiple-step phosphorelay in prokaryotes: Lateral domain recruitment involved in the formation of hybrid-type histidine kinases. *Microbiology*. 10.1099/mic.0.27987-0

65. Mikkelsen, H., Sivaneson, M., and Filloux, A. (2011) Key two-component regulatory systems that control biofilm formation in *Pseudomonas aeruginosa*. *Environ. Microbiol.* **13**, 1666–1681

66. Goodman, A. L., Kulasekara, B., Rietsch, A., Boyd, D., Smith, R. S., and Lory, S. (2004) A signaling network reciprocally regulates genes associated with acute infection and chronic persistence in *Pseudomonas aeruginosa*. *Dev. Cell*. **7**, 745–754

67. Francis, V. I., Stevenson, E. C., and Porter, S. L. (2017) Two-component systems required

for virulence in *Pseudomonas aeruginosa*. *FEMS Microbiol. Lett.* 10.1093/femsle/fnx104

68. Lyczak, J. B., Cannon, C. L., and Pier, G. B. (2000) Establishment of *Pseudomonas aeruginosa* infection: Lessons from a versatile opportunist. *Microbes Infect.* **2**, 1051–1060

69. Lyczak, J. B., Cannon, C. L., and Pier, G. B. (2002) Lung infections associated with cystic fibrosis. *Clin. Microbiol. Rev.* **15**, 194–222

70. Yahr, T. L., and Greenberg, E. P. (2004) The genetic basis for the commitment to chronic versus acute infection in *Pseudomonas aeruginosa*. *Mol. Cell*. **16**, 497–498

71. Intile, P. J., Balzer, G. J., Wolfgang, M. C., and Yahr, T. L. (2015) The RNA helicase DeaD stimulates ExsA translation to promote expression of the *Pseudomonas aeruginosa* type III secretion system. *J. Bacteriol.* **197**, 2664–2674

72. Furukawa, S., Kuchma, S. L., and O'Toole, G. A. (2006) Keeping their options open: Acute versus persistent infections. *J. Bacteriol.* 10.1128/JB.188.4.1211-1217.2006

73. Engel, J., and Balachandran, P. (2009) Role of *Pseudomonas aeruginosa* type III effectors in disease. *Curr. Opin. Microbiol.* **12**, 61–66

74. Lorenz, A., Preuße, M., Bruchmann, S., Pawar, V., Grahl, N., Pils, M. C., Nolan, L. M., Filloux, A., Weiss, S., and Häussler, S. (2019) Importance of flagella in acute and chronic *Pseudomonas aeruginosa* infections. *Environ. Microbiol.* 10.1111/1462-2920.14468

75. Moradali, M. F., Ghods, S., and Rehm, B. H. A. (2017) *Pseudomonas aeruginosa* lifestyle: A paradigm for adaptation, survival, and persistence. *Front. Cell. Infect. Microbiol.* 10.3389/fcimb.2017.00039

76. Hauser, A. R. (2009) The type III secretion system of *Pseudomonas aeruginosa*: Infection by injection. *Nat. Rev. Microbiol.* **7**, 654–665

77. Laskowski, M. A., Osborn, E., and Kazmierczak, B. I. (2004) A novel sensor kinase-

response regulator hybrid regulates type III secretion and is required for virulence in *Pseudomonas aeruginosa*. *Mol. Microbiol.* **54**, 1090–1103

78. Korotkov, K. V., Sandkvist, M., and Hol, W. G. J. (2012) The type II secretion system: Biogenesis, molecular architecture and mechanism. *Nat. Rev. Microbiol.* 10.1038/nrmicro2762

79. Rossez, Y., Wolfson, E. B., Holmes, A., Gally, D. L., and Holden, N. J. (2015) Bacterial Flagella: Twist and Stick, or Dodge across the Kingdoms. *PLoS Pathog.* 10.1371/journal.ppat.1004483

80. Liu, R., and Ochman, H. (2007) Stepwise formation of the bacterial flagellar system. *Proc. Natl. Acad. Sci. U. S. A.* 10.1073/pnas.0700266104

81. Craig, L., Forest, K. T., and Maier, B. (2019) Type IV pili: dynamics, biophysics and functional consequences. *Nat. Rev. Microbiol.* 10.1038/s41579-019-0195-4

82. Ryder, C., Byrd, M., and Wozniak, D. J. (2007) Role of polysaccharides in *Pseudomonas aeruginosa* biofilm development. *Curr. Opin. Microbiol.* **10**, 644–648

83. Irie, Y., Borlee, B. R., O'Connor, J. R., Hill, P. J., Harwood, C. S., Wozniak, D. J., and Parsek, M. R. (2012) Self-produced exopolysaccharide is a signal that stimulates biofilm formation in *Pseudomonas aeruginosa*. *Proc. Natl. Acad. Sci. U. S. A.* **109**, 20632–20636

84. Vasseur, P., Vallet-Gely, I., Soscia, C., Genin, S., and Filloux, A. (2005) The pel genes of the *Pseudomonas aeruginosa* PAK strain are involved at early and late stages of biofilm formation. *Microbiology*. **151**, 985–997

85. Ciofu, O., and Tolker-Nielsen, T. (2019) Tolerance and resistance of *Pseudomonas aeruginosa* biofilms to antimicrobial agents-how *P. aeruginosa* Can escape antibiotics. *Front. Microbiol.* 10.3389/fmicb.2019.00913

86. Wozniak, D. J., Wyckoff, T. J. O., Starkey, M., Keyser, R., Azadi, P., O'Toole, G. A., and Parsek, M. R. (2003) Alginate is not a significant component of the extracellular polysaccharide matrix of PA14 and PAO1 *Pseudomonas aeruginosa* biofilms. *Proc. Natl. Acad. Sci. U. S. A.* 10.1073/pnas.1231792100

87. Colvin, K. M., Irie, Y., Tart, C. S., Urbano, R., Whitney, J. C., Ryder, C., Howell, P. L., Wozniak, D. J., and Parsek, M. R. (2012) The Pel and Psl polysaccharides provide *Pseudomonas aeruginosa* structural redundancy within the biofilm matrix. *Environ. Microbiol.* **14**, 1913–1928

88. Santajit, S., and Indrawattana, N. (2016) Mechanisms of Antimicrobial Resistance in ESKAPE Pathogens. *Biomed Res. Int.* 10.1155/2016/2475067

89. Langendonk, R. F., Neill, D. R., and Fothergill, J. L. (2021) The Building Blocks of Antimicrobial Resistance in *Pseudomonas aeruginosa*: Implications for Current Resistance-Breaking Therapies. *Front. Cell. Infect. Microbiol.* 10.3389/fcimb.2021.665759

90. Mulani, M. S., Kamble, E. E., Kumkar, S. N., Tawre, M. S., and Pardesi, K. R. (2019) Emerging strategies to combat ESKAPE pathogens in the era of antimicrobial resistance: A review. *Front. Microbiol.* 10.3389/fmicb.2019.00539

91. Armbruster, C. R., Lee, C. K., Parker-Gilham, J., De Anda, J., Xia, A., Zhao, K., Murakami, K., Tseng, B. S., Hoffman, L. R., Jin, F., Harwood, C. S., Wong, G. C. L., and Parsek, M. R. (2019) Heterogeneity in surface sensing suggests a division of labor in *Pseudomonas aeruginosa* populations. *Elife*. 10.7554/eLife.45084

92. Ha, D.-G., and O'Toole, G. A. (2015) c-di-GMP and its Effects on Biofilm Formation and Dispersion: a *Pseudomonas aeruginosa* Review . *Microbiol. Spectr.*

10.1128/microbiolspec.mb-0003-2014

93. Pestrak, M. J., and Wozniak, D. J. (2020) Regulation of Cyclic di-GMP Signaling in *Pseudomonas aeruginosa*. in *Microbial Cyclic Di-Nucleotide Signaling*, 10.1007/978-3-030-33308-9_28

94. O'Toole, G. A., and Kolter, R. (1998) Flagellar and twitching motility are necessary for *Pseudomonas aeruginosa* biofilm development. *Mol. Microbiol.* 10.1046/j.1365-2958.1998.01062.x

95. van Gestel, J., Vlamakis, H., and Kolter, R. (2015) Division of Labor in Biofilms: the Ecology of Cell Differentiation. *Microbiol. Spectr.* 10.1128/microbiolspec.mb-0002-2014

96. Toutain, C. M., Caizza, N. C., Zegans, M. E., and O'Toole, G. A. (2007) Roles for flagellar stators in biofilm formation by *Pseudomonas aeruginosa*. *Res. Microbiol.* 10.1016/j.resmic.2007.04.001

97. Caiazza, N. C., and O'Toole, G. A. (2004) SadB is required for the transition from reversible to irreversible attachment during biofilm formation by *Pseudomonas aeruginosa* PA14. *J. Bacteriol.* 10.1128/JB.186.14.4476-4485.2004

98. Luo, Y., Zhao, K., Baker, A. E., Kuchma, S. L., Coggan, K. A., Wolfgang, M. C., Wong, G. C. L., and O'Toole, G. A. (2015) A hierarchical cascade of second messengers regulates *Pseudomonas aeruginosa* Surface Behaviors. *MBio*. 10.1128/mBio.02456-14

99. Caiazza, N. C., Merritt, J. H., Brothers, K. M., and O'Toole, G. A. (2007) Inverse regulation of biofilm formation and swarming motility by *Pseudomonas aeruginosa* PA14. *J. Bacteriol.* 10.1128/JB.01685-06

100. Jennings, L. K., Dreifus, J. E., Reichhardt, C., Storek, K. M., Secor, P. R., Wozniak, D. J., Hisert, K. B., and Parsek, M. R. (2021) *Pseudomonas aeruginosa* aggregates in cystic

fibrosis sputum produce exopolysaccharides that likely impede current therapies. *Cell Rep.* 10.1016/j.celrep.2021.108782

101. Borlee, B. R., Goldman, A. D., Murakami, K., Samudrala, R., Wozniak, D. J., and Parsek, M. R. (2010) *Pseudomonas aeruginosa* uses a cyclic-di-GMP-regulated adhesin to reinforce the biofilm extracellular matrix. *Mol. Microbiol.* 10.1111/j.1365-2958.2009.06991.x

102. Passos da Silva, D., Matwichuk, M. L., Townsend, D. O., Reichhardt, C., Lamba, D., Wozniak, D. J., and Parsek, M. R. (2019) The *Pseudomonas aeruginosa* lectin LecB binds to the exopolysaccharide Psl and stabilizes the biofilm matrix. *Nat. Commun.* 10.1038/s41467-019-10201-4

103. Quan, K., Hou, J., Zhang, Z., Ren, Y., Peterson, B. W., Flemming, H. C., Mayer, C., Busscher, H. J., and van der Mei, H. C. (2021) Water in bacterial biofilms: pores and channels, storage and transport functions. *Crit. Rev. Microbiol.* 10.1080/1040841X.2021.1962802

104. Wilking, J. N., Zaburdaev, V., De Volder, M., Losick, R., Brenner, M. P., and Weitz, D. A. (2013) Liquid transport facilitated by channels in *Bacillus subtilis* biofilms. *Proc. Natl. Acad. Sci. U. S. A.* 10.1073/pnas.1216376110

105. Rasamiravaka, T., Labtani, Q., Duez, P., and El Jaziri, M. (2015) The formation of biofilms by *Pseudomonas aeruginosa*: A review of the natural and synthetic compounds interfering with control mechanisms. *Biomed Res. Int.* 10.1155/2015/759348

106. Ozer, E., Yaniv, K., Chetrit, E., Boyarski, A., Meijler, M. M., Berkovich, R., Kushmaro, A., and Alfonta, L. (2021) An inside look at a biofilm: *Pseudomonas aeruginosa* flagella biotracking. *Sci. Adv.* 10.1126/sciadv.abg8581

107. Karatan, E., and Watnick, P. (2009) Signals, Regulatory Networks, and Materials That Build and Break Bacterial Biofilms. *Microbiol. Mol. Biol. Rev.* 10.1128/mmbr.00041-08

108. Rutherford, S. T., and Bassler, B. L. (2012) Bacterial quorum sensing: Its role in virulence and possibilities for its control. *Cold Spring Harb. Perspect. Med.* 10.1101/cshperspect.a012427

109. Kostylev, M., Kim, D. Y., Smalley, N. E., Salukhe, I., Peter Greenberg, E., and Dandekar, A. A. (2019) Evolution of the *Pseudomonas aeruginosa* quorum-sensing hierarchy. *Proc. Natl. Acad. Sci. U. S. A.* 10.1073/pnas.1819796116

110. Yan, S., and Wu, G. (2019) Can Biofilm Be Reversed Through Quorum Sensing in *Pseudomonas aeruginosa*? *Front. Microbiol.* 10.3389/fmicb.2019.01582

111. Venturi, V. (2006) Regulation of quorum sensing in *Pseudomonas*. *FEMS Microbiol. Rev.* 10.1111/j.1574-6976.2005.00012.x

112. Lee, J., Wu, J., Deng, Y., Wang, J., Wang, C., Wang, J., Chang, C., Dong, Y., Williams, P., and Zhang, L. H. (2013) A cell-cell communication signal integrates quorum sensing and stress response. *Nat. Chem. Biol.* 10.1038/nchembio.1225

113. Lin, J., Cheng, J., Wang, Y., and Shen, X. (2018) The *Pseudomonas* quinolone signal (PQS): Not just for quorum sensing anymore. *Front. Cell. Infect. Microbiol.* 10.3389/fcimb.2018.00230

114. Wang, J., Wang, C., Yu, H. B., Dela Ahator, S., Wu, X., Lv, S., and Zhang, L. H. (2019) Bacterial quorum-sensing signal IQS induces host cell apoptosis by targeting POT1–p53 signalling pathway. *Cell. Microbiol.* 10.1111/cmi.13076

115. Lee, J., and Zhang, L. (2015) The hierarchy quorum sensing network in *Pseudomonas aeruginosa*. *Protein Cell*. 10.1007/s13238-014-0100-x

116. Turkina, M. V., and Vikström, E. (2019) Bacteria-Host Crosstalk: Sensing of the Quorum in the Context of *Pseudomonas aeruginosa* Infections. *J. Innate Immun.* 10.1159/000494069

117. Cornelis, P. (2020) Putting an end to the *Pseudomonas aeruginosa* IQS controversy. *Microbiologyopen*. 10.1002/mbo3.962

118. Valentini, M., and Filloux, A. (2016) Biofilms and Cyclic di-GMP (c-di-GMP) signaling: Lessons from *Pseudomonas aeruginosa* and other bacteria. *J. Biol. Chem.* 10.1074/jbc.R115.711507

119. Pultz, I. S., Christen, M., Kulasekara, H. D., Kennard, A., Kulasekara, B., and Miller, S. I. (2012) The response threshold of *Salmonella* PilZ domain proteins is determined by their binding affinities for c-di-GMP. *Mol. Microbiol.* 10.1111/mmi.12066

120. Belas, R. (2014) Biofilms, flagella, and mechanosensing of surfaces by bacteria. *Trends Microbiol.* 10.1016/j.tim.2014.05.002

121. Moscoso, J. A., Mikkelsen, H., Heeb, S., Williams, P., and Filloux, A. (2011) The *Pseudomonas aeruginosa* sensor RetS switches Type III and Type VI secretion via c-di-GMP signalling. *Environ. Microbiol.* 10.1111/j.1462-2920.2011.02595.x

122. Matsuyama, B. Y., Krasteva, P. V., Baraquet, C., Harwood, C. S., Sondermann, H., and Navarro, M. V. A. S. (2016) Mechanistic insights into c-di-GMP-dependent control of the biofilm regulator FleQ from *Pseudomonas aeruginosa*. *Proc. Natl. Acad. Sci. U. S. A.* 10.1073/pnas.1523148113

123. Visaggio, D., Pasqua, M., Bonchi, C., Kaever, V., Visca, P., and Imperi, F. (2015) Cell aggregation promotes pyoverdine-dependent iron uptake and virulence in *Pseudomonas aeruginosa*. *Front. Microbiol.* 10.3389/fmicb.2015.00902

124. Webster, S. S., Lee, C. K., Schmidt, W. C., Wong, G. C. L., and O'Toole, G. A. (2021) Interaction between the type 4 pili machinery and a diguanylate cyclase fine-tune c-di-GMP levels during early biofilm formation. *Proc. Natl. Acad. Sci. U. S. A.* 10.1073/pnas.2105566118

125. Li, Z., Chen, J. H., Hao, Y., and Nair, S. K. (2012) Structures of the PelD cyclic diguanylate effector involved in pellicle formation in *Pseudomonas aeruginosa* PAO1. *J. Biol. Chem.* 10.1074/jbc.M112.378273

126. Whitney, J. C., Colvin, K. M., Marmont, L. S., Robinson, H., Parsek, M. R., and Howell, P. L. (2012) Structure of the cytoplasmic region of PelD, a degenerate diguanylate cyclase receptor that regulates exopolysaccharide production in *Pseudomonas aeruginosa*. *J. Biol. Chem.* 10.1074/jbc.M112.375378

127. Liu, C., Sun, D., Zhu, J., Liu, J., and Liu, W. (2020) The Regulation of Bacterial Biofilm Formation by cAMP-CRP: A Mini-Review. *Front. Microbiol.* 10.3389/fmicb.2020.00802

128. Almblad, H., Harrison, J. J., Rybtke, M., Groizeleau, J., Givskov, M., Parsek, M. R., and Tolker-Nielsen, T. (2015) The cyclic AMP-Vfr signaling pathway in *Pseudomonas aeruginosa* is inhibited by cyclic Di-GMP. *J. Bacteriol.* 10.1128/JB.00193-15

129. Almblad, H., Rybtke, M., Hendiani, S., Andersen, J. B., Givskov, M., and Tolker-Nielsen, T. (2019) High levels of cAMP inhibit *Pseudomonas aeruginosa* biofilm formation through reduction of the c-di-GMP content. *Microbiol. (United Kingdom).* 10.1099/mic.0.000772

130. Fuchs, E. L., Brutinel, E. D., Klem, E. R., Fehr, A. R., Yahr, T. L., and Wolfgang, M. C. (2010) In vitro and in vivo characterization of the *Pseudomonas aeruginosa* cyclic AMP (cAMP) phosphodiesterase CpdA, required for cAMP homeostasis and virulence factor

regulation. *J. Bacteriol.* 10.1128/JB.00168-10

131. Lapouge, K., Schubert, M., Allain, F. H. T., and Haas, D. (2008) Gac/Rsm signal transduction pathway of γ-proteobacteria: From RNA recognition to regulation of social behaviour. *Mol. Microbiol.* **67**, 241–253

132. Janssen, K. H., Diaz, M. R., Golden, M., Graham, J. W., Sanders, W., Wolfgang, M. C., and Yahr, T. L. (2018) Functional analyses of the RsmY and RsmZ small noncoding regulatory RNAs in *Pseudomonas aeruginosa*. *J. Bacteriol.* 10.1128/JB.00736-17

133. Valverde, C., Lindell, M., Wagner, E. G. H., and Haas, D. (2004) A repeated GGA motif is critical for the activity and stability of the riboregulator RsmY of *Pseudomonas fluorescens*. *J. Biol. Chem.* 10.1074/jbc.M401870200

134. Brencic, A., McFarland, K. A., McManus, H. R., Castang, S., Mogno, I., Dove, S. L., and Lory, S. (2009) The GacS/GacA signal transduction system of *Pseudomonas aeruginosa* acts exclusively through its control over the transcription of the RsmY and RsmZ regulatory small RNAs. *Mol. Microbiol.* **73**, 434–445

135. Bordi, C., Lamy, M. C., Ventre, I., Termine, E., Hachani, A., Fillet, S., Roche, B., Bleves, S., Méjean, V., Lazdunski, A., and Filloux, A. (2010) Regulatory RNAs and the HptB/RetS signalling pathways fine-tune *Pseudomonas aeruginosa* pathogenesis. *Mol. Microbiol.* **76**, 1427–1443

136. Brencic, A., and Lory, S. (2009) Determination of the regulon and identification of novel mRNA targets of *Pseudomonas aeruginosa* RsmA. *Mol. Microbiol.* 10.1111/j.1365-2958.2009.06670.x

137. Heurlier, K., Williams, F., Heeb, S., Dormond, C., Pessi, G., Singer, D., Cámara, M., Williams, P., and Haas, D. (2004) Positive Control of Swarming, Rhamnolipid Synthesis,

and Lipase Production by the Posttranscriptional RsmA/RsmZ System in *Pseudomonas aeruginosa* PAO1. *J. Bacteriol.* 10.1128/JB.186.10.2936-2945.2004

138. Heeb, S., and Haas, D. (2001) Regulatory roles of the GacS/GacA two-component system in plant-associated and other Gram-negative bacteria. *Mol. Plant-Microbe Interact.* **14**, 1351–1363

139. Latour, X. (2020) The evanescent gacs signal. *Microorganisms*. **8**, 1–25

140. Monzel, C., and Unden, G. (2015) Transmembrane signaling in the sensor kinase DcuS of *Escherichia coli*: A long-range piston-type displacement of transmembrane helix 2. *Proc. Natl. Acad. Sci. U. S. A.* 10.1073/pnas.1507217112

141. Chambonnier, G., Roux, L., Redelberger, D., Fadel, F., Filloux, A., Sivaneson, M., de Bentzmann, S., and Bordi, C. (2016) The Hybrid Histidine Kinase LadS Forms a Multicomponent Signal Transduction System with the GacS/GacA Two-Component System in *Pseudomonas aeruginosa*. *PLoS Genet.* 10.1371/journal.pgen.1006032

142. Ventre, I., Goodman, A. L., Vallet-Gely, I., Vasseur, P., Soscia, C., Molin, S., Bleves, S., Lazdunski, A., Lory, S., and Filloux, A. (2006) Multiple sensors control reciprocal expression of *Pseudomonas aeruginosa* regulatory RNA and virulence genes. *Proc. Natl. Acad. Sci. U. S. A.* **103**, 171–176

143. Broder, U. N., Jaeger, T., and Jenal, U. (2016) LadS is a calcium-responsive kinase that induces acute-to-chronic virulence switch in *Pseudomonas aeruginosa*. *Nat. Microbiol.* 10.1038/nmicrobiol.2016.184

144. Jing, X., Jaw, J., Robinson, H. H., and Schubot, F. D. (2010) Crystal structure and oligomeric state of the Ret S signaling kinase sensory domain. *Proteins Struct. Funct. Bioinforma.* **78**, 1631–1640

145. Ryan Kaler, K. M., Nix, J. C., and Schubot, F. D. (2021) RetS inhibits *Pseudomonas aeruginosa* biofilm formation by disrupting the canonical histidine kinase dimerization interface of GacS. *J. Biol. Chem.* **297**, 101193

146. Le Roux, M., Kirkpatrick, R. L., Montauti, E. I., Tran, B. Q., Brook Peterson, S., Harding, B. N., Whitney, J. C., Russell, A. B., Traxler, B., Goo, Y. A., Goodlett, D. R., Wiggins, P. A., and Mougous, J. D. (2015) Kin cell lysis is a danger signal that activates antibacterial pathways of *Pseudomonas aeruginosa*. *Elife*. **2015**, 1–65

147. Wang, B. X., Wheeler, K. M., Cady, K. C., Lehoux, S., Cummings, R. D., Laub, M. T., and Ribbeck, K. (2021) Mucin Glycans Signal through the Sensor Kinase RetS to Inhibit Virulence-Associated Traits in *Pseudomonas aeruginosa*. *Curr. Biol.* **31**, 90-102.e7

148. Hsu, J. L., Chen, H. C., Peng, H. L., and Chang, H. Y. (2008) Characterization of the histidine-containing phosphotransfer protein B-mediated multistep phosphorelay system in *Pseudomonas aeruginosa* PAO1. *J. Biol. Chem.* **283**, 9933–9944

149. Lin, C. T., Huang, Y. J., Chu, P. H., Hsu, J. L., Huang, C. H., and Peng, H. L. (2006) Identification of an HptB-mediated multi-step phosphorelay in *Pseudomonas aeruginosa* PAO1. *Res. Microbiol.* **157**, 169–175

150. Bouillet, S., Ba, M., Houot, L., Iobbi-Nivol, C., and Bordi, C. (2019) Connected partner-switches control the life style of *Pseudomonas aeruginosa* through RpoS regulation. *Sci. Rep.* **9**, 1–11

151. Valentini, M., Laventie, B. J., Moscoso, J., Jenal, U., and Filloux, A. (2016) The Diguanylate Cyclase HsbD Intersects with the HptB Regulatory Cascade to Control *Pseudomonas aeruginosa* Biofilm and Motility. *PLoS Genet.* 10.1371/journal.pgen.1006354

152. Petrova, O. E., and Sauer, K. (2011) SagS contributes to the motile-sessile switch and acts in concert with BfiSR to enable *Pseudomonas aeruginosa* biofilm formation. *J. Bacteriol.* **193**, 6614–6628

153. Petrova, O. E., and Sauer, K. (2010) The novel two-component regulatory system BfiSR regulates biofilm development by controlling the small RNA rsmZ through CafA. *J. Bacteriol.* 10.1128/JB.00387-10

154. Petrova, O. E., and Sauer, K. (2009) A novel signaling network essential for regulating *Pseudomonas aeruginosa* biofilm development. *PLoS Pathog.* 10.1371/journal.ppat.1000668

155. Zschiedrich, C. P., Keidel, V., and Szurmant, H. (2016) Molecular Mechanisms of Two-Component Signal Transduction. *J. Mol. Biol.* **428**, 3752–3775

156. Podgornaia, A. I., and Laub, M. T. (2013) Determinants of specificity in two-component signal transduction. *Curr. Opin. Microbiol.* **16**, 156–162

157. Assmann, G., Brehm, W., and Diederichs, K. (2016) Identification of rogue datasets in serial crystallography. *J. Appl. Crystallogr.* 10.1107/S1600576716005471

158. Ulrich, L. E., and Zhulin, I. B. (2005) Four-helix bundle: A ubiquitous sensory module in prokaryotic signal transduction. *Bioinformatics*. 10.1093/bioinformatics/bti1204

159. Albanesi, D., Martín, M., Trajtenberg, F., Mansilla, M. C., Haouz, A., Alzari, P. M., De Mendoza, D., and Buschiazzo, A. (2009) Structural plasticity and catalysis regulation of a thermosensor histidine kinase. *Proc. Natl. Acad. Sci. U. S. A.* **106**, 16185–16190

160. Ashenberg, O., Keating, A. E., and Laub, M. T. (2013) Helix bundle loops determine whether histidine kinases autophosphorylate in *cis* or in *trans*. *J. Mol. Biol.* **425**, 1198–1209

161. Kinoshita-Kikuta, E., Kinoshita, E., Eguchi, Y., and Koike, T. (2016) Validation of *cis* and *trans* modes in multistep phosphotransfer signaling of bacterial tripartite sensor kinases by using phos-tag SDS-pagE. *PLoS One*. 10.1371/journal.pone.0148294

162. Workentine, M. L., Chang, L., Ceri, H., and Turner, R. J. (2009) The GacS-GacA two-component regulatory system of *Pseudomonas fluorescens*: A bacterial two-hybrid analysis. *FEMS Microbiol. Lett.* **292**, 50–56

163. Yan, Q., Lopes, L. D., Shaffer, B. T., Kidarsa, T. A., Vining, O., Philmus, B., Song, C., Stockwell, V. O., Raaijmakers, J. M., McPhail, K. L., Andreote, F. D., Chang, J. H., and Loper, J. E. (2018) Secondary metabolism and interspecific competition affect accumulation of spontaneous mutants in the GacS-GacA regulatory system in *Pseudomonas protegens*. *MBio*. 10.1128/mBio.01845-17

164. Wei, X., Huang, X., Tang, L., Wu, D., and Xu, Y. (2013) Global control of GacA in secondary metabolism, primary metabolism, secretion systems, and motility in the rhizobacterium *Pseudomonas aeruginosa* M18. *J. Bacteriol.* **195**, 3387–3400

165. Sonnleitner, E., and Haas, D. (2011) Small RNAs as regulators of primary and secondary metabolism in *Pseudomonas* species. *Appl. Microbiol. Biotechnol.* **91**, 63–79

166. Mann, T. H., and Shapiro, L. (2018) Integration of cell cycle signals by multi-PAS domain kinases. *Proc. Natl. Acad. Sci. U. S. A.* **115**, E7166–E7173

167. Vincent, F., Round, A., Reynaud, A., Bordi, C., Filloux, A., and Bourne, Y. (2010) Distinct oligomeric forms of the Pseudomonas aeruginosa RetS sensor domain modulate accessibility to the ligand binding site. *Environ. Microbiol.* 10.1111/j.1462-2920.2010.02264.x

168. Qiu, D., Damron, F. H., Mima, T., Schweizer, H. P., and Yu, H. D. (2008) PBAD-based

shuttle vectors for functional analysis of toxic and highly regulated genes in *Pseudomonas* and *Burkholderia* spp. and other bacteria. *Appl. Environ. Microbiol.* **74**, 7422–7426

169. Mancl, J. M. (2018) *Molecular Investigations of Protein Assemblies Involved in Prokaryotic Virulence*. Ph.D. thesis

170. Evans, P. R., and Murshudov, G. N. (2013) How good are my data and what is the resolution? *Acta Crystallogr. Sect. D Biol. Crystallogr.* 10.1107/S0907444913000061

171. Evans, P. R. (2011) An introduction to data reduction: Space-group determination, scaling and intensity statistics. *Acta Crystallogr. Sect. D Biol. Crystallogr.* 10.1107/S090744491003982X

172. Kabsch, W. (2010) *XDS*. *Acta Crystallogr. Sect. D Biol. Crystallogr.*

173. Adams, P. D., Afonine, P. V., Bunkóczi, G., Chen, V. B., Echols, N., Headd, J. J., Hung, L. W., Jain, S., Kapral, G. J., Grosse Kunstleve, R. W., McCoy, A. J., Moriarty, N. W., Oeffner, R. D., Read, R. J., Richardson, D. C., Richardson, J. S., Terwilliger, T. C., and Zwart, P. H. (2011) The Phenix software for automated determination of macromolecular structures. *Methods*. **55**, 94–106

174. McCoy, A. J., Grosse-Kunstleve, R. W., Adams, P. D., Winn, M. D., Storoni, L. C., and Read, R. J. (2007) Phaser crystallographic software. *J. Appl. Crystallogr.* 10.1107/S0021889807021206

175. Emsley, P., Lohkamp, B., Scott, W. G., and Cowtan, K. (2010) Features and development of Coot. *Acta Crystallogr. Sect. D Biol. Crystallogr.* 10.1107/S0907444910007493

176. Guss, J. M. (2011) *Biomolecular Crystallography: Principles, Practice, and Application to Structural Biology, by Bernard Rupp*, Garland Science, Taylor & Francis Group, LLC, 10.1080/08893111003621289

177. Vagin, A. A., Steiner, R. A., Lebedev, A. A., Potterton, L., McNicholas, S., Long, F., and Murshudov, G. N. (2004) REFMAC5 dictionary: Organization of prior chemical knowledge and guidelines for its use. *Acta Crystallogr. Sect. D Biol. Crystallogr.* **60**, 2184–2195

178. DeLano, W. L. (2020) The PyMOL Molecular Graphics System, Version 2.3. *Schrödinger LLC*

179. Karimova, G., Dautin, N., and Ladant, D. (2005) Interaction network among *Escherichia coli* membrane proteins involved in cell division as revealed by bacterial two-hybrid analysis. *J. Bacteriol.* **187**, 2233–2243

180. Zhang, X., and Bremer, H. (1995) Control of the *Escherichia coli rrnB* P1 promoter strength by ppGpp. *J. Biol. Chem.* **270**, 11181–11189

181. O'Toole, G. A. (2010) Microtiter dish Biofilm formation assay. *J. Vis. Exp.* 10.3791/2437

182. Laskowski, R. A., Jabłońska, J., Pravda, L., Vařeková, R. S., and Thornton, J. M. (2018) PDBsum: Structural summaries of PDB entries. *Protein Sci.* 10.1002/pro.3289

183. Rowland, M. A., and Deeds, E. J. (2014) Crosstalk and the evolution of specificity in two-component signaling. *Proc. Natl. Acad. Sci. U. S. A.* 10.1073/pnas.1317178111

184. Agrawal, R., Sahoo, B. K., and Saini, D. K. (2016) Cross-talk and specificity in two-component signal transduction pathways. *Future Microbiol.* 10.2217/fmb-2016-0001

185. Bem, A. E., Velikova, N., Pellicer, M. T., Baarlen, P. Van, Marina, A., and Wells, J. M. (2015) Bacterial histidine kinases as novel antibacterial drug targets. *ACS Chem. Biol.* 10.1021/cb5007135

186. Ganesh, I., Kim, T. W., Na, J. G., Eom, G. T., and Hong, S. H. (2019) Engineering *Escherichia coli* to Sense Non-native Environmental Stimuli: Synthetic Chimera Two-

component Systems. *Biotechnol. Bioprocess Eng.* 10.1007/s12257-018-0252-2

187. Selvamani, V., Ganesh, I., Maruthamuthu, M. kannan, Eom, G. T., and Hong, S. H. (2017) Engineering chimeric two-component system into *Escherichia coli* from *Paracoccus denitrificans* to sense methanol. *Biotechnol. Bioprocess Eng.* 10.1007/s12257-016-0484-y

188. Hori, M., Oka, S., Sugie, Y., Ohtsuka, H., and Aiba, H. (2017) Construction of a photo-responsive chimeric histidine kinase in *Escherichia coli*. *J. Gen. Appl. Microbiol.* 10.2323/jgam.2016.07.005

189. Ward, S. M., Delgado, A., Gunsalus, R. P., and Manson, M. D. (2002) A NarX-Tar chimera mediates repellent chemotaxis to nitrate and nitrite. *Mol. Microbiol.* 10.1046/j.1365-2958.2002.02902.x

190. Xie, W., Y. Blain, K., Meng-Chiang Kuo, M., and Choe, S. (2010) Protein Engineering of Bacterial Histidine Kinase Receptor Systems. *Protein Pept. Lett.* 10.2174/092986610791306706

191. Utsumi, R., Brissette, R. E., Rampersaud, A., Forst, S. A., Oosawa, K., and Inouye, M. (1989) Activation of bacterial porin gene expression by a chimeric signal transducer in response to aspartate. *Science (80-.).* 10.1126/science.2476847

192. Zhu, Y., and Inouye, M. (2003) Analysis of the role of the EnvZ linker region in signal transduction using a chimeric Tar/EnvZ receptor protein, Tez1. *J. Biol. Chem.* 10.1074/jbc.M300916200

193. Cheung, J., and Hendrickson, W. A. (2009) Structural Analysis of Ligand Stimulation of the Histidine Kinase NarX. *Structure*. 10.1016/j.str.2008.12.013

194. Salvi, M., Schomburg, B., Giller, K., Graf, S., Unden, G., Becker, S., Lange, A., and Griesinger, C. (2017) Sensory domain contraction in histidine kinase CitA triggers

transmembrane signaling in the membrane-bound sensor. *Proc. Natl. Acad. Sci. U. S. A.* 10.1073/pnas.1620286114

195. Kaspar, S., Perozzo, R., Reinelt, S., Meyer, M., Pfister, K., Scapozza, L., and Bott, M. (1999) The periplasmic domain of the histidine autokinase CitA functions as a highly specific citrate receptor. *Mol. Microbiol.* 10.1046/j.1365-2958.1999.01536.x

196. Sevvana, M., Vijayan, V., Zweckstetter, M., Reinelt, S., Madden, D. R., Herbst-Irmer, R., Sheldrick, G. M., Bott, M., Griesinger, C., and Becker, S. (2008) A Ligand-Induced Switch in the Periplasmic Domain of Sensor Histidine Kinase CitA. *J. Mol. Biol.* 10.1016/j.jmb.2008.01.024

197. Reinelt, S., Hofmann, E., Gerharz, T., Bott, M., and Madden, D. R. (2003) The structure of the periplasmic ligand-binding domain of the sensor kinase CitA reveals the first extracellular pas domain. *J. Biol. Chem.* 10.1074/jbc.M305864200

198. Henke, J. M., and Bassler, B. L. (2004) Three parallel quorum-sensing systems regulate gene expression in *Vibrio harveyi*. *J. Bacteriol.* 10.1128/JB.186.20.6902-6914.2004

199. Timmen, M., Bassler, B. L., and Jung, K. (2006) AI-1 influences the kinase activity but not the phosphatase activity of LuxN of *Vibrio harveyi*. *J. Biol. Chem.* 10.1074/jbc.M604108200

200. Jung, K., Odenbach, T., and Timmen, M. (2007) The quorum-sensing hybrid histidine kinase LuxN of *Vibrio harveyi* contains a periplasmically located N terminus. *J. Bacteriol.* 10.1128/JB.01723-06

201. Ke, X., Miller, L. C., and Bassler, B. L. (2015) Determinants governing ligand specificity of the *Vibrio harveyi* LuxN quorum-sensing receptor. *Mol. Microbiol.* 10.1111/mmi.12852

202. Hurley, A., and Bassler, B. L. (2017) Asymmetric regulation of quorum-sensing receptors drives autoinducer-specific gene expression programs in *Vibrio cholerae*. *PLoS Genet.* 10.1371/journal.pgen.1006826

203. Ng, W. L., Wei, Y., Perez, L. J., Cong, J., Long, T., Koch, M., Semmelhack, M. F., Wingreen, N. S., and Bassler, B. L. (2010) Probing bacterial transmembrane histidine kinase receptor-ligand interactions with natural and synthetic molecules. *Proc. Natl. Acad. Sci. U. S. A.* 10.1073/pnas.1001392107

204. Van Alst, N. E., Picardo, K. F., Iglewski, B. H., and Haidaris, C. G. (2007) Nitrate sensing and metabolism modulate motility, biofilm formation, and virulence in *Pseudomonas aeruginosa*. *Infect. Immun.* 10.1128/IAI.00201-07

205. Mangalea, M. R., and Borlee, B. R. (2020) The NarX-NarL two-component system is a global regulator of biofilm formation, natural product biosynthesis, and host-associated survival in *Burkholderia pseudomallei*. *bioRxiv*. 10.1101/2020.06.25.170712

206. Park, J. S., Choi, H. Y., and Kim, W. G. (2020) The nitrite transporter facilitates biofilm formation via suppression of nitrite reductase and is a new antibiofilm target in *Pseudomonas aeruginosa*. *MBio*. 10.1128/mBio.00878-20

207. Taylor, P. K., Zhang, L., and Mah, T.-F. (2019) Loss of the Two-Component System TctD-TctE in *Pseudomonas aeruginosa* Affects Biofilm Formation and Aminoglycoside Susceptibility in Response to Citric Acid . *mSphere*. 10.1128/msphere.00102-19

208. Möglich, A., Ayers, R. A., and Moffat, K. (2009) Structure and Signaling Mechanism of Per-ARNT-Sim Domains. *Structure*. 10.1016/j.str.2009.08.011

Appendix A: Chimeric RetS Response to Sensory Domain Stimulation

Introduction

Elusive signals stimulate the sensory domains of many histidine kinases (HKs). The paralogous and modular nature of HKs enables the genetic engineering of chimeric HKs in which the N-terminal sensory domain from a protein with a known ligand is fused to the C-terminal catalytic region of an HK whose ligand is unknown, enabling the assessment of sensory domain stimulation's impact on the catalytic HK region (186–190). Previously, chimeric constructs were engineered between the methyl accepting chemotaxis protein Tar and the HK EnvZ of *Escherichia coli* (190–192). Tar and EnvZ share a similar domain organization; both comprise a periplasmic sensory domain, two transmembrane regions, a cytoplasmic HAMP signal transduction domain followed by catalytic cytoplasmic domains (190). EnvZ responds to changes in osmolarity via regulation of expression of two outer membrane porin genes *ompF* and *ompC,* but the exact signal remains unknown (190). Tar mediates chemotaxis via response to several ligands including aspartate (190). Two chimeric constructs were engineered. Taz1, which includes the periplasmic sensory domain, the transmembrane region and the HAMP domain from Tar fused to the HK region of EnvZ, was demonstrated to respond to aspartate stimulation, while Tez1, which comprises the periplasmic sensory domain and the transmembrane region from Tar fused to the HAMP domain and HK region of EnvZ, did not respond to aspartate (191, 192). Mutational analysis of Tez1 identified a single alanine insertion N-terminal to the HAMP domain that enabled Tez1 to respond to aspartate, which suggests that signal transmission is dependent on a specific alignment between the helical transmembrane region with the helical HAMP domain (192). The successful engineering of signal responsive chimeric proteins

suggests that the two proteins likely share a mechanism of signal transduction through the transmembrane region and HAMP domain (190).

Previously, the signals that stimulate the sensory domain of RetS were unknown. To determine if RetS could be controlled via sensory domain stimulation we engineered several chimeric constructs. The codons encoding the all helical nitrate sensory domain, the transmembrane signal transduction region, and the HAMP domain in NarX, a nitrate stimulated HK in *E. coli* K-12, were fused to the codons encoding the HK region through the C-terminus of RetS from *Pseudomonas aeruginosa* PAK to create the chimeric constructs Netx and Netx2 (Table A.1) (5, 20, 193). The codons encoding the citrate PDC/PAS sensory domain, the transmembrane signal transduction region, and the PAS signal transduction domain in CitA, a citrate stimulated HK from *Klebsiella pneumoniae*, were fused to the codons encoding the N-terminus of the HK region through the C-terminus of RetS creating the chimeric constructs CitA-RetS1 and CitA-RetS2 (Table A.1) (194–197). The codons encoding the sensory domain which is predicted to be comprised of nine transmembrane regions separated by short periplasmic regions in LuxN, a quorum sensing HK from *Vibrio harveyi* that interacts with autoinducer-1 (AI-1), were fused to the codons encoding the N-terminus of the HK region through the C-terminus of RetS creating the chimeric constructs LuxN-RetS1 and LuxN-RetS2 (Table A.1) (198–201). The codons encoding the sensory domain which is predicted to be comprised of six transmembrane regions separated by short periplasmic regions in CqsS, a quorum sensing HK from *Vibrio cholerae* that interacts with cholera autoinducer-1 (CAI-1), were fused to the codons encoding the N-terminus of the HK region through the C-terminus of RetS creating the chimeric constructs CqsS-RetS1 and CqsS-RetS2 (Table A.1) (202, 203). The constructs were expressed from an arabinose inducible, low-copy number plasmid in the *P. aeruginosa* PAK *retS* mutant

strain. The crystal violet (CV) cell attachment assay was used as a proxy for exopolysaccharide production to examine the effects of signaling through RetS on the Gac/Rsm pathway (181).

Results and Discussion

The initial CV cell attachment assays suggested that the Netx construct is functional and responds to sensory domain stimulation at the 13.5 and 15-hour time point as a clear difference was observed in the absorbance measurements at 590 nm between the PAKΔ*retS*+pHERD20T*netx* strain in the presence and absence of nitrate (Fig. A.1). An arabinose concentration of 1% (w/v) was identified as the most consistent concentration of arabinose under which the differential +/- nitrate phenotype was observed in PAKΔ*retS*+pHERD20T*netx* (Fig. A.2). In later CV cell attachment assays the nitrate responsive phenotype that was previously observed for the PAKΔ*retS*+pHERD20T*netx* strain was not observed, so we engineered a second Netx construct, termed Netx2. Netx2 did not display a nitrate responsive phenotype in the CV cell attachment assay at 15 hours with 1% (w/v) arabinose (Fig. A.3). The control PAKΔ*retS* + pHERD20T demonstrated a nitrate responsive phenotype similar to the nitrate responsive phenotype observed for PAKΔ*retS* + pHERD20T-*netx* at 15 hours with 1% (w/v) arabinose (Fig. A.3). This suggested that the initial nitrate responsive phenotype that was observed for the PAKΔ*retS*+pHERD20T*netx* was not due to RetS sensory domain stimulation but due to the impact of nitrate on biofilm formation, although PAKΔ*retS*+pHERD20T*netx* did demonstrate a nitrate responsive phenotype with increasing arabinose concentration which suggested that the nitrate responsive phenotype was dependent on the expression of *netx*. Given that the native Nar system in *P. aeruginosa* plays a role in biofilm

formation (with a Nar system knockout displaying a hyperbiofilm phenotype) and the observed nitrate responsive phenotype in the control, this suggests that nitrate may contribute to biofilm formation through means other than the NarX-RetS chimera (204). Biofilm formation and c-di-GMP production in *Burkholderia pseudomallei* is inhibited by nitrate, which could also be the case in *P. aeruginosa*, as nitric oxide is involved in both biofilm formation and dissolution in *P. aeruginosa* (205, 206). This led us to generate other chimeric RetS constructs (CitA-RetS1, CitA-RetS2, LuxN-RetS1, LuxN-RetS2, CqsS-RetS1 and CqsS-RetS2) (Table A.1). The CitA-RetS constructs were examined in the CV cell attachment assay and PAKΔ*retS* + pHERD20T-*citA-retS1* demonstrated a citrate responsive phenotype, as did the control PAKΔ*retS* + pHERD20T after incubation at 37 °C for 8 hours with 1% (w/v) arabinose and +/- 20 mM sodium citrate (Fig. A.4). The observed citrate responsive phenotype in both the control and PAKΔ*retS* + pHERD20T-*citA-retS1* could be due to the impact of citrate on biofilm formation not related to the chimeric CitA-RetS construct given that *P. aeruginosa* PA14 has demonstrated a reduction in biofilm mass with 20 mM exogenous citrate, although we did not observe the same impact on the wildtype strain (207). The LuxN-RetS constructs were examined in the CV cell attachment assay and neither displayed an AI-1 responsive phenotype with PAKΔ*retS* + pHERD20T-*luxN-retS1* displaying a phenotype similar to the *retS* knockout strain and PAKΔ*retS* + pHERD20T-*luxN-retS2* displaying a phenotype similar to the *retS* complement strain (Fig. A.5).

Difficulty in generating signal responsive chimeric RetS constructs is likely due to the stringent requirements for connections between signal transducing regions. The lack of a HAMP domain in RetS may explain why a chimeric NarX-RetS construct did not respond to sensory domain stimulation. The previously mentioned Tar-EnvZ fusion Tez1, which only responded to

aspartate after the insertion of an alanine residue N-terminal to the HAMP domain, demonstrates the importance of the alignment between the transmembrane regions and the HAMP domain in signal transmission (191, 192). It is also likely that the alignment between the helical HAMP domain and the helical DHp domain of the HK region is important in signal transmission. Similarly, the PAS signal transduction domain (comprising an antiparallel β-sheet flanked by several α helices) in CitA likely needs a specific alignment with the DHp domain of RetS to form a signal responsive chimera (208). LuxN is not predicted to contain a signal transduction domain C-terminal to the transmembrane region, although it likely contains the signaling helix (S-helix) which connects the transmembrane region to the catalytic HK region in many HKs (3, 30). While the LuxN-RetS1 construct contains the S-helix from RetS, the LuxN-RetS2 construct contains the predicted S-helix from LuxN. An incorrect alignment between the helices likely inhibited signal transmission which resulted in a lack of a signal responsive phenotype. Also, an output other than cell attachment as a proxy for biofilm formation may provide better insight into the signal responsive phenotypes of the chimeric constructs. Biofilm formation is a complex process that is regulated by multiple signal transduction pathways, thus the impact that a signal has on biofilm formation could be due to interactions with proteins other than the chimeric RetS constructs.

RetS contains a periplasmic sensory 7 TMR-DISM2 domain, a domain which contains a carbohydrate binding motif, followed by a 7 TMR-DISM-7TM region, which can both transduce signals across the inner membrane and interact with sensory stimuli (21, 142). We now know that RetS binds a component of kin cell lysis as well as host cell mucins via its 7 TMR-DISM2 sensory domain (146, 147). While binding to a component of kin cell lysis triggers the relief of GacS inhibition, binding of host cell mucins result in GacS inhibition (146, 147). This distinction

between the signaling outputs suggests that RetS may possess a complex sensory domain capable of transmitting disparate signals perhaps through differing signal transmission mechanisms.

Experimental Procedures

Chimeric Construct Synthesis

RetS chimeric constructs were synthesized by Genewiz and inserted into pHERD20T (Table A.1).

Crystal Violet Cell Attachment Assay

P. aeruginosa PAK strains were examined in the crystal violet cell attachment assay. The strains were plated to LB agar containing 300 μg/mL carbenicillin. Individual colonies were used to inoculate LB containing 300 μg/mL carbenicillin which was then incubated at 37 °C overnight while shaking at 225 rpm. The strains were sub-cultured into modified M63 media containing 0, 0.4, 0.8, or 1% (w/v) arabinose and 300 μg/mL carbenicillin which were incubated at 37 °C overnight while shaking at 225 rpm (181). The OD_{600} of the cultures was adjusted to 0.05 using modified M63 media containing 0, 0.4, 0.8 or 1% (w/v) arabinose, 300 μg/mL carbenicillin and +/- 1 mM KNO_3. 100 μL of each culture was dispensed into 96-well plates (Corning # 3896) (181). Plates were covered with lids and incubated at 37 °C for the given time periods (6, 13.5, 15 or 24 hours). Following incubation, the media were removed via pipette and the wells were washed with water via pipette. The wells were stained with 0.1% crystal violet for 10 minutes, and then washed with water via pipette (181). The remaining crystal violet-stained cells were solubilized in 125 μL of 30% acetic acid for 15 minutes (181). 100 μL of the solution was transferred to a 96-well plate (Corning # 3370) and absorbance at 590 or 600 nm was measured using a Tecan M200 plate reader.

Figures

Table A.1. Chimeric RetS constructs

Construct	NarX, CitA, LuxN and CqsS residues	RetS residues
Netx	NarX: 1 – 396	420 – 942
Netx2	NarX: 1 – 224	387 – 942
CitA-RetS1	CitA: 1 – 326	389 – 942
CitA-RetS2	CitA: 1 – 345	420 – 942
LuxN-RetS1	LuxN: 1 – 438	390 – 942
LuxN-RetS2	LuxN: 1 – 469	423 – 942
CqsS-RetS1	CqsS: 1 – 188	419 – 942
CqsS-RetS2	CqsS: 1 – 172	388 – 942

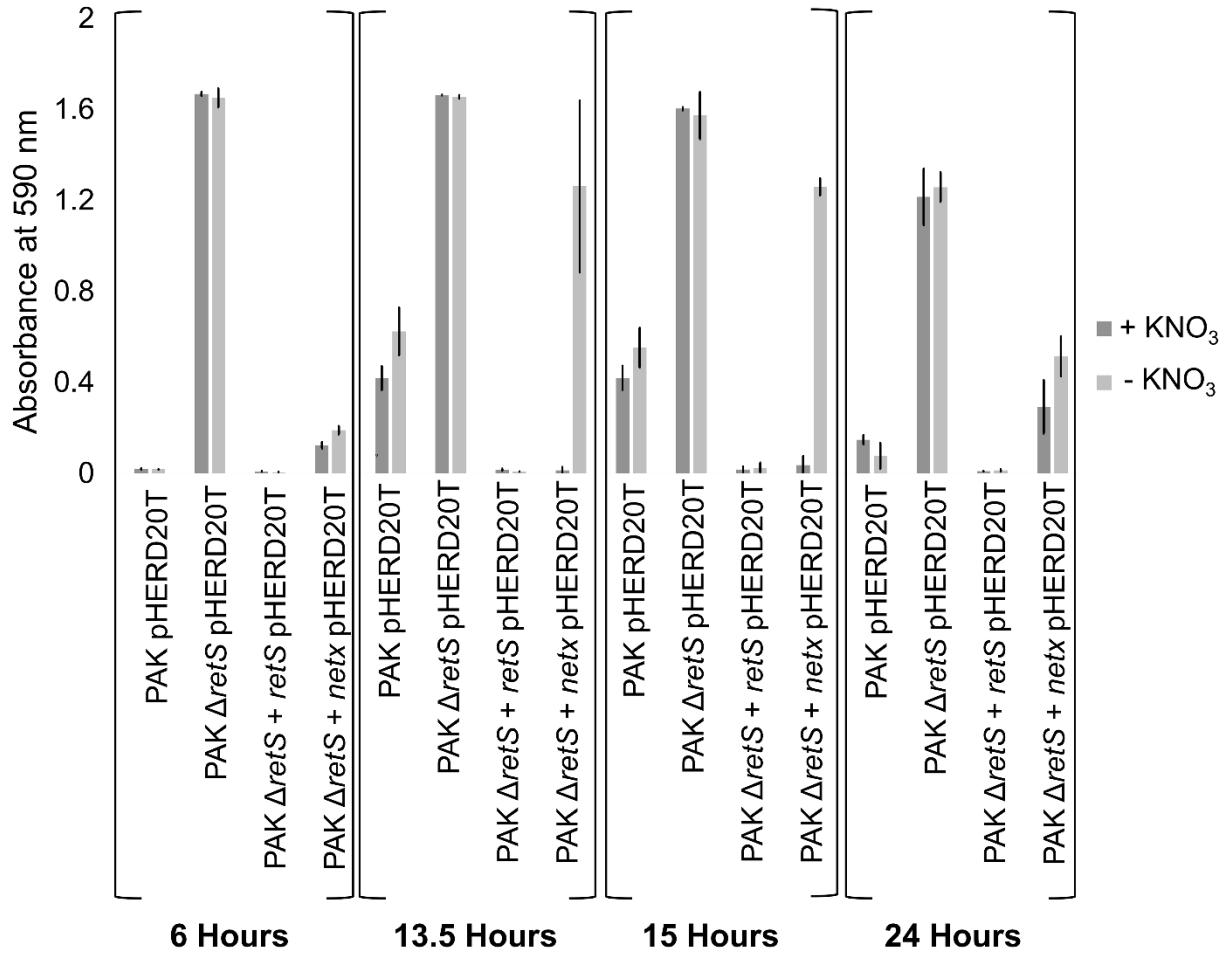

Figure A.1. Nitrate responsive chimeric Netx. Biofilm production assessed by the crystal violet cell attachment assay. PAKΔ*retS* + pHERD20T-*netx* was demonstrated to have a nitrate responsive phenotype in the crystal violet biofilm assay after incubation at 37 °C for 13.5 and 15 hours with 1% (w/v) arabinose and +/- 1 mM KNO_3. Assay was performed in triplicate.

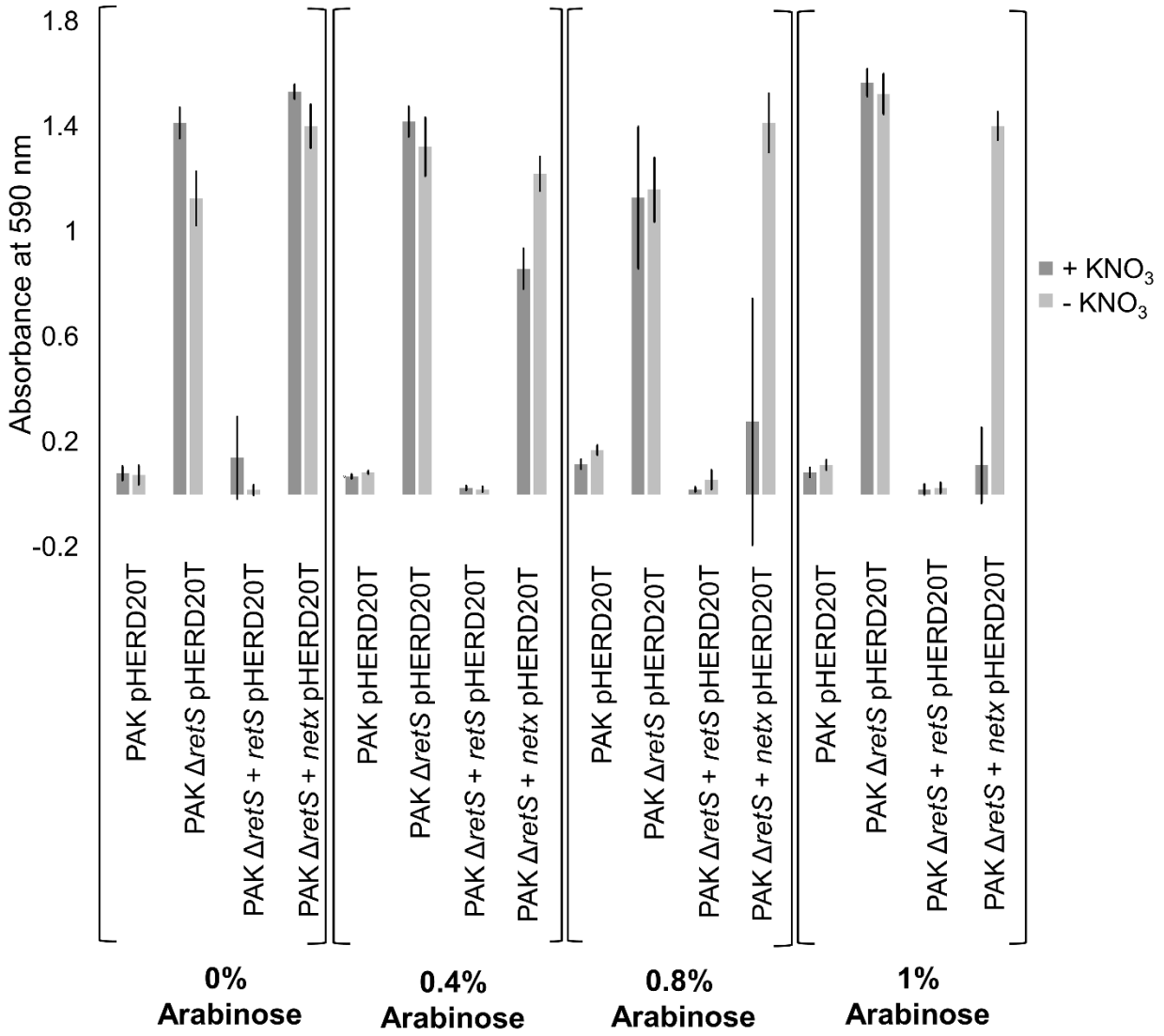

Figure A.2. Nitrate responsive chimeric Netx with 1% (w/v) arabinose. Biofilm production assessed by the crystal violet cell attachment assay. PAKΔ*retS* + pHERD20T-*netx* was demonstrated to have a nitrate responsive phenotype in the crystal violet biofilm assay after incubation at 37 °C for 15 hours with 1% (w/v) arabinose and +/- 1 mM KNO_3. Assay was performed in triplicate.

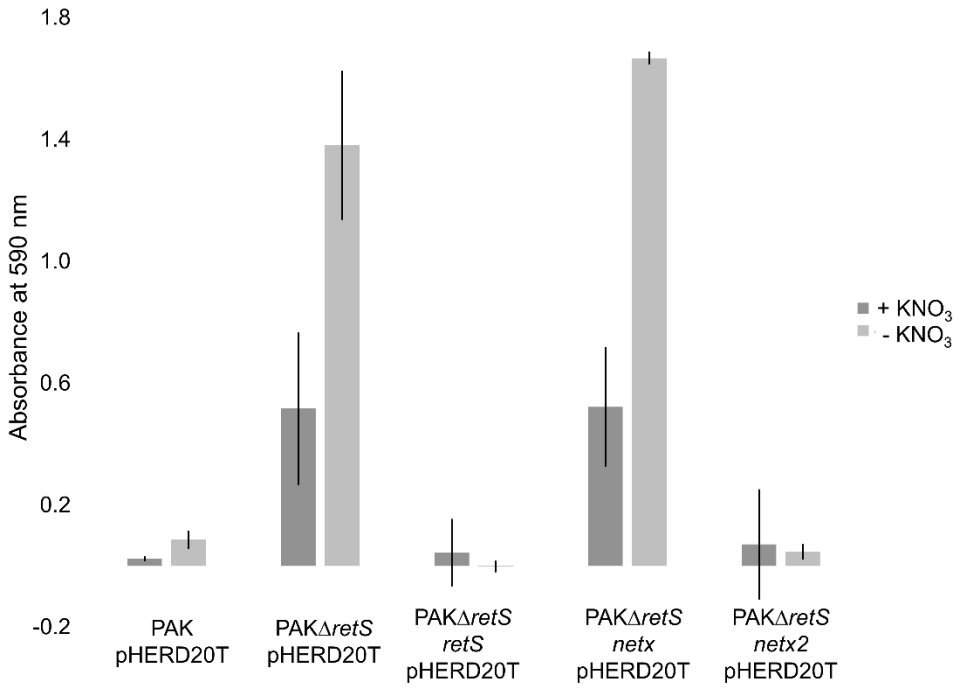

Figure A.3. Nitrate responsive phenotype observed in control. Biofilm production assessed by the crystal violet cell attachment assay. The control PAKΔ*retS* + pHERD20T demonstrated the same nitrate responsive phenotype as that observed for PAKΔ*retS* + pHERD20T-*netx* in the crystal violet biofilm assay after incubation at 37 °C for 15 hours with 1% (w/v) arabinose and +/- 1 mM KNO_3. Assay was performed in triplicate.

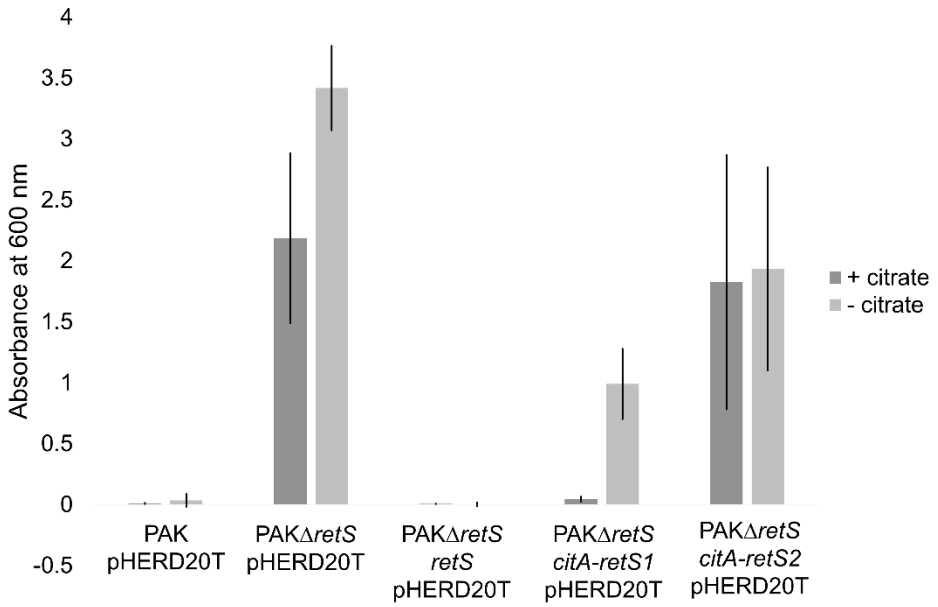

Figure A.4. Citrate responsive phenotype observed for CitA-RetS1 construct and control. Biofilm production assessed by the crystal violet cell attachment assay. PAKΔ*retS* + pHERD20T-*citA-retS1* was demonstrated to have a citrate responsive phenotype in the crystal violet biofilm assay after incubation at 37 °C for 8 hours with 1% (w/v) arabinose and +/- 20 mM sodium citrate. The control PAKΔ*retS* + pHERD20T also demonstrated a citrate responsive phenotype. Assay was performed in triplicate.

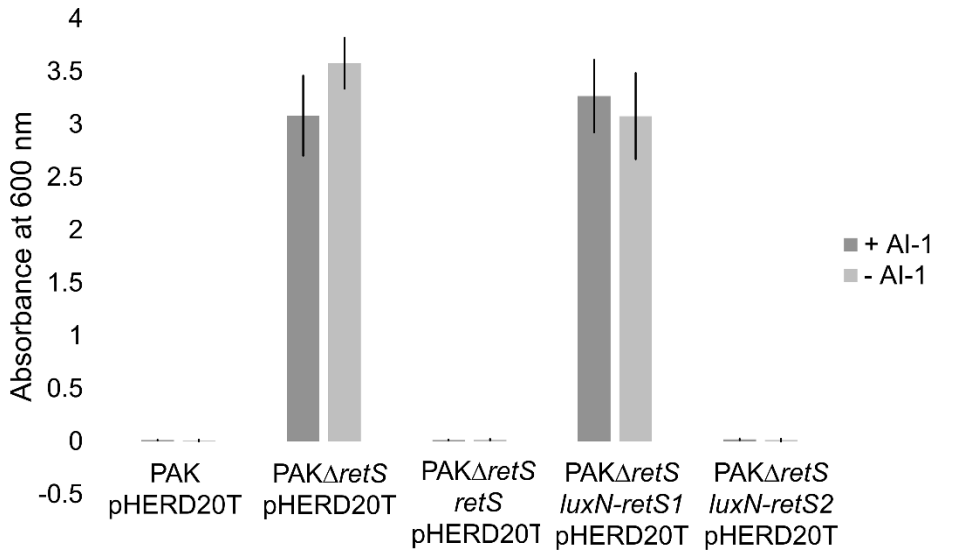

Figure A.5. LuxN-RetS constructs did not display an AI-1 responsive phenotype. Biofilm production assessed by the crystal violet cell attachment assay. Neither LuxN-RetS construct displayed an AI-1 responsive phenotype in the CV biofilm assay after incubation at 37 °C for 8 hours with 1% (w/v) arabinose and +/- 20 μM AI-1. Assay was performed in triplicate.

Table A.2. Strains and recombinant DNA

Strains	
Pseudomonas aeruginosa PAK	A. Filloux
P. aeruginosa PAKΔ*retS*	A. Filloux
Recombinant DNA	
pHERD20T	Qiu et al., 2018 (168)
pHERD20T-*retS*	Mancl et al., 2019 (36)
pHERD20T-*netx*	This study via Genewiz
pHERD20T-*netx2*	This study via Genewiz
pHERD20T-citA-retS1	This study via Genewiz
pHERD20T-citA-retS2	This study via Genewiz
pHERD20T-luxN-retS1	This study via Genewiz
pHERD20T-luxN-retS2	This study via Genewiz
pHERD20T-cqsS-retS1	This study via Genewiz
pHERD20T-cqsS-retS2	This study via Genewiz